九州大学学術情報リポジトリ
Kyushu University Institutional Repository

Theoretical studies on alternative life-history tactics from a physiological and an eco-evolutionary perspective

堀田, 淳之介

https://hdl.handle.net/2324/4784428

出版情報：Kyushu University, 2021, 博士（理学）, 課程博士
バージョン：
権利関係：

Theoretical studies on alternative life-history tactics from a physiological and an eco-evolutionary perspective

Junnosuke Horita

Submitted to the faculty of the Graduate School

in partial fulfillment of the requirements

for the degree

Doctor of Philosophy

in Science

Kyushu University

January 2022

Preface

"Alternative life-history tactics" indicates the discontinuous patterns of variation expressed within a population at the same life stage, and it is realized by divergent developmental programs (Roff, 1996). For example, some insects have two tactics, one has short or no wings and the other has normal or large wings based on their population density (Kishimoto, 1956; Roff, 1986; Denno et al., 1989; Zera and Denno, 1997), and some coral fishes change their sexes based on their social rank and body size (Fricke and Fricke 1977; Warner and Robertson 1978; Kuwamura and Nakashima, 1998; Munday et al., 2009).

Salmonids exhibit distinct alternative life-history tactics. Some individuals migrate to the sea for feeding migration, grow to a much larger size, and return to the same stream for reproduction (migratory tactic), meanwhile others mature early and complete their total life cycle in freshwater streams (resident tactic) (Morita and Nagasawa, 2010; Morita et al., 2014). Male juveniles that larger ones tend to choose the resident tactic, which is common throughout salmonids (Aubin-Horth & Dodson, 2004; Piché et al., 2008). This trend can be explained by the competition among individuals, as residents are affected by strong competition for both feeding and spawning opportunities, resulting in a dominance hierarchy among residents (Nakano, 1995; Esteve, 2011). Therefore, the reproductive success of an individual adopting the resident tactic strongly correlates with their body size in the juvenile state, because they mature at younger ages without experiencing a feeding migration (Morita et al., 2014).

Alternative behaviors or morphological types represent the result of complex physiological pathways controlled by gene expression (Oliveira, 2009). In salmonids, several factors such as growth and stress have been proposed to mediate seaward migrating behavior (Clements & Schreck, 2004; Ojima & Iwata, 2010). However, how these physiological factors relate to the development of alternative tactics and its association with body size are still unclear.

In this thesis, firstly I proposed simple mathematical models to describe the mechanisms that emerges the polymorphisms such as alternative life-history tactics by considering the relationships between the physiological dynamics and the competition among juveniles. Secondly, I investigated the effect of interaction between juveniles and adult residents on population dynamics. I considered the case in which the density of adult residents suppresses juvenile growth and investigated the dynamics of alternative life-history tactics and the evolution of threshold size by using the framework of eco-evolutionary dynamics.

In Chapter1, I assumed that the level of a key hormone changes in response to competitive interaction with other individuals, and that the consequence of the distribution of hormone levels exhibits two or more clusters, causing different phenotypes. I constructed a simple mathematical model that describes the positive feedback between hormonal and behavioral dynamics, with the expectation of establishing multiple discrete clusters of hormone levels leading to differentiation of life-history tactics. The assumptions were that winning probability in fighting depends both on the body size and hormone level of the two contestants. An individual with a

higher hormone level would be more likely to win the competition, which further enhanced hormone production, forming a positive feedback loop between hormone level and fighting ability. If the positive feedback was strong but not excessive, discrete clusters of hormone level formed.

In Chapter 2, I consider the case in which the density of adult residents modifies juvenile growth, which then affect the fraction of alternative tactics. Because smaller juveniles tend to be migrant, when the density of the adult residents is high, juvenile growth is suppressed and more juveniles exhibit the migratory tactic that year, resulting in a decrease in the density of residents in the subsequent year. If the density of adult residents is reduced, the growth of juveniles is improved and the body size exceeds the threshold for more individuals than those in the case of high density. A larger fraction of juveniles then adopts the resident tactic and the number of residents is high in the subsequent year. This forms a negative feedback loop. I demonstrated that this feedback loop can result in unstable population dynamics. Furthermore, we consider the evolution of threshold size, which occurs within the same time scale as ecological dynamics (i.e., eco-evolutionary dynamics).

In Chapter 3, I consider the size of individuals affected by climate change, represented as a monotonic change of temperature, that might either increase or decrease their growth rate. Abiotic factors also affect the status and consequences of decision-making. I examined how their eco-evolutionary dynamics as well as the fraction of migrant tactics and the evolution of the threshold status, responds to climate change. Consequently, I showed that the eco-evolutionary dynamics exhibit a qualitative shift in

the population dynamics in case that the environmental changes occur faster than the rate of evolutionary adaptation.

References

Aubin Horth, N., & Dodson, J. J. (2004). Influence of individual body size and variable thresholds on the incidence of a sneaker male reproductive tactic in Atlantic salmon. *Evolution*, *58*(1), 136-144.

Clements, S., & Schreck, C. B. (2004). Central administration of corticotropin-releasing hormone alters downstream movement in an artificial stream in juvenile chinook salmon (Oncorhynchus tshawytscha). *General and comparative endocrinology*, *137*(1), 1-8.

Denno, R. F., Olmstead, K. L., & McCLOUD, E. R. I. C. (1989). Reproductive cost of flight capability: a comparison of life history traits in wing dimorphic planthoppers. *Ecological Entomology*, *14*(1), 31-44.

Esteve, M., McLennan, D. A., & Kawahara, M. (2011). Sexual behaviour of a masu salmon parr, with implications for the evolution of parr sexual behaviour in the salmonines. *Ecology of Freshwater Fish*, *20*(3), 492-494.

Fricke, H., & Fricke, S. (1977). Monogamy and se*x* change by aggressive dominance in coral reef fish. *Nature*, *266*(5605), 830-832.

Kishimoto, R. 1956. Effect of crowding during the larval period on the determination of the wing-form of an adult plant-hopper. *Nature*, **176**: 641–642.

Kuwamura, T., & Nakashima, Y. (1998). New aspects of sex change among reef fishes: recent studies in Japan. In *Fish biology in Japan: an anthology in honour of*

Hiroya Kawanabe (pp. 125-135). Springer Netherlands.

Nakano, S. (1995). Individual differences in resource use, growth and emigration under the influence of a dominance hierarchy in fluvial red-spotted masu salmon in a natural habitat. *Journal of Animal Ecology*, 75-84.

Morita, K., & Nagasawa, T. (2010). Latitudinal variation in the growth and maturation of masu salmon (Oncorhynchus masou) parr. *Canadian Journal of Fisheries and Aquatic Sciences*, 67(6), 955-965.

Morita, K., Tamate, T., Kuroki, M., & Nagasawa, T. (2014). Temperature-dependent variation in alternative migratory tactics and its implications for fitness and population dynamics in a salmonid fish. *Journal of Animal Ecology*, *83*(6), 1268-1278.

Munday, P. L., Buston, P. M., & Warner, R. R. (2006). Diversity and flexibility of sex-change strategies in animals. *Trends in Ecology & Evolution*, *21*(2), 89-95.

Ojima, D., & Iwata, M. (2010). Central administration of growth hormone-releasing hormone and corticotropin-releasing hormone stimulate downstream movement and thyroxine secretion in fall-smolting coho salmon (Oncorhynchus kisutch). *General and comparative endocrinology*, *168*(1), 82-87.

Oliveira, R. F. (2009). Social behavior in context: hormonal modulation of behavioral plasticity and social competence. *Integrative and Comparative Biology*, *49*(4), 423-440.

Piché, J., Hutchings, J. A., & Blanchard, W. (2008). Genetic variation in threshold reaction norms for alternative reproductive tactics in male Atlantic salmon, Salmo

salar. *Proceedings of the Royal Society of London B: Biological Sciences*, *275*(1642), 1571-1575.

Roff, D. A. (1986). The evolution of wing dimorphism in insects. *Evolution*, *40*(5), 1009-1020.

Roff, D. A. (1996). The evolution of threshold traits in animals. *The Quarterly Review of Biology*, *71*(1), 3-35.

Warner, R. R., & Robertson, D. R. (1978). Sexual Patterns in the Labroicl Fishes of the Western Caribbean, I: The Wrasses (Labridae). *Smithsonian Contributions to Zoology*, *254*, 1-27.

Zera, A. J., & Denno, R. F. (1997). Physiology and ecology of dispersal polymorphism in insects. *Annual review of entomology*, *42*(1), 207-230.

Acknowledgement

I would like to express my special appreciation and thanks to my advisors Dr. Yuuya Tachiki, Dr. Akiko Satake and Dr. Yoh Iwasa, for their great support on my research activities. They constantly encouraged me throughout my research life. I could not have continued my research without their supports. I am thankful to the members and alumni of Mathematical Biology Laboratory at Kyushu University, for stimulating discussion from the points of view of their various interests. Especially, I am grateful to professors Shingo Iwami, Hiroshi Haeno, Koji Noshita, Ryo Yamaguchi, Shinsuke Satoi, Yusuke Kakizoe and Akane Hara for their advice on my research. I would like to thank the following people for their helpful comments and fruitful discussion on my study: Eiiti Kasuya, Takuya Sato, Takenori Takada, Kentaro Morita, Itsuro Koizumi, Hiroshi Araki, Jun-Ichiro Suzuki. I also thank to my family and friends; Kenichiro Horita, Kazuko Horita, Ayumi Horita, Shinnosuke Horita, Shuzo Iwanishi, Kengo Nagata, Tomohiro Hirano, Koichiro Yamashita, Hajime Arimitsu, Kazuaki Yoshida, Takuya Toma, Shun Kataoka and Hitomi Isaka. They gave me a lot of kind words. Finally, this work was financially supported by a Research Fellowship for Young Scientists (DC1) by JSPS.

Contents

Chapter 1 Positive feedback between behavioral and hormonal dynamics leads to differentiation of life-history tactics

The study in this chapter, done in collaboration with Dr. Yuuya Tachiki and Dr. Yoh Iwasa, was published in The American Naturalist 196(6): 679-689 in 2020.

Abstract

Competitive interaction among individuals of a single population may result in the differentiation of two or more distinct life-history tactics. For example, although they exhibit unimodal size distribution,male juveniles of salmonids differentiate into those going down to the ocean to grow and returning to the natal stream after several years to reproduce (migratory tactic) and those staying in the stream and reproducing for multiple years (resident tactic). In this study, we developed a simple mathematical model for the positive feedback between hormonal and behavioral dynamics, with the expectation of establishing multiple discrete clusters of hormone levels leading to differentiation of life-history tactics. The assumptions were that probability of winning in fighting depends both on the body size and hormone level of the two contestants. An individual with a higher hormone level would be more likely to win the competition, which further enhanced hormone production, forming a positive feedback loop between hormone level and fighting ability. If the positive feedback was strong but not excessive, discrete clusters of hormone levels emerged from a continuous distribution. In contrast, no clear clustering structure appeared in the distribution of hormone levels if the probability of winning in fighting was controlled by the body size.

1. Introduction

Alternative life-history tactics comprise discontinuous patterns of phenotypic variation arising from the continuous status, realized by divergent developmental programs (Roff, 1996). For example, in scarab beetles, large males develop horns and behave as fighters, whereas the others become sneakers (Emlen, 1997). Some coral fishes change their sex based on body size and social rank (Fricke and Fricke 1977; Warner and Robertson 1978; Kuwamura and Nakashima, 1998; Munday et al., 2006). Generally, individuals choose a tactic at a particular time in their life based on a given environment and/or their status in the population.

Salmonid fishes exhibit extreme alternative life-history tactics. Some individuals migrate to the ocean to feed, grow to a much larger size, and return to the natal stream for reproduction (migratory tactic), whereas others mature early and complete their entire life cycle in freshwater streams (resident tactic) (Morita and Nagasawa, 2010; Morita et al., 2014). Larger male juveniles tend to choose the resident tactic, which is common throughout salmonids (Aubin-Horth & Dodson, 2004; Piché et al., 2008). This trend can be explained by the competition among these fishes, as residents suffer from intensive competition for both spawning and feeding opportunities, resulting in a dominance hierarchy among residents (Nakano, 1995; Esteve, 2011). Consequently, the reproductive success of an individual adopting the resident tactic strongly correlates with their body size in the juvenile state, because they mature at younger ages without experiencing a feeding migration (Morita et al., 2014).

Alternative behaviors or morphological types represent the output of complex physiological pathways controlled by gene expression (Oliveira, 2009). In salmonids, several factors including growth and stress have been proposed to mediate seaward migrating behavior (Clements & Schreck, 2004; Ojima & Iwata, 2010). However, how these physiological factors relate to the development of alternative tactics and its association with body size are still unclear.

In modeling salmonid population dynamics, the life-history decision of male juveniles has been assumed to follow a threshold rule (Tachiki & Koizumi, 2016; Horita et al., 2018), in which the individuals remain in the stream if the body size (or a status parameter) is larger than a threshold, otherwise migrating to the ocean. However, although the mean body size of juveniles adopting the resident tactic is larger than that of migratory juveniles, the actual body size distribution exhibits a single peak without a clear separation of two groups of individuals (Morita & Nagasawa, 2010). This implies that an endocrine system drives different developmental pathways depending on the status of each individual, even if the body size is similar among individuals. The purpose of this study is to propose a system that could explain the induction of discrete patterns of physiological states serving to establish the threshold assumed by prior studies.

We conjectured that the level of a key hormone changes in response to competitive interaction with other individuals, and that the resultant distribution of the hormone levels exhibits two or more clusters, leading to the distinct developmental fates. For Salmonids, one candidate for the key hormone in juvenile males' life-history choice is

11-ketotestosterone (11-KT) as in many animals, maturation is induced by sex steroids (Devlin & Nagahama, 2002). In Salmonids, 11-KT functions as an androgen, whereas estradiol-17β (E_2) serves as the estrogen. These hormones contain a steroid nucleus and are synthesized from testosterone. Moreover, in masu salmon, the plasma level of 11-KT and testosterone of mature males is higher than that of immature males, and the migration of individuals could be suppressed when 11-KT and testosterone were artificially injected (Munakata, 2012).

The production of steroid hormones is induced by several factors including both biotic (e.g., competition: Perry & Grober, 2003) and abiotic (e.g., water quality: Awata et al, 2011) factors, which may vary among seasons (Munakata et al., 2001; Munakata, 2012). Social interaction is one of the most important stimuli that affect hormone production (Perry & Grober, 2003; Lorenzi & Grober, 2012). The results of competitive interaction affect the production of sex steroid hormone, modify the behavior of the individual, and change the results of future competition (Wingfield and Wada, 1989). For example, the plasma level of androgen significantly differs between the winner and loser in *Neolamprologus pulcher* (Taves et al, 2009). Because androgen enhances activity and renders behavior more aggressive (Nelson & Kriegsfeld, 2016; Hirschenhauser & Oliveira, 2006; Taves et al, 2009), an individual who wins a competition becomes more likely to win the next competition, which is termed the winner-loser effect (Earley et al., 2013; Li et al., 2014). Salmonid fishes compete over food resources and space in streams, forming a dominance hierarchy (Nakano, 1995).

The social interaction may thus affect the life-history choice of an individual through differentiation of the endocrine level.

In this study, we constructed a mathematical model for the hormonal dynamics that are coupled with individual growth and competitive interactions, and investigated how the distribution of hormone levels in the population changed depending on the physiological and ecological processes (Fig. 1). We demonstrated that the distribution of hormone level formed multiple clusters when the hormone level largely contributes to the winning probability. Our study shows that ecological interactions such as competition can give rise to discrete phenotypes for diverse traits such as life-history tactics via hormonal dynamics without assuming the presence of a threshold.

2. Materials and methods

Life histories and sex steroids of Salmonids

We considered a mathematical model for competitive interaction among juveniles and analyzed the resultant patterns of individual growth and hormone level. In this study, we focused on masu salmon (*Oncorhynchus masou masou*) because it exhibits a typical and relatively simple life history of salmonids. Some males complete their entire life cycle in freshwater streams (residents) whereas others migrate to the ocean (migrants).

Among factors previously proposed to determine the life-history choice, the concentration of key hormones, lipid storage, and growth efficiency have been shown to affect the propensity to realize alternative phenotypes (Dodson et al, 2013). We here

considered the situation in which the proximal factor of the decision-making is endocrine status (i.e., hormone level) and the correlation between decision-making and body size results from the correlation between hormone level and body size. Empirical evidence suggests that a sexual hormone constitutes a key factor for life-history choice in masu salmon. As Munakata (2012) measured the time series of plasma androgen levels of 0+ male and showed that the plasma levels of testosterone and 11-KT in mature males were significantly higher than those in non-mature males, in the present study we considered testosterone as a factor inducing maturation.

Androgen production is induced by both biotic and abiotic factors. Here, we focused on social interaction, especially competition that stimulates hormone production (Perry & Grober, 2003; Lorenzi & Grober, 2012). We also considered that the steroid hormone changes the behavior of the individual and modifies the result of future competition. In particular, an individual retaining a higher hormone concentration is likely to win a competition (Taves et al., 2009).

Scheme of individual-based simulation

In the model, we considered a population consisting of $N = 100$ juveniles. The body size and hormone level of individual i ($i = 1,2, \dots, N$) at time t were denoted by $s_{i,t}$ and $h_{i,t}$, respectively. The initial body size and hormone level of each individual was a stochastic variable following a bivariate normal distribution. We assumed that the growth rate and hormone plasma level were affected by the outcomes of fighting with other individuals. We traced the dynamics of hormone level and body size of each

individual in terms of a continuous-time stochastic individual-based model (Gillespie, 1977). A single time step in the simulation model consisted of the following three processes:

[1] The time lapse Δt until the next event is drawn from an exponential distribution with mean $1/E$, where E represents the event rate and is defined as follows:

$$E = qN(N-1) \quad , \tag{1}$$

where q is a rate constant for an individual to encounter with an opponent. When E is larger, fighting events occur more frequently.

[2] Two individuals are randomly chosen from the population. These individuals fight each other with one declared as the winner. The probability that individual i wins the fighting against individual j is denoted by $\varepsilon_{i,j,t}$. We assume that $\varepsilon_{i,j,t}$ is given as:

$$\varepsilon_{i,j,t} = \frac{1}{1+\left(\frac{s_{j,t}}{s_{i,t}}\right)^{\lambda_{\mathrm{s}}}\left(\frac{h_{j,t}}{h_{i,t}}\right)^{\lambda_{\mathrm{h}}}} \quad . \tag{2}$$

Note that $\varepsilon_{i,j,t} = 1 - \varepsilon_{j,i,t}$ is satisfied. Also note that the winning probability of i against j is an increasing function of the ratio of $(s_{i,t})^{\lambda_{\mathrm{s}}}(h_{i,t})^{\lambda_{\mathrm{h}}}$ to $(s_{j,t})^{\lambda_{\mathrm{s}}}(h_{j,t})^{\lambda_{\mathrm{h}}}$. Hence, the winning probability depends both on the relative body size and the relative hormone level. The weighting factor for the body size is λ_{s} and that for the hormone level is λ_{h}. Suffixes s and h represent size and hormone, respectively. λ indicates the sensitivity of each element to the winning probability. When λ_{s} (λ_{h}) is large, a slight difference in size (hormone level) between individuals becomes a large difference in winning probability. λ is larger if an organism is capable of recognizing their relative competitive ability more accurately. As $s_{i,t}$ (or $h_{i,t}$) increases, $\varepsilon_{i,j,t}$ increases

and finally converges to 1. If both $s_i = s_j$ and $h_i = h_j$ are satisfied, the two contestants have equal chance of winning: $\varepsilon_{i,j} = 0.5$.

[3] Winners can obtain more resources, resulting in a faster growth rate than that of losers. In addition, winners synthesize testosterone and enhance the hormone level. Size growth dynamics are modeled according to the von Bertalanffy model of the first order, which is commonly used in fishery sciences for describing the growth of body length (rather than body weight) (von Bertalanffy, 1938; Snover et al., 2005; Kiso et al., 1992). We assume that the hormone is synthesized at a constant rate and is decomposed in proportion to the current level. If individual i wins the competition, the body size and hormone level of the individual change according to the following equations until the next fighting event:

$$\frac{ds_i}{dt} = \alpha_{\mathrm{s}}(1+\gamma) - \beta_{\mathrm{s}} s_i \ , \tag{3a}$$

$$\frac{dh_i}{dt} = \alpha_{\mathrm{h}} - \beta_{\mathrm{h}} h_i. \tag{3b}$$

In contrast, if individual i loses, the body size and hormone level of the individual change with the following equations:

$$\frac{ds_i}{dt} = \alpha_{\mathrm{s}} - \beta_{\mathrm{s}} s_i, \tag{4a}$$

$$\frac{dh_i}{dt} = -\beta_{\mathrm{h}} h_i. \tag{4b}$$

In these equations (3 and 4), α_{s} and γ are coefficients of anabolism and β_{s} is a coefficient of catabolism (von Bertalanffy, 1938). α_{h} is the rate of hormone synthesis and β_{h} is the rate of degradation. The winner increases with regard to both size and

hormone level, rendering the individual more likely to win in subsequent encounters. The body sizes and hormone levels of all individuals are updated until the next fighting event. We assume that the rate of hormonal change is much faster than that of size growth (Lindstedt & Calder,1981), i.e., α_{s} and β_{s} is smaller than α_{h} and β_{h}. Juveniles of masu salmon emerge when they are approximately 22.0–28.0 mm (Fujioka, 1990), and make their decision regarding life tactic when they are 50.0–100.0 mm (Morita & Nagasawa, 2010). This is considered when choosing the standard set of parameter values.

We repeated these processes until *t* reached $T = 100$ and obtained the time series of size and hormone levels of all individuals in the population. Examples are shown in Fig. 2.

Cluster analysis

Cluster analysis is the method of grouping a set of data in such a way that data in the same group (called a cluster) are more similar (in character) to each other than to those in other clusters. Establishment of an alternative tactic is generally triggered by the physiological status and expressed as a consequence of intrinsic signaling pathways (Arterbery et al., 2010; Feng and Bass, 2017; Genova et al., 2012). We here explored the condition in which the competitive interactions divide the population into multiple clusters differing in the expression level of a key hormone. We identified the number of clusters using the following two steps:

[1] In order to perform the cluster analysis, the distribution of data should be either random or clumped. Thus, before performing cluster analysis, we calculated I_δ-index (Morisita, 1971) to identify the datasets showing uniform distribution and to remove them from the cluster analysis. This is defined as follows:

$$I_\delta = p\sum_{l=1}^{p} x_l(x_l - 1)/\sum_{l=1}^{p} x_l\left(\sum_{l=1}^{p} x_l - 1\right), \qquad (5)$$

where, p determines how many the range of data is divided into and x_l is the number of individuals in unit l. When $I_\delta < 1$, distribution is uniform, whereas when $I_\delta > 1$, distribution is clumped (note that when the distribution follows a Poisson distribution, $I_\delta = 1$ holds). If the distribution is uniform ($I_\delta < 1$), all individuals are grouped into a single cluster. In such case, the number of clusters was regarded as unity. If $I_\delta > 1$, we adopted the following analysis to determine the number of clusters in the population. Note that p is an arbitrary positive integer, we set $p = 7$. We performed the analysis using various values of p, and confirmed that the results were not altered substantively.

[2] We classified the distribution of the hormone level in the population by using the gap statistics in R package termed "cluster" (Tibshirani et al., 2001). This package calculates the optimal number of clusters for a given observation based on gap statistics. We adopted the K-means clustering algorithm to determine the optimal clustering for a given number of clusters *k*, where *k* is an integer from 1 to 10. Then, the gap statistic was calculated for each *k* and we identified the optimal number of clusters as the value of *k* that achieved the maximum gap statistics.

3. Results

Formation of multiple clusters in the hormone level distribution

Figure 2 illustrates an example of the simulation. A video of the dynamics of this example can be found in the online appendix (Appendix C). Initially, the hormone level and size of individuals in a population were distributed following a bivariate normal distribution. Once the simulation began, for some individuals the hormone level increased rapidly, whereas for others the hormonal level remained low. Individuals became separated into two distinct clusters differing in hormone level. In Fig. 3a, these are indicated by filled and open circles. Body size distribution remained unimodal (Fig. 3b). This result was quite similar to the pattern of alternative life-history tactics observed in salmonid (Morita & Nagasawa, 2011). Hormonal distribution consisted of some individuals with markedly high hormone levels and others with low levels (Fig. 3c). We expected that the former individuals would achieve earlier sexual maturation. Figs. 3d-f illustrate the results in which 10 runs are pooled, which reveal that the patterns did not substantially change among runs.

Figure 4a shows a heat map of the number of clusters averaged over 10 replicates for each pair of parameters. Vertical and horizontal axes indicate the importance of hormone (λ_{h}) and body size (λ_{s}) to the winning probability, respectively. When both λ_{h} and λ_{s} were small, as indicated by “I” in Fig. 4a, no correlation existed between size and hormone level (Fig. 4b). Specifically, the difference in hormone level among individuals was small. When λ_{h} was larger, the size–hormone distribution showed multiple clusters (Fig. 4c). In this case, winners synthesize more hormone than losers,

rendering the winner more likely to win the next competition. The positive feedback between behavior and hormone eventually split the population into two or more distinct types of individuals.

As λ_h increased further, the winning probability strongly depended on the hormone level. This meant that a small difference in hormone level could determine the outcome of the competition; hence, a clear dominance hierarchy was formed depending on the initial hormone level. This effect affected a regular, rather than clumped, distribution of hormone levels, as shown in Fig. 4d.

The correlation between body size and hormone level increased with an increase in λ_s (Fig. 4e). However, a small difference in body size determined the outcome of the competition, resulting in higher rates of both hormone production and size growth. Under this distribution, clustering did not occur because the number of optimal clusters was one. Discrete clusters, as expected for alternative tactics, appeared most clearly when the λ_h was large but not too large, as illustrated in Fig. 4c. In contrast, only a single cluster was identified when λ_h was small, as illustrated in Fig. 4b, and also when λ_h was very large, as shown in Figs. 4d and 4e.

The parameters mediating hormonal dynamics also affect the adoption of alternative tactics in the population. If individuals belonging to the cluster with the highest hormone level will mature and become residents, the fraction of residents in the population would decrease with an increase in the contribution of hormone level to the winning probability λ_h, as illustrated in Fig. 5. Here λ_s is fixed at 0.5 (see Fig. 4a). As λ_h increased, the number of clusters increased and the number of individuals belonging

to the top cluster decreased (Fig. 4a and Fig. 5). The further increase in λ_{h} made the cluster disappeared, and the number of clusters decreased (Fig. 4a).

Accuracy of decision-making

In order to examine the stability of the dominance hierarchy and the predictability of life-history choice, we defined the accuracy of decision making as the probability for an individual to be classified to the cluster predicted from the initial order of hormone level. In Fig. 6a, as the reaction rate q increased, the hormone level at the end of simulation more strongly reflected the initial state. The hormone level fluctuated less as the coefficient of reaction rate q increased (Fig. 6b). Because q mediates the number of encounters with opponents per unit time, the increase in the number of competitions provides more accurate information regarding an individual's status in the population.

4. Discussion

Numerous classical models of alternative life history assume the existence of threshold values of continuous traits, such as body size, and that distinct patterns of life history are adopted depending on whether the trait is above or below the threshold (Gross, 1996; Roff, 1996; Tachiki & Koizumi, 2016; Horita et al., 2018). Underlying these assumptions are physiological processes realizing life history choices. From initially similar states, two distinct internal physiological states are eventually formed. In behavioral endocrinology, the positive feedback between hormone level and behavior (e.g., fighting, aggression) has been considered responsible for the process of forming

distinct types (Wingfield & Wada, 1989; Nelson & Kriegsfeld, 2016). In this study, we provided a simple mathematical model as a candidate representation of this process. We assumed that the hormone level constitutes a key factor in the decision-making and described the competitive interaction between juveniles and the hormone synthesis of each individual. Notably, the distribution of hormone levels could exhibit multiple discrete clusters whereas the body size distribution could remain unimodal (i.e. no distinct clusters). This indicates the possibility of discrete clusters of traits (i.e. alternative tactics) arising from a continuous distribution without a threshold rule, as observed in salmonids (Morita & Nagasawa, 2010) and also in other organisms (Emlen, 1997; Tomkins, 1999).

Forming multiple clusters within the distribution of hormone levels

The distribution of hormone levels exhibited multiple clusters when the winning probability was sensitive to the between-individual difference of hormone levels (i.e., λ_{h} was large but not too large), and when hormonal dynamics processed much more rapidly than the size growth (i.e., α_{h} was much larger than $\alpha_{\mathrm{s}}(1+\gamma)$) (Fig. 4c). After a competitive interaction, the winner synthesizes more androgen and becomes more likely to win in the subsequent fighting. This positive feedback causes the distribution to exhibit multiple peaks. As λ_{h} is larger, the contribution of hormone level to the winning probability is stronger and the difference of winning probability becomes more pronounced than the case with small λ_{h}. A strong positive feedback between victory in fighting and enhanced hormone synthesis expands the difference between individuals

with initial small differences. Hence, the likelihood of forming multiple clusters within the distribution of hormone levels increases.

In Eqs. (3) and (4), the dynamics of hormone level and body size are qualitatively similar, with both exhibiting a positive feedback loop with the behavioral dynamics (i.e., winning probability in fighting). Although alternative tactics are characterized by bimodal or multimodal trait distribution of behavior and physiology (Taborsky et al., 2001), we only observed a bimodal distribution with regard to hormone level (Fig. 4c). This might be explained in terms of the difference in parameter values that mediate the speed of hormone processing dynamics. It is plausible that hormone levels change more quickly than morphology, such as increase in body size (Lindstedt & Calder,1981). If we assumed that the size growth was much faster than the speed of hormonal processing dynamics (although this is unrealistic), the body size distribution became bimodal and the hormonal distribution became unimodal when the winning probability was controlled by the body size more strongly than by hormone level (i.e. $\lambda_{\mathrm{h}} < \lambda_{\mathrm{s}}$) (Fig. S1 in Appendix A). Hence, the multimodal distribution of hormone levels and unimodal distribution of body sizes observed in the wild (Morita & Nagasama, 2010) may be the result of differenced in parameter values.

A larger weighting factor for the process that responds slower (λ_{s} in the case of Fig. 4e) did not contribute to the formation of multiple clusters. Rather, multiple cluster formation was suppressed with larger weighting factor (see Fig. 4e). When the contribution of the body size to the winning probability, λ_{s}, is large, large individuals

become likely to win in the competition, and the importance of hormone level toward winning probability decreases. Hence, an increase in λ_s weakens the feedback between winning probability and hormone synthesis, leading to the disappearance of hormone level dimorphism.

Multiple clusters in the evolutionarily endpoint

In the present study, we evaluated a simple mechanistic model for the formation of multiple clusters of a competitive trait (e.g., hormone level). In some publications, the coexistence of multiple types along the spectrum of competitive ability has been discussed as a result of adaptive evolution. When many types continuously compete among on another, the outcome is typically an evolutionarily stable community consisting of discrete and often finite numbers of types. Sasaki and Ellner (1995) derived this result mathematically in the case where the competition kernel between genotypes constituted a Gaussian function of between-genotypes difference in the trait. An elegant result is their mathematical proof of discreteness (in the sense of exact mathematics) when the competition kernel constitutes an analytic function and the resource distribution is not analytic (such as establishing the truncation in the high and low ends of resource distributions). In the context of community ecology, a similar pattern was found by Pacala and Tilman (1994) who discussed the limiting similarity of coexisting species. Following these seminal papers, diverse examples of coexisting multiple types have been discussed including discrete multiple types of phenology of trees (Kubo and Iwasa, 1996), mutation rate (Haraguchi & Sasaki 2000), and prey-

predator coevolution. In the context of honest signaling of male quality, Johnstone & Grafen (1994) discussed the coexistence of discrete clusters of phenotypes indicating male quality, which answered the puzzle of "typical intensity" of animal signals in the science of animal behavior. The appearance of multiple clusters of hormonal levels in the present study might be regarded an example of this same general principle.

We note that the results of our study show that multiple clusters of hormone levels might automatically emerge as a result of plausible competitive interaction between individuals, in whom no evolutionary adaptation was assumed. This sheds light on an aspect different from that of the numerous theoretical works focusing on adaptive significance. To promote our understanding of the ecological process of alternative tactics, we need to incorporate the studies of molecular mechanisms, such as epigenetic control (Champagne, 2012), gene expression (Martin et al., 2010; Johansson et al., 2016), and their association with social interactions and endocrine systems.

Variability of hormone levels

The coefficient of variation of the hormone level along the time series decreased with the increase in the frequency of encounter q. When q was smaller, the updating of individual status occurs less often and the hormone level fluctuates more strongly. When q was larger, hormone values fluctuated less strongly (Fig. 6b) because individuals could estimate their social rank more accurately (see Tachiki & Koizumi, 2016).

We note that, if the growth rate is small, bimodal size distribution may not be observed before the appearance of matured individuals, and the observed size distribution may have a single peak (Morita and Nagasawa, 2010).

Implications for future studies

We incorporated the hormone level in our model as this can be experimentally measured to predict future behavior. Hormone levels have been evaluated in previous studies (Devlin & Nagahama, 2002; Taves et al, 2009; Munakata, 2012). Nevertheless, it would be very useful if we could estimate how androgen contributes to the aggressiveness of individuals and correlates with the probability of winning.

It would also be very informative to understand how juveniles make contact with each other because considerable behavioral diversity exists among individuals in the same population. In natural situations, individuals may adjust their endocrine system through contacts that may not be clearly observable. It is therefore necessary to record the behavior of individuals and to quantify parameters, such as q and λ_s. For example, Butail et al. (2012) reconstructed the trajectory of flying mosquitoes from video data. The estimation of these parameters in fishes may thus be possible through the development of specialized measuring devices.

In this study, we demonstrated that dimorphism emerges from the interaction between the hormone level and social interaction. Many organisms estimate their own social rank in the population and behave appropriately considering their status (Taves et al., 2009). Both the nervous and endocrine system process social information. For example,

androgen enhances the aggressiveness of behavior, whereas stress hormones (e.g., cortisol) inhibit behavior. Animals are able to estimate the previous experience and predict the future behavior just by measuring their hormone levels. This is likely useful for energetically efficient decision-making, considering the cost of maintaining neural and endocrine systems (Kappeler, 2010). These systems should contribute to understanding of biological phenomena which have discreteness. For instance, some birds have partial migration (Wingfield, 2005). In male elk, variation in ornaments signals male status and is related to androgen level (Bartos & Bubenik, 2011; Bartos et al., 2012). In termites, caste specialization is induced by interaction with other individuals via modification of juvenile hormone titer, and this contributes to the maintenance of colony (Watanabe et al., 2014). In mandrills, there is a clear hierarchy which is formed by behavioral interactions and endocrine systems (Setchell, 2010).

Nevertheless, in natural conditions, the behavior of animals is likely to be more complex than that assumed herein. For example, hormone level may modify the frequency of encounters among individuals; in turn, this effect may induce polymorphism, which should be considered future theoretical studies.

We further showed that the ratio of strategies was not substantively affected by the initial condition and environmental fluctuation (Figs. S2 and S3 in Appendix B). This robustness is caused by the feedback between social interactions and hormone synthesis. Decision-making based on the social interaction contributes to the stability of a population (Tachiki & Koizumi, 2016; Horita et al., *under review*). Thus, clarifying

the relationship between intrinsic states and social interactions along with its ecological consequence is very important for understanding the system.

5. **Conclusion**

Behavior and hormone synthesis affect each other; thus, clarifying the relationship between hormonal level and behavior is very important. The data of endocrine status and behavior of the same individual sampled over time are useful for understanding the mechanism of decision making. Ecological sciences would therefore markedly benefit by incorporating endocrinological mechanisms when considering the factors influencing decision-making in animal behavior.

Acknowledgments

This work was supported by a Research Fellowship for Young Scientists (DC1) from the Japan Society for the Promotion of Science (JSPS) to J.H., by a Grant-in-Aid for JSPS Fellows award (19J21686) to J.H., and by a Grant-in-Aid for Young Scientists award (17K1597, 20K15876), a Grant-in-Aid for Scientific Research (B) award (16H04845), and the Tokyo Metropolitan University strategic research fund to Y.T. We thank A. Hara, S. Iwami, A. Munakata, K. Nagata, K.Noshita,A. Satake, T. Sato, and J. I. Suzuki for their helpful comments. The authors declare no conflicts of interest, financial or otherwise.

References

Arterbery, A. S., Deitcher, D. L., & Bass, A. H. (2010). Corticosteroid receptor expression in a teleost fish that displays alternative male reproductive tactics. *General and comparative endocrinology*, *165*(1), 83-90.

Aubin Horth, N., & Dodson, J. J. (2004). Influence of individual body size and variable thresholds on the incidence of a sneaker male reproductive tactic in Atlantic salmon. *Evolution*, *58*(1), 136-144.

Awata, S., Tsuruta, T., Yada, T., & Iguchi, K. I. (2011). Effects of suspended sediment on cortisol levels in wild and cultured strains of ayu Plecoglossus altivelis. *Aquaculture*, *314*(1-4), 115-121.

Bartos, L., & Bubenik, G. A. (2011). Relationships between rank-related behaviour, antler cycle timing and antler growth in deer: behavioural aspects. *Animal production science*, *51*(4), 303-310.

Bartos, L., Bubenik, G. A., & Kuzmova, E. (2012). Endocrine relationships between rank-related behavior and antler growth in deer. *Frontiers in Bioscience*, *4*, 1111-1126.

Butail, S., Manoukis, N., Diallo, M., Ribeiro, J. M., Lehmann, T., & Paley, D. A. (2012). Reconstructing the flight kinematics of swarming and mating in wild mosquitoes. *Journal of The Royal Society Interface*, *9*(75), 2624-2638.

Champagne, F. A. (2012). Interplay between social experiences and the genome: epigenetic consequences for behavior. In *Advances in genetics* (Vol. 77, pp. 33-57). Academic Press.

Clements, S., & Schreck, C. B. (2004). Central administration of corticotropin-releasing hormone alters downstream movement in an artificial stream in juvenile chinook salmon (Oncorhynchus tshawytscha). *General and comparative endocrinology*, *137*(1), 1-8.

Devlin, R. H., & Nagahama, Y. (2002). Sex determination and sex differentiation in fish: an overview of genetic, physiological, and environmental influences. *Aquaculture*, *208*(3-4), 191-364.

Dodson, J. J., Aubin-Horth, N., Thériault, V., & Páez, D. J. (2013). The evolutionary ecology of alternative migratory tactics in salmonid fishes. *Biological Reviews*, *88*(3), 602-625.

Earley, R. L., Lu, C. K., Lee, I. H., Wong, S. C., & Hsu, Y. (2013). Winner and loser effects are modulated by hormonal states. *Frontiers in zoology*, *10*(1), 6.

Emlen, D. J. (1997). Alternative reproductive tactics and male-dimorphism in the horned beetle Onthophagus acuminatus (Coleoptera: Scarabaeidae). *Behavioral Ecology and Sociobiology*, *41*(5), 335-341.

Esteve, M., McLennan, D. A., & Kawahara, M. (2011). Sexual behaviour of a masu salmon parr, with implications for the evolution of parr sexual behaviour in the salmonines. *Ecology of Freshwater Fish*, *20*(3), 492-494.

Fujioka, Y. (1990). Biwa salmon : its ecological and morphological characteris, *Fish and eggs*, *159*, 25-38. (in Japanese)

Feng, N. Y., & Bass, A. H. (2017). 2.04–Neural, hormonal, and genetic mechanisms of alternative reproductive tactics: vocal fish as model systems. *Hormones, Brain and Behavior.(Third Edition). Academic Press, Oxford*, 47-68.

Fricke, H., & Fricke, S. (1977). Monogamy and sex change by aggressive dominance in coral reef fish. *Nature*, *266*(5605), 830.

Genova, R. M., Marchaterre, M. A., Knapp, R., Fergus, D., & Bass, A. H. (2012). Glucocorticoid and androgen signaling pathways diverge between advertisement calling and non-calling fish. *Hormones and behavior*, *62*(4), 426-432.

Gillespie, D. T. (1977). Exact stochastic simulation of coupled chemical reactions. *The journal of physical chemistry*, *81*(25), 2340-2361.

Gross, M. R. (1996). Alternative reproductive strategies and tactics: diversity within sexes. *Trends in Ecology and Evolution*, *11*(2), 92-98.

Haraguchi, Y., & Sasaki, A. (2000). The evolution of parasite virulence and transmission rate in a spatially structured population. *Journal of Theoretical Biology*, *203*(2), 85-96.

Hirschenhauser, K., & Oliveira, R. F. (2006). Social modulation of androgens in male vertebrates: meta-analyses of the challenge hypothesis. *Animal Behaviour*, *71*(2), 265-277.

Horita, J., Iwasa, Y., & Tachiki, Y. (2018). Evolutionary bistability of life history decision in male masu salmon. *Journal of theoretical biology*, *448*, 104-111.

Johansson, L. H., Timmerhaus, G., Afanasyev, S., Jørgensen, S. M., & Krasnov, A. (2016). Smoltification and seawater transfer of Atlantic salmon (Salmo salar L.) is

associated with systemic repression of the immune transcriptome. *Fish & shellfish immunology*, *58*, 33-41.

Johnstone, R.A., & Grafen, A. (1994) Dishonesty and the handicap principle. *Anim. Behav.* 46: 759-764.

Kappeler, P. (ed.) (2010). "*Animal behaviour: evolution and mechanisms*." Springer Science & Business Media.

Kiso, K., & Matsumiya, Y. (1992). Growth of fluviatile form masu salmon Oncorhynchus masou in southern Sanriku district, Honshu, Japan. *Bulletin of the Japanese Society of Scientific Fisheries (Japan)*.

Kubo, T. & Iwasa, Y. (1996). Phenological pattern of tree regeneration in a model for forest species diversity. *Theoretical Population Biology* **49**:90-117

Kuwamura, T., & Nakashima, Y. (1998). New aspects of sex change among reef fishes: recent studies in Japan. *Environmental Biology of Fishes*, *52*(1-3), 125-135.

Li, C. Y., Earley, R. L., Huang, S. P., & Hsu, Y. (2014). Fighting experience alters brain androgen receptor expression dependent on testosterone status. *Proceedings of the Royal Society B: Biological Sciences*, *281*(1796), 20141532.

Lindstedt, S. L., & Calder III, W. A. (1981). Body size, physiological time, and longevity of homeothermic animals. *The Quarterly Review of Biology*, *56*(1), 1-16.

Lorenzi, V., Earley, R. L., & Grober, M. S. (2012). Differential responses of brain, gonad and muscle steroid levels to changes in social status and sex in a sequential and bidirectional hermaphroditic fish. *PLoS One*, *7*(12), e51158.

Martin, S. A., Douglas, A., Houlihan, D. F., & Secombes, C. J. (2010). Starvation alters the liver transcriptome of the innate immune response in Atlantic salmon (Salmo salar). *BMC genomics*, *11*(1), 418.

Miner, B. G., Sultan, S. E., Morgan, S. G., Padilla, D. K., & Relyea, R. A. (2005). Ecological consequences of phenotypic plasticity. *Trends in ecology & evolution*, *20*(12), 685-692.

Morisita, M. (1971). Composition of the Iδ-index. *Population Ecology*, *13*(1), 1-27.

Morita, K., & Nagasawa, T. (2010). Latitudinal variation in the growth and maturation of masu salmon (Oncorhynchus masou) parr. *Canadian Journal of Fisheries and Aquatic Sciences*, *67*(6), 955-965.

Morita, K., Tamate, T., Kuroki, M., & Nagasawa, T. (2014). Temperature-dependent variation in alternative migratory tactics and its implications for fitness and population dynamics in a salmonid fish. *Journal of Animal Ecology*, *83*(6), 1268-1278.

Munakata, A. (2012). *Migratory behaviors in masu salmon (Oncorhynchus masou) and the influence of endocrinological factors*. Terrapub.

Munakata, A., Amano, M., Ikuta, K., Kitamura, S., & Aida, K. (2001). The involvement of sex steroid hormones in downstream and upstream migratory behavior of masu salmon. *Comparative Biochemistry and Physiology Part B: Biochemistry and Molecular Biology*, *129*(2-3), 661-669.

Munday, P. L., Buston, P. M., & Warner, R. R. (2006). Diversity and flexibility of sex-change strategies in animals. *Trends in Ecology & Evolution*, *21*(2), 89-95.

Nakano, S. (1995). Individual differences in resource use, growth and emigration under the influence of a dominance hierarchy in fluvial red-spotted masu salmon in a natural habitat. *Journal of Animal Ecology*, 75-84.

Nelson, R.J., & Kriegsfeld, L.J. (2016). An introduction to behavioral endocrinology(5th ed.), Sinauer, Sunderland.

Ojima, D., & Iwata, M. (2010). Central administration of growth hormone-releasing hormone and corticotropin-releasing hormone stimulate downstream movement and thyroxine secretion in fall-smolting coho salmon (Oncorhynchus kisutch). *General and comparative endocrinology*, *168*(1), 82-87.

Oliveira, R. F. (2009). Social behavior in context: hormonal modulation of behavioral plasticity and social competence. *Integrative and Comparative Biology*, *49*(4), 423-440.

Pacala, S. W., & Tilman, D. (1994). Limiting similarity in mechanistic and spatial models of plant competition in heterogeneous environments. *The American Naturalist*, *143*(2), 222-257.

Perry, A. N., & Grober, M. S. (2003). A model for social control of sex change: interactions of behavior, neuropeptides, glucocorticoids, and sex steroids. *Hormones and Behavior*, *43*(1), 31-38.

Piché, J., Hutchings, J. A., & Blanchard, W. (2008). Genetic variation in threshold reaction norms for alternative reproductive tactics in male Atlantic salmon, Salmo salar. *Proceedings of the Royal Society of London B: Biological Sciences*, *275*(1642), 1571-1575.

Roff, D.A. (1996). Evolution of threshold trait in animals. *Q. Rev. Biol.* 71: 3-35.

Sasaki, A., & Ellner, S. (1995). The evolutionarily stable phenotype distribution in a random environment. *Evolution*, *49*(2), 337-350.

Setchell, J. M., Smith, T., Wickings, E. J., & Knapp, L. A. (2010). Stress, social behaviour, and secondary sexual traits in a male primate. *Hormones and Behavior*, *58*(5), 720-728.

Sinervo, B., Miles. D.B., Frankino, W.A., Klukowski, M., & DeNardo, D.F. (2000). Testosterone, endurance, and Darwinian fitness: natural and sexual selection on the physiological bases of alternative male behaviors in side-blotched lizards. Horm Behav. 2000 38:222-233.

Snover, M. L., Watters, G. M., & Mangel, M. (2005). Interacting effects of behavior and oceanography on growth in salmonids with examples for coho salmon (Oncorhynchus kisutch). *Canadian Journal of Fisheries and Aquatic Sciences*, *62*(6), 1219-1230.

Taborsky, M., Oliveira, R. F., & Brockmann, H. J. (2008). The evolution of alternative reproductive tactics: concepts and questions. *Alternative reproductive tactics: an integrative approach*, *1*, 21.

Tachiki, Y. and Koizumi, I. (2016). Absolute versus relative assessments of individual status in status-dependent strategies in stochastic environments. *Am Natur* 188: 131-123

Taves, M. D., Desjardins, J. K., Mishra, S., & Balshine, S. (2009). Androgens and dominance: sex-specific patterns in a highly social fish (Neolamprologus pulcher). *General and Comparative Endocrinology*, *161*(2), 202-207.

Tibshirani, R., Walther, G., & Hastie, T. (2001). Estimating the number of clusters in a data set via the gap statistic. *Journal of the Royal Statistical Society: Series B (Statistical Methodology)*, *63*(2), 411-423.

Tomkins, J. L. (1999). Environmental and genetic determinants of the male forceps length dimorphism in the European earwig Forficula auricularia L. *Behavioral Ecology and Sociobiology*, *47*(1-2), 1-8.

von Bertalanffy, L. (1938). A quantitative theory of organic growth (inquiries on growth laws. II). *Human biology*, *10*(2), 181-213.

Warner, R. R., & Robertson, D. R. (1978). Sexual patterns in the labroid fishes of the western Caribbean, I the wrasses (Labridae). *Smithsonian Contributions to Zoology*.

Watanabe, D., Gotoh, H., Miura, T., & Maekawa, K. (2014). Social interactions affecting caste development through physiological actions in termites. *Frontiers in physiology*, *5*, 127.

Wingfield, J.C. & Wada, M. (1989) Changes in plasma levels of testosterone during male-male interactions in the song sparrow *Melospiza melodia*: time course and specificity of response. *Journal of Comparative Physiology A*, 166: 189–194

Wingfield, J. C. (2005). Flexibility in annual cycles of birds: implications for endocrine control mechanisms. *Journal of ornithology*, *146*(4), 291-304.

Appendix A

When hormonal dynamics are much slower than body size growth

In the main text, we focused on cases in which the rate of change in hormonal level is much faster than the growth of body size. Here, we considered the opposite situation in which hormonal level changes much slower than the growth rate of body size. The mathematical model is the same as in the main text but the parameter values are different. Figure S1 illustrates the results in the same manner as in Fig. 4 in the text, but the roles of two weights: λ_{h} and λ_{s} are switched. The mean cluster number of hormonal dynamics is large when λ_{h} is small and when λ_{s} is not excessively large. It can be observed that the distribution of hormonal levels has a single peak whereas that of body sizes tends to have two peaks, as shown in Fig. S1(c).

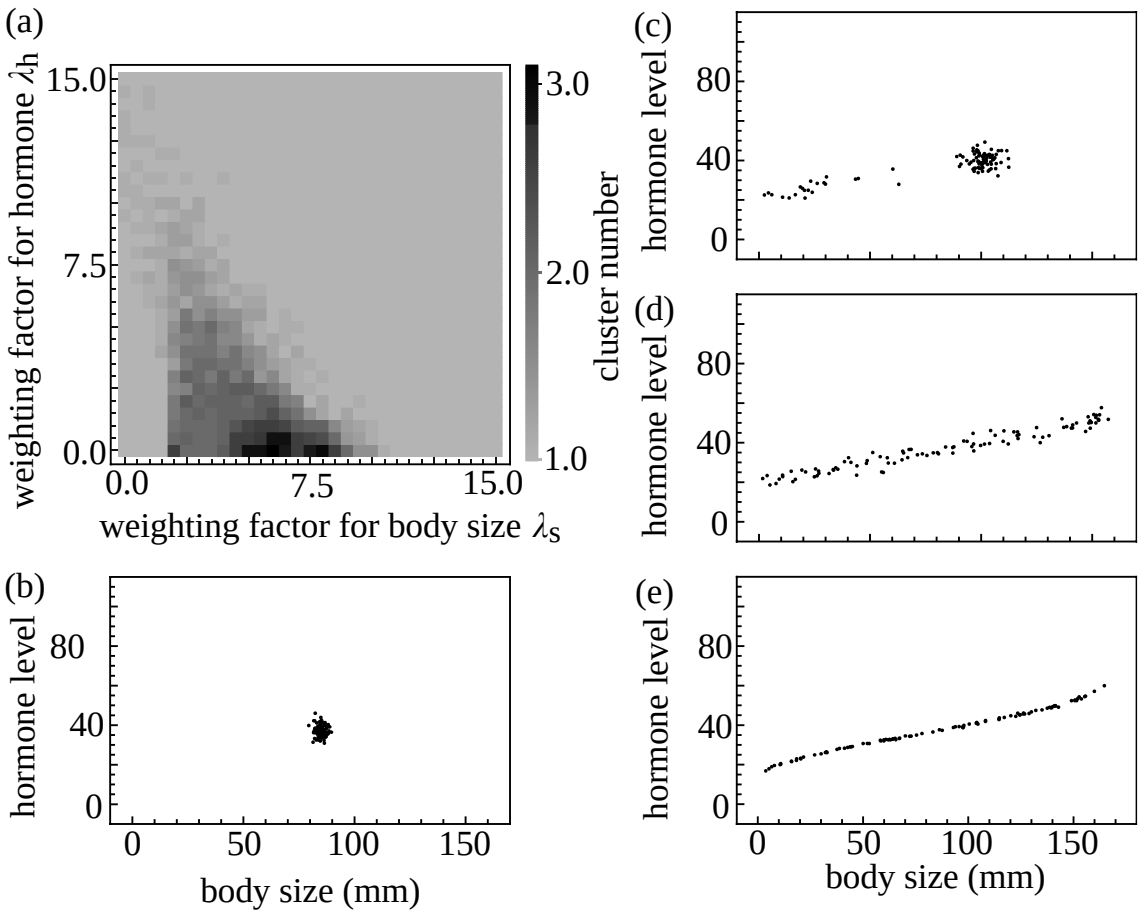

Figure S1:

Parameter dependence of the dynamics when hormone level dynamics are slower than body size growth. (a) Heat map of the mean cluster number. Darker areas indicate the parameter sets representing larger cluster size. I–IV correspond to the outcome of distribution shown in (b)–(e). (b) When both λ_s and λ_h are small, the distribution of body sizes shows a single cluster and the variance is small. Parameters were: $\lambda_s = 0.0$, $\lambda_h = 0.0$. (c) When λ_s is larger, the distribution of hormonal levels exhibits multiple clusters. Parameters were: $\lambda_s = 2.5$, $\lambda_h = 0.0$. (d) When λ_s is very large, a single cluster is again formed, although the variance of body size becomes larger. Parameters were: $\lambda_s = 2.5$, $\lambda_h = 10.0$. (e) When λ_h is large, the variance of body size becomes larger. Parameters were: $\lambda_s = 15.0$, $\lambda_h = 0.0$. Other parameters were: $\alpha_s = 0.5$, $\gamma = 100.0$, $\beta_s = 0.3$ $\alpha_h = 0.3$ $\beta_h = 0.001$, $N = 100$, and $q = 4.0$.

Appendix B

Conditions of initial distribution and size growth

We studied the effect of the initial distribution on outcomes. We focused on the shape and the variance of the distribution of outcomes. First, we formed the initial distribution of the hormone level as a bimodal distribution formed by the sum of two unimodal distributions with three different weights: 10–90, 50–50, and 90–10. Second, we also studied the dependency on the variance of the initial distribution. Third, we simulated the model both under a constant environment and under a fluctuating environment where the growth rate α_{s} was sampled from the normal distribution with the mean $\mu = 0.2$ and the standard deviation $\sigma = 0.04$.

Fig. S3 and S4 illustrate the fraction of the residents among juveniles obtained by the simulations (the mean of 10 replicates). The fraction of the residents was affected neither by the different weights of the two unimodal distributions nor by the standard deviation of the initial distribution of the hormone level (Fig. S3). Under the fluctuating environment, the outcome of the individuals among the residents was the same as that under the constant environment (Fig. S4).

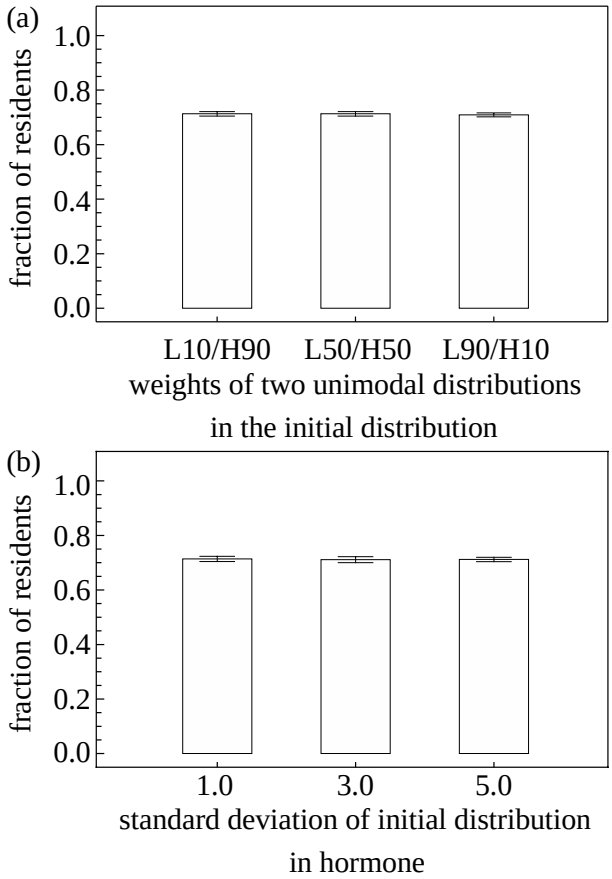

Figure S2:

Dependence of the fraction of residents among juveniles on the initial distribution of hormonal levels. Bar chart and error bar (SD) calculated using 10 replicates for each parameter set. (a) Results when the initial distribution of the hormone level was formed from the sum of two unimodal distributions. L10/H90 indicates the distribution constructed using 10 individuals who had low hormone levels and 90 having high hormone levels. L50/H50 and L90/H10 were derived in a similar manner. The fraction of residents was independent of the initial situation. Parameters were: $\alpha_{\mathrm{s}} = 0.3$, $\gamma = 0.3$, $\beta_{\mathrm{s}} = 0.001$ $\alpha_{\mathrm{h}} = 100.0$ $\beta_{\mathrm{h}} = 0.3$, $N = 100$, $q = 4.0$. $\lambda_{\mathrm{h}} = 3.0$, $\lambda_{\mathrm{s}} = 0.1$, $\mu_{11} = 60.0, \sigma_{11} = 3.0, \mu_{12} = 30.0, \sigma_{12} = 3.0, \rho_1 = 0.5, \mu_{21} = 60.0, \sigma_{21} = 3.0, \mu_{22} = 100.0, \sigma_{22} = 3.0$ and $\rho_2 = 0.5$, where, μ_{11} and μ_{21} are the averages of body sizes, μ_{12} and μ_{22} are the averages of hormone levels, σ_{11} and σ_{21} are the standard deviation of the body sizes, σ_{12} and σ_{22} are the standard deviation of hormone levels, and ρ_1 and ρ_2 are correlation coefficients.

(b) The fraction of residents in relation to the standard deviation of the initial distribution

of hormonal level. Parameters were: $\alpha_s = 0.3$, $\gamma = 0.3$, $\beta_s = 0.001$ $\alpha_h = 100.0$ $\beta_h = 0.3$, $N = 100$, $q = 4.0$. $\lambda_h = 3.0$ and $\lambda_s = 0.1$.

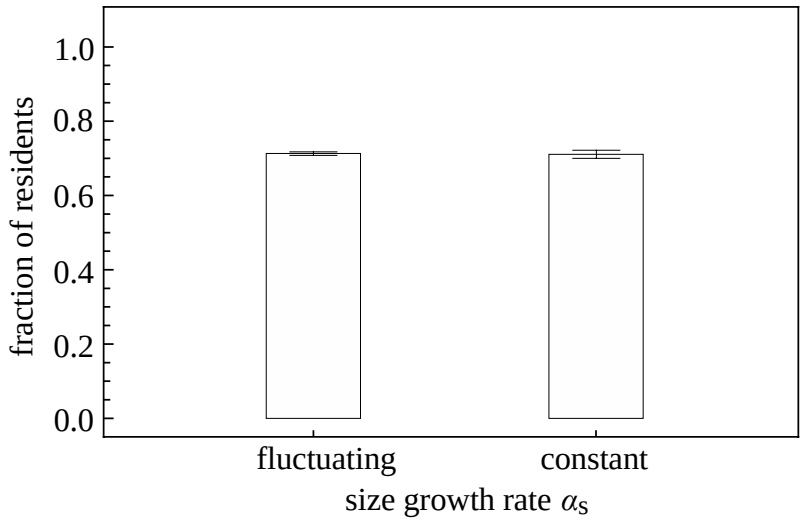

Figure S3:

Fraction of residents among juveniles. We compared the results under constant and fluctuating environments. Bar chart and error bar (SD) were calculated using 10 replicates. Calculations were performed for both a constant (right) and randomly chosen (left) growth rate. The outcome did not change substantively. Parameters were: $\alpha_s = 0.3$, $\gamma = 0.3$, $\beta_s = 0.001$ $\alpha_h = 100.0$ $\beta_h = 0.3$, $N = 100$, $q = 4.0$. $\lambda_h = 3.0$, and $\lambda_s = 0.1$. In the fluctuating environment, α_s was chosen from the normal distribution, for which the mean value is 0.2 and standard deviation is 0.04.

Video

Video 1. Animation of size growth and hormonal dynamics. In the scatterplot, the vertical axis represents size and the horizontal axis represents hormone level. The bottom histogram represents the size distribution and the right histogram represents the distribution of hormone level.

https://www.journals.uchicago.edu/doi/video_original/10.1086/711414/Video1.mp4

Download Original Video (1.5 MB)

Figures

Figure 1 Scheme of the model

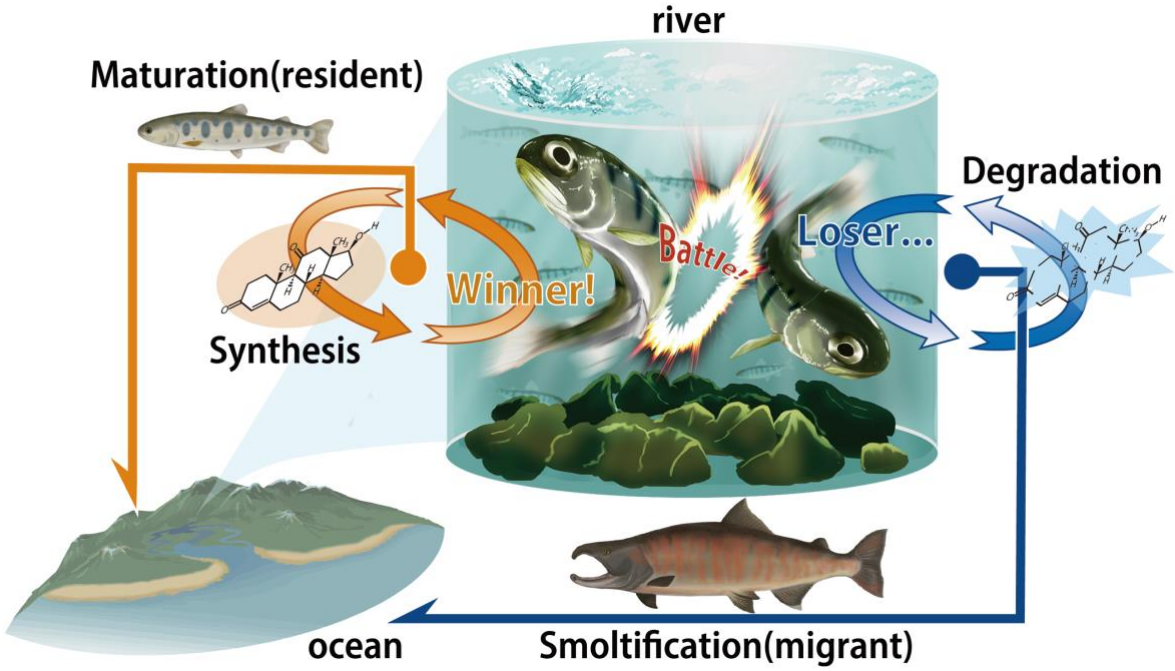

All individuals hatch in the river and make the decision regarding whether they stay in the river or migrate to the sea. Juveniles compete with each other and the winners synthesize more androgen than the losers. Winners become more likely to win in subsequent competitive events because androgen enhances aggressiveness, resulting in two distinct types of juveniles differing markedly in androgen level. As androgen also induces maturation, the juveniles with high androgen levels become residents whereas those with low androgen levels migrate to the sea.

Figure 2 Dynamics of hormone level and body size

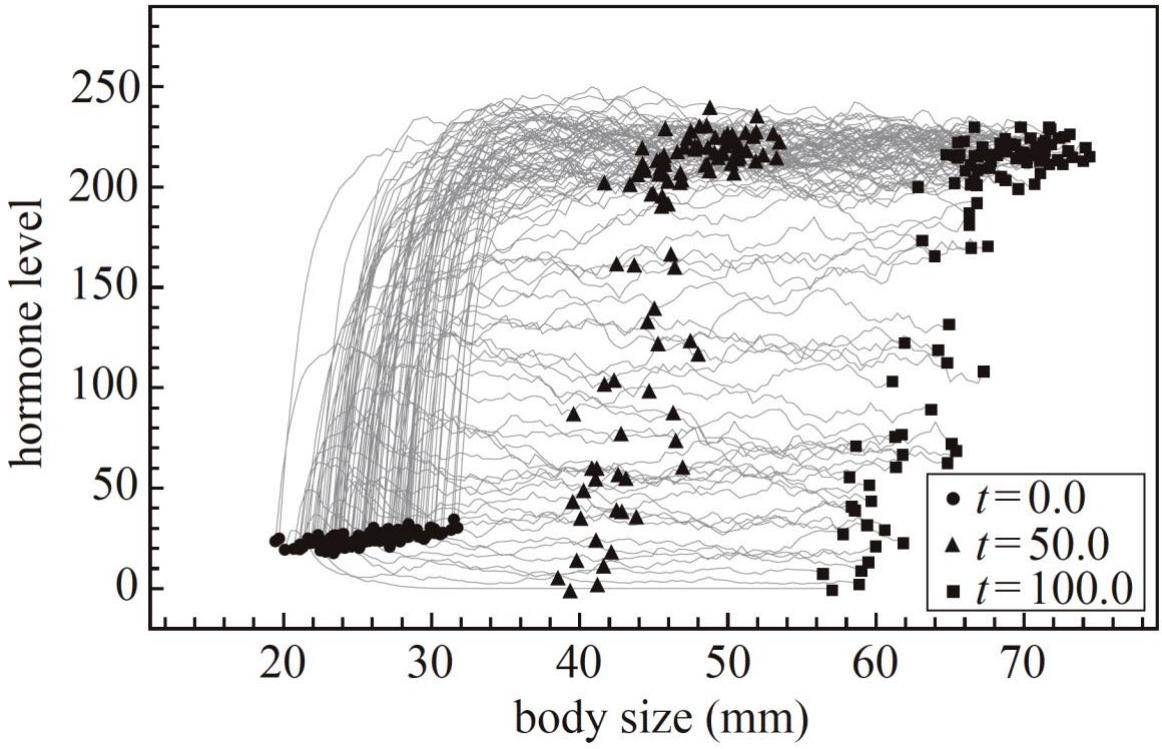

Lines represent the trajectories of individuals. When $t = 0.0$, individuals formed a single cluster (circles). Over time, they become separated into two groups that markedly differ with regard to hormone level (triangles; $t = 50.0$, squares; $t = 100.0$), although their body size distribution remained in a single cluster. Parameters were: $\alpha_{\mathrm{s}} = 0.3$, $\gamma = 0.2$, $\beta_{\mathrm{s}} = 0.001$, $\alpha_{\mathrm{h}} = 100.0$, $\beta_{\mathrm{h}} = 0.3$, $N = 100$, $q = 4.0$. $\lambda_{\mathrm{h}} = 3.0$ and $\lambda_{\mathrm{s}} = 0.0$.

Figure 3 Distributions of hormone levels and body sizes at the end of simulation

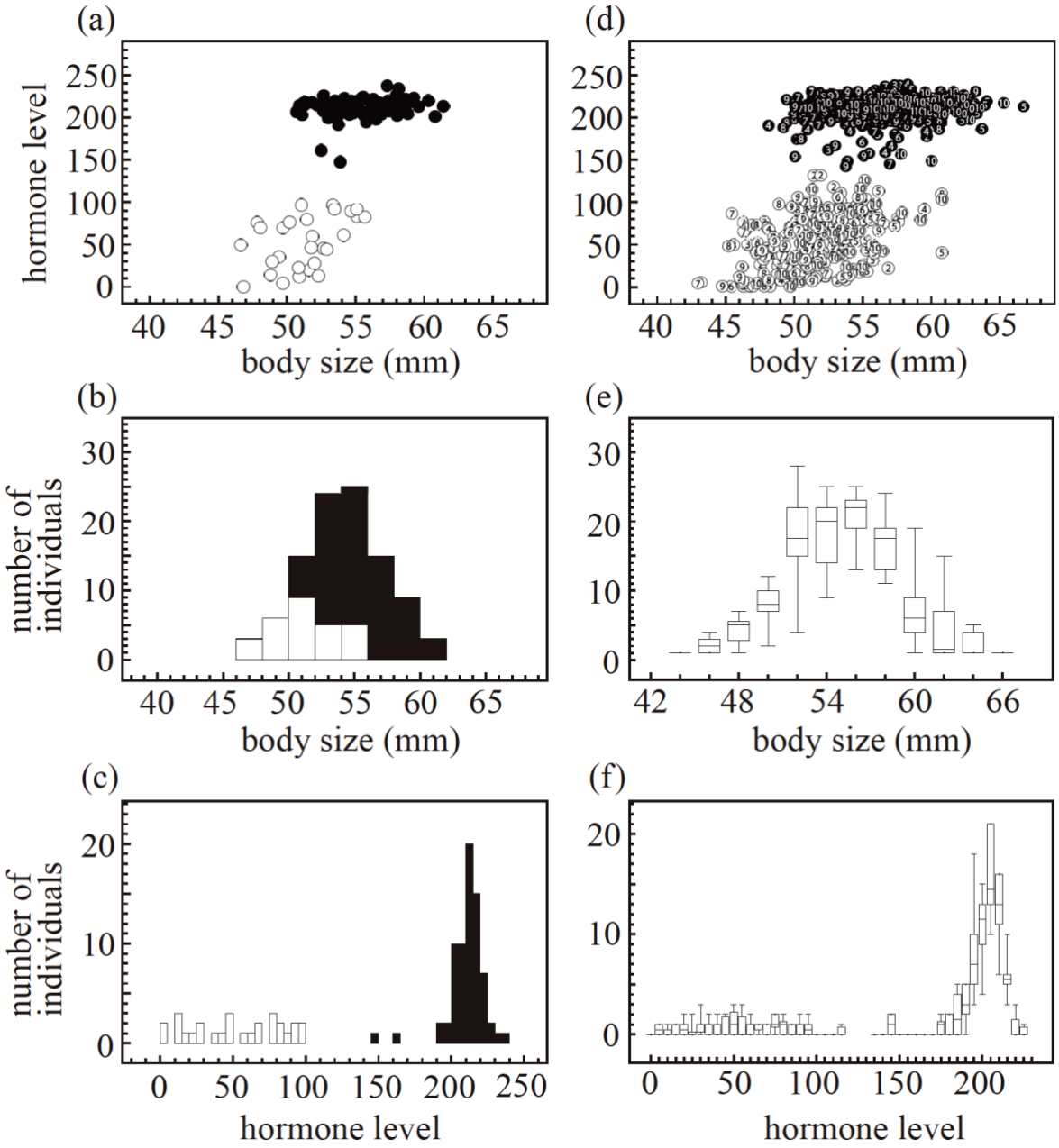

(a) Filled and open circles represent individuals with high and low hormone levels, respectively. Note that circles are separated with regard to hormone levels but body sizes of the two groups overlapped. (b) Number of individuals with different body sizes. Black and white plot bars indicate individuals with high and low hormone levels,

respectively. Individuals with high hormone levels tend to be larger in body size than those with low hormone levels, although their distributions are overlapped. (c) Number of individuals with different hormone levels. Two peaks can be observed, representing higher and lower hormone levels, with the latter being widely distributed. The two clusters are separated at about 130. (d-f) Results from combining 10 replicates of runs. (d) The numbers within each circle distinguish different runs. Filled/open circles represent individuals with high and low hormone levels, respectively. (e) Box-whisker plot of body size. Error bars indicate the standard deviation, and the bars in the boxes indicate median value. Body size distribution in which the results of 10 runs were pooled showed a single peak. (f) Box-whisker plot of hormone level distribution in which the results of 10 runs were pooled. Distribution of hormone level was bimodal. Parameters were: $\alpha_{\mathrm{s}} = 0.3$, $\gamma = 0.2$, $\beta_{\mathrm{s}} = 0.001$, $\alpha_{\mathrm{h}} = 100.0$, $\beta_{\mathrm{h}} = 0.3$, $N = 100$, $q = 4.0$. $\lambda_{\mathrm{h}} = 3.0$, and $\lambda_{\mathrm{s}} = 0.0$.

Figure 4 Parameter dependence of the dynamics

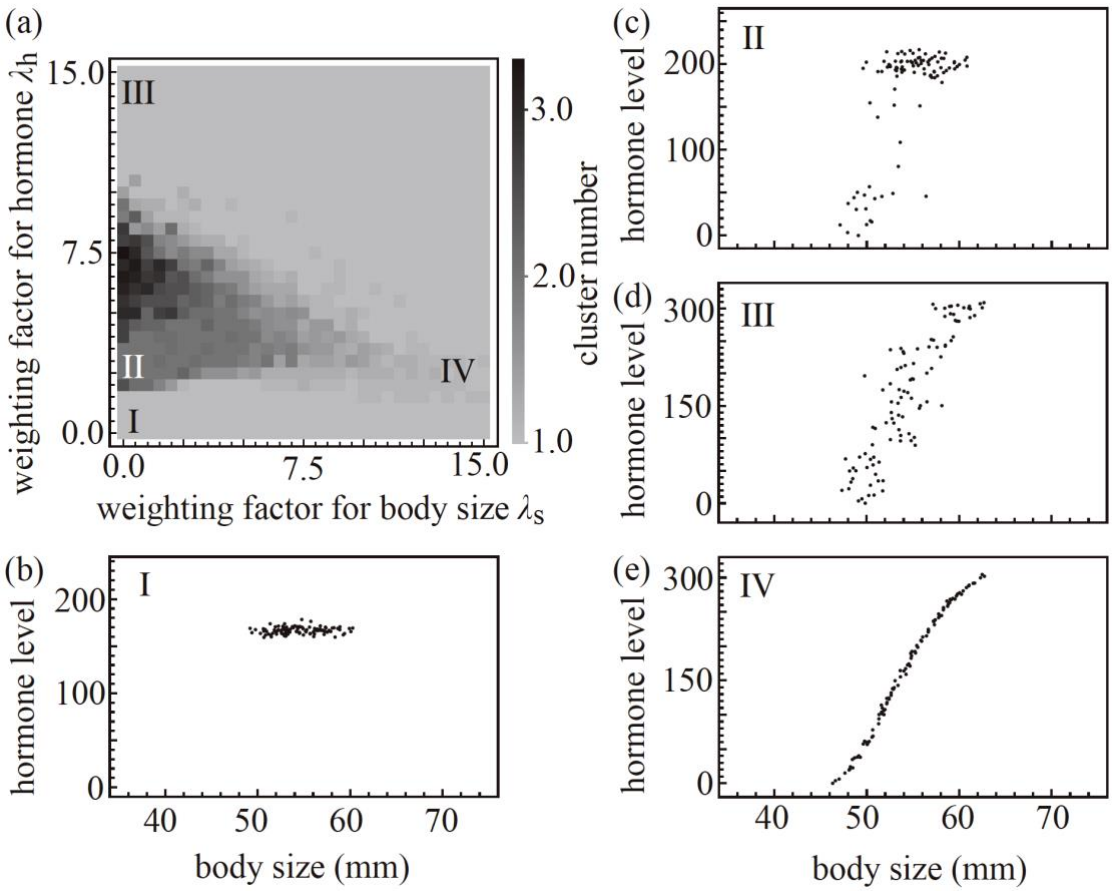

(a) Heat map of the mean cluster number, where darker area indicates a larger mean cluster number of hormonal distribution. Roman numbers I–IV correspond to the situation shown in (b)–(e). (b–e) Distributions of hormonal levels and body sizes in a population. (b) When both λ_s and λ_h are small, the hormonal distribution has a single peak with small variance. Parameters were: $\lambda_h = 0.5$, $\lambda_s = 0.0$. (c) When λ_h is larger, the hormonal distribution exhibits two peaks with multiple clusters. Parameters were: $\lambda_h = 2.5$, $\lambda_s = 0.0$. (d) When λ_h was too large, the hormone level distribution shows a large variance but has a single peak (cluster number is one). The distribution of body sizes also shows a single peak. Parameters were: $\lambda_h = 15.0$, $\lambda_s = 0.0$. (e) When λ_s is large, the

variance of hormone level becomes larger but the cluster number was one. The hormonal levels and body sizes of individuals become strongly correlated. Parameters were: $\lambda_{\mathrm{h}} = 2.5$, $\lambda_{\mathrm{s}} = 15.0$. Other parameters were: $\alpha_{\mathrm{s}} = 0.3$, $\gamma = 0.2$, $\beta_{\mathrm{s}} = 0.001$ $\alpha_{\mathrm{h}} = 100.0$ $\beta_{\mathrm{h}} = 0.3$, $N = 100$, $q = 4.0$.

Figure 5 Fraction of residents among juveniles

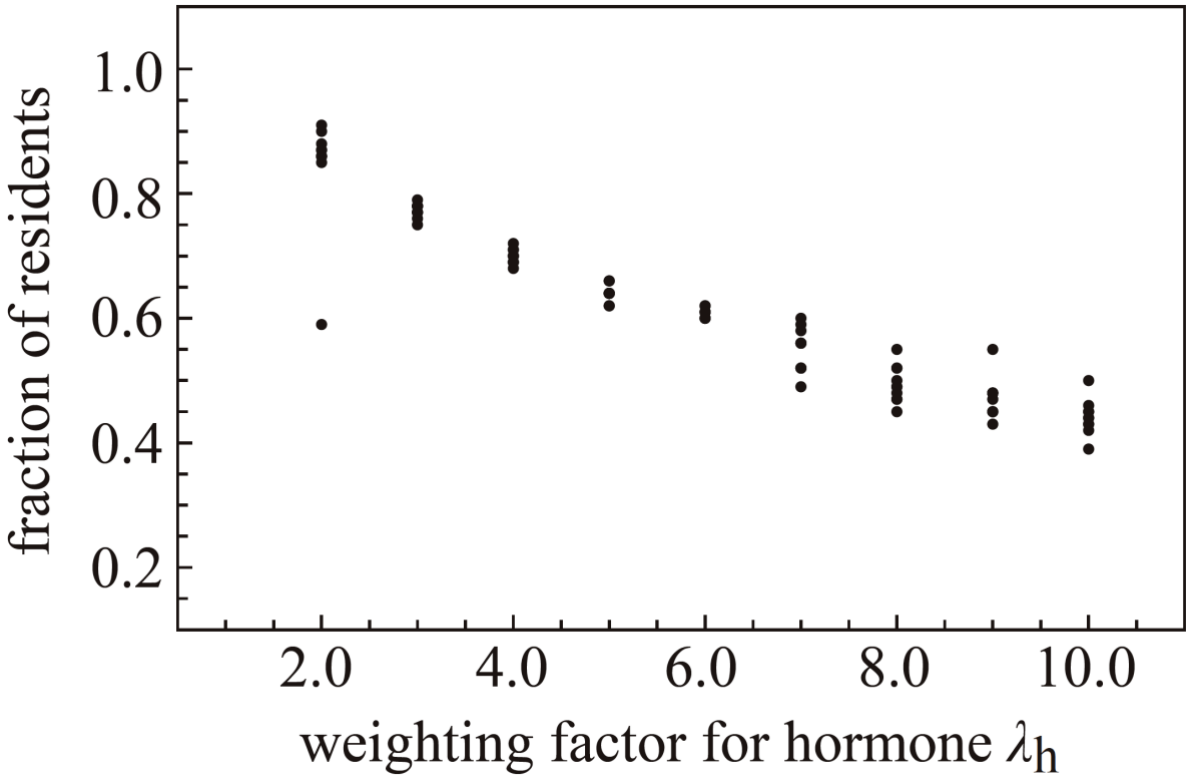

The results of 10 replicates are shown for each parameter value. Parameters were: $\alpha_{\mathrm{s}} = 0.3$, $\gamma = 0.2$, $\beta_{\mathrm{s}} = 0.001$ $\alpha_{\mathrm{h}} = 100.0$ $\beta_{\mathrm{h}} = 0.3$, $N = 100$, $q = 4.0$. $\lambda_{\mathrm{h}} = 3.0$, $\lambda_{\mathrm{s}} = 0.1$.

Figure 6 Tendency of changing rank of individuals over time

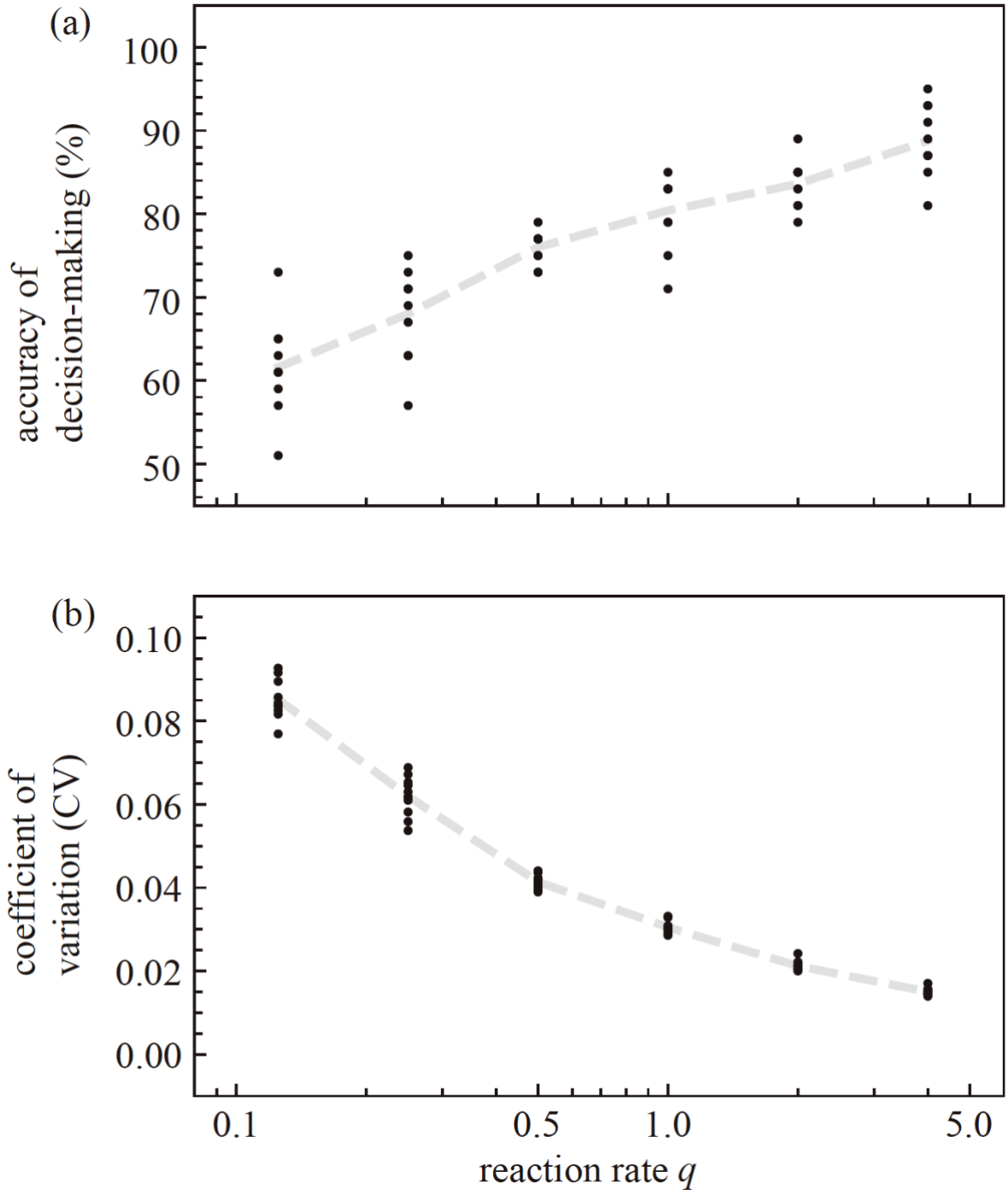

(a) Accuracy of decision making. The results of 10 replicates are shown. (b) Coefficient of variation of hormone level CV. The CV decreased with increasing q. Parameters

were: $\alpha_{\mathrm{s}} = 0.3$, $\gamma = 0.2$, $\beta_{\mathrm{s}} = 0.001$ $\alpha_{\mathrm{h}} = 100.0$ $\beta_{\mathrm{h}} = 0.3$, $N = 100$, $q = 4.0$. $\lambda_{\mathrm{h}} = 3.0$, and $\lambda_{\mathrm{s}} = 0.1$.

Chapter 2 Evolutionary bistability of life history decision in male masu salmon

The study in this chapter, done in collaboration with Dr. Yuuya Tachiki and Dr. Yoh Iwasa, was published in Journal of Theoretical Biology 448: 104-111 in 2018.

Abstract

Within the salmonid species, some male juveniles after spawning in fresh water stream migrate to the ocean and return to their natal streams after maturation, while others stay and mature in the fresh water stream only. Migration is relative to the size of the individuals. This is an evolutionary outcome according to the status-dependent strategy model, which assumes that the juveniles exhibit the optimal tactic based on their status. In this paper, we consider the case in which the density of adult residents suppresses juvenile growth, and explore the dynamics of alternative tactics and the evolution of threshold size. We show that a fraction of the migratory tactic that might converge into a stable state or continue to fluctuate wildly, and that the evolutionary outcome might be evolutionarily bistable, resulting in a clearly different threshold size. In the case of evolutionary bistability, two threshold sizes differ in ecological dynamics either by stable fraction of migratory tactic or showing two-year periodic fluctuation.

Keywords: interference competition, alternative life-history tactics, anadromous fish, status-dependent strategy

1. Introduction

"Alternative life-history tactics" refers to the discontinuous patterns of variation expressed at the same life stage within a population, which is realized by divergent developmental programs (Roff, 1996). For example, some coral fishes change their sexes based on their body size and social rank (Fricke and Fricke 1977; Warner and Robertson 1978; Kuwamura and Nakashima, 1998; Munday et al., 2009), and some insects have two life-histories, one with short or no wings and the other with normal or large wings based on their population density (Kishimoto, 1956; Roff, 1986; Denno et al., 1989; Zera and Denno, 1997).

Several species of salmonids exhibit one of the two alternative life-history tactics that result in polymorphisms at a particular point in life. Some individuals complete their life cycle in freshwater streams (resident tactic), whereas others migrate to the ocean to feed and mature (migratory tactic) (Morita and Nagasawa, 2010; Morita et al., 2014). The coexistence of alternative tactics within a population is often explained by a status-dependent strategy (SDS; Gross, 1996). If multiple tactics are available, and if the fitness of each tactic is a function of the status of the individual (e.g., body size) at a given point in life, each individuals should choose one of tactics which achieves a highest fitness gain. This results in a response to the status at which the tactics change in the individuals based on whether the status is above or below a specific threshold. A general trend observed throughout salmonids is that larger juveniles tend to remain in their natal streams (residents) whereas others undergo feeding migration (Piche et al., 2008). The estimation of demographic parameters and

fitness functions for both resident and migratory tactics revealed that fitness gain through resident tactic is higher than that through migratory tactic when the body size when juvenile is larger than the specific threshold size (Morita et al., 2014).

In salmonids, body size, measured by fork length or body mass, determines whether the fish stays in or leaves its natal stream (Dodson et al., 2013). On the other hand, body size may vary due to several factors, such as interactions among individuals, environmental stochasticity, and climate change. These processes result in a change in the fraction of juvenile salmonids that employ the two tactics. For example, juvenile salmonid growth is suppressed by competing with other individuals in a stream comprising both juveniles and adult residents. The size and number of juveniles decreases with an increase in the density of adult residents (Brown trout: Jenkins et al.,1999; Rainbow trout: Post et al., 1999). Moreover, considering juveniles, Daufresne et al. (2009) suggested that an increase in the water temperature results in a decrease in the body size of aquatic organisms due to their increased metabolic activity, and also decreases the number of residents. These and other factors can cause variations in the juvenile body size. However, the mechanism of these to affect the individual tactics remains unclear.

In this paper, we construct a mathematical model for organisms that exhibit alternative life-history tactics, focusing especially on salmonids. We consider the case in which the density modifies juvenile growth, which then affect the fraction of alternative tactics. When the density of the adult residents is high, juvenile growth is suppressed and more juveniles exhibit the migratory tactic that year, resulting in a decrease in the

density of residents in the subsequent year. If the density of adult residents is reduced, the growth of juveniles is improved and the body size exceeds the threshold for more individuals than those in the case of high density. A larger fraction of juveniles then adopts the resident tactic and the number of residents is high in the subsequent year. This forms a negative feedback loop or "ecological feedback." We demonstrate that this feedback loop can result in unstable population dynamics. In addition, we consider the evolution of threshold size, which occurs within the same time scale as ecological dynamics (i.e., eco-evolutionary dynamics). Due to the nonlinearity caused by the ecological feedback, the system may exhibit evolutionary bistability, in which the evolutionary endpoint depends on the initial value of threshold size. In this case, the two evolutionary outcomes differ significantly in the population dynamics: one shows a stable equilibrium and the other shows large-amplitude oscillation. This suggests that the dynamical behavior of the population can differ among the local populations or between closely related species, and that the population dynamics may reveal a sudden big change as the parameter of the model gradually changes due to climate change.

2. Model for Life-History Characteristics

We develop a mathematical model for the life-history of masu salmon (*Oncorhynchus masou*). Masu salmon shows remarkable alternative migratory tactics and has a relatively simple life cycle compared with other salmonids. Most of demographic parameters had already been estimated (Morita et al. 2014). Only males show dimorphism within a population, whereas all females undergo feeding migration

(Dodson et al., 2013). Some males complete their entire life cycle in freshwater streams (residents), whereas others migrate to the ocean (migrants; Fig. 1). Residents can start reproducing in the year they hatch and survive and further reproduce for multiple years (iteroparity). In contrast, migrants mature in the ocean, reproduce after returning to their natal stream at the age of 2+ years, and then die (semelparity). Large juveniles tend to be residents (Piche et al., 2008), which was considered as the optimal tactic according to the status-dependent strategy model of this species (Morita et al., 2014).

In this paper, we focus on the fraction of males who go to the sea and return to the spawning site versus those who stay in the stream. Since all the females have the same life history and no environmental fluctuation is considered, the total number of juveniles is the same between years.

2.1. Juvenile tactics

We assume for this model that the body size x of each juvenile when the tactic is exhibited, follows normal distribution in which the mean and standard deviation are μ_t and σ, respectively:

$$\hat{p}_t(x, \mu_t) = \frac{1}{\sqrt{2\pi}\sigma} \exp\left(-\frac{(x-\mu_t)^2}{2\sigma^2} \right). \quad (1)$$

Mean body size μ_t can vary over the years because it is affected by competition for food and space with other river residents, as explained further. In this paper, we focus on the dynamics of the males who exhibit two life-history tactics, because all females are migrants.

We assume that a juvenile becomes a resident if its body size x is larger than a threshold x_{T}, and a migrant if x is smaller than x_{T}. We denote the total number of new born individuals be N. The density of stream residents in year t, denoted by D_t, is obtained by integrating the size distribution Equation (1) multiplied by N with respect to size x. We have:

$$D_t = \sum_{\tau=1}^{\infty} S_{\mathrm{R}}{}^{\tau} N \int_{x_{\mathrm{T}}}^{\infty} \hat{p}_t(x, \mu_{t-\tau})\, dx. \quad (2)$$

In Equation (2), S_{R} represents annual survivorship.

2.2 Growth suppression

We consider that the growth rate of juveniles depends on the density of the residents, where juvenile body size decreases with the density of the residents (Brown trout: Jenkins et.al., 1999;Rainbow trout: Post et al., 1999). A high density of residents suppresses the growth of juveniles and small juveniles become migrants, leading to a reduced number of juveniles remaining in the stream. This then results in a smaller biomass of residents in the following year. This negative feedback loop might lead to a greatly fluctuating population size in the stream. To explore this possibility, we here consider the following equation for the mean size of juveniles as a decreasing function of the resident density:

$$\mu_t = \mu_0 + \mu_1 \mathrm{erf}\,[k(\theta - D_t)]. \quad (3)$$

The average body size of juveniles in year t. μ_t converges to $\mu_0 + \mu_1 \mathrm{erf}\,(k\theta)$when the density of the residents is very small, and to $\mu_0 - \mu_1$when it is very large. θ represents the population density that is equal to the mean $\mu_t = \mu_0$. k determines the

slope of the function, which we designate as the "strength of ecological feedback."

Because μ_t in Equation (3) is a function of the density of residents, the size distribution of juveniles in year *t* is given by $p_t(x, D_t) = \hat{p}_t\big(x, \mu_t(D_t)\big)$ as a function of D_t.

The residents in a subsequent year comprise the resident juveniles of the current year who remain in the stream plus residents in the current year. Then:

$$D_{t+1} = S_{\mathrm{R}} N \int_{x_{\mathrm{T}}}^{\infty} p_t(x, D_t)\, dx + S_{\mathrm{R}} D_t, \tag{4}$$

where $S_{\mathrm{R}} N \int_{x_{\mathrm{T}}}^{\infty} p_t(x, D_t)\, dx$ indicates the contribution by the juveniles of the present year who remain in the stream, and $S_{\mathrm{R}} D_t$ represents the residents in the present year. Equation (4) indicates that the density of residents in year $t + 1$ can be calculated only from the density in year *t*. When the dynamics reach equilibrium, then

$$D^* = S_{\mathrm{R}} N \int_{x_{\mathrm{T}}}^{\infty} p_t(x, D^*)\, dx + S_{\mathrm{R}} D^* \ , \tag{5}$$

is satisfied, where D^* is the equilibrium density. Notably, the equilibrium density, even if it exists, might be unstable.

2.3 Fluctuating size distribution

We explored the stability of ecological dynamics. Figure 2(a) illustrates the bifurcation of the system. The horizontal and vertical axes represent the strength of feedback k and the fraction of residents D_t, respectively. When $k < 0.82$, the fraction of residents has reached a stable equilibrium; if not, the equilibrium has fluctuated. When $0.82 < k < 1.90$, the system reveals fluctuation within a period of 2 years. For the intermediate

values of k(~$2.2 < k < 3.0$), the system reveals chaotic fluctuation. When k increases substantially, the fraction of the residents fluctuates within a period of 3 years. We analytically derived the condition that the dynamics of μ_t becomes locally stable as follows:

$$\left| S_{\mathrm{R}} \left\{ 1 - \frac{\sqrt{2} S_{\mathrm{R}} k \mu_1}{\pi \sigma} \exp\left[-\left(\frac{x_{\mathrm{T}} - \mu^*}{\sqrt{2}\sigma} \right)^2 - k^2 (\theta - D^*)^2 \right] \right\} \right| < 1 \ . \tag{6}$$

The derivation is explained in Appendix A. This indicates that as the difference between x_{T} and μ^* becomes larger, the system becomes more stable (Fig. 2b), and the system becomes unstable with increasing S_{R} and μ_1. From Equation 6, we created Figure 2(b), in which the horizontal and vertical axes represent the strength of feedback k and the threshold x_{T}, respectively. The area assigned I indicates stability of the system, whereas other areas indicate its instability. The system becomes stable in region I, whereas it becomes unstable in the other regions (for details, see Fig. 2).

3. Evolution of Threshold Size

We consider the evolution of threshold trait x_{T}, which is expressed only in males. We adopted the fitness function formalized by Tachiki and Koizumi (2016), in which fitness of a male is defined as lifetime siring success for each tactic. Notably, the population growth is independent of the threshold trait and population size does not change because all females are migrants. In contrast, the evolutionary change in the threshold trait might affect the fraction of males who exhibit an alternative life-history.

A spawning group of masu salmon consists of a single female and several males comprising both migrants and residents (Watanabe et al., 2008). Migrant males attack resident males, whereas resident males adopt a sneaking tactic (Koseki and Maekawa, 2000; Watanabe et al., 2008). Sneaker males attack each other, resulting in a dominance hierarchy among residents (Koseki and Maekawa, 2000).

In this model, we assumed that the number of new born individuals *N* is constant and the population size is not change.

3.1 Competitive ability

Because of the interference competition among the residents, the competitive ability of resident males with body size *x* is a decreasing function of the density of resident males larger than *x*. We assume that the competitive ability of a male with size *x* is as follows:

$$C_t(x|x_{\mathrm{T}}) = c_0 \exp\left[-c_1 \int_x^{\infty} n_{\mathrm{R},t}(y|x_{\mathrm{T}})\, dy\right] \quad (7),$$

where c_0 is the relative competitive ability of the strongest resident toward a migrant, and c_1 is a constant that mediates the strength of the interference competition among the residents. $n_{\mathrm{R},t}(y)$ is the size distribution of the residents and its calculations are explained in Appendix B. Equation (7) could be interpreted as the product of c_0 and the probability that an individual with size *x* does not encounter larger individuals in the same spawning group. The number of spawning females and eggs produced do not change between the years because all females are migrants and the sex ratio and survivorship are constant. The migrants return to their natal stream after feeding and maturing in the ocean. Miyakoshi and Saitoh (2011) reported that the adult size and

ocean survival of masu salmon are independent of their size at smoltification. We assume here that the competitive ability of a migrant can be expressed as the product of a constant survivorship S_{M} and the size-independent competitive ability of the migrant, which is normalized to 1. We derived the fitness of masu salmon according to the aforementioned description. Let N be the number of juveniles at the timing of decision making, which is the product of the number of females fertilized in year $t-1$, number of eggs per female, sex ratio, and survivorship of juveniles from hatching to exhibiting the tactic. We consider mate competition among males in a spawning season.

The fitness of a mutant male with threshold size x'_{T} in a population dominated by males with threshold size x_{T} is given as follows (Tachiki and Koizumi, 2016):

$$W(x'_{\mathrm{T}}|x_{\mathrm{T}}) = K\left\{S_{\mathrm{M}}\int_0^{x'_{\mathrm{T}}} p_{t-2}(x, D_{t-2})dx + \int_{x'_{\mathrm{T}}}^{\infty}\sum_{\tau=0}^{\infty} S_{\mathrm{R}}{}^{\tau} C_t(x+\tau\Delta l|x_{\mathrm{T}})\, p_{t-\tau}(x, D_{t-\tau})dx\right\}, \quad (8)$$

where K might depend on x_{T} but is independent of x'_{T}. $S_{\mathrm{M}}\int_0^{x_T} p(x, D_{t-2})dx$ is the reproductive success as migrants. The survivorship (S_{M}) is multiplied by the probability that a juvenile migrates to the ocean. The annual increment in body size, measured in terms of fork length, is assumed to be constant Δl, which is an assumption commonly adopted in fishery sciences and used in a study by Tachiki and Koizumi (2016). Notably, the mating success of migrants when they safely return to their natal stream is normalized as unity.

$\int_{x_{\mathrm{T}}}^{\infty}\sum_{\tau=0}^{\infty} S_{\mathrm{R}}{}^{\tau} C(x+\tau\Delta l|x_{\mathrm{T}})\}p(x, D_{t-2})dx$ is the contribution as residents. The

residents can survive for multiple years with an annual survivorship of S_{R}. It is the product of survivorship during τ years and competitive ability summed over the years and averaged with the probability distribution.

Here, we adopt the evolutionary dynamics as follows:

$$x_{\mathrm{T}_{t+1}} = x_{\mathrm{T}_t} + \Lambda \frac{\partial \ln W}{\partial x'_{\mathrm{T}}}\bigg|_{x'_{\mathrm{T}}=x_{\mathrm{T}}}, \qquad ,(9)$$

where the derivative is evaluated at $x'_{\mathrm{T}} = x_{\mathrm{T}}$. Λ is equal to the additive genetic variance (Iwasa et al., 1991) and mediates the speed of evolution. Noting that the fitness is equal to 1 at $x'_{\mathrm{T}} = x_{\mathrm{T}}$, Equation (9) becomes $\Delta x_{\mathrm{T}_t} = \Lambda\, \partial \ln W / \partial\, x'_{\mathrm{T}}|_{x'_{\mathrm{T}}=x_{\mathrm{T}}}$, which has been proposed based on intuitive arguments (e.g., Brown and Vincent, 1987; Rosenzweig, 1987) or on the adaptive dynamics argument (Dieckmann and Law, 1996). Using Equations (8) and (9), we numerically tested the stability of eco-evolutionary dynamics in this system.

4. Outcome of Eco-Evolutionary Dynamics

Figure 3 illustrates the evolution of the threshold trait x_{T}, beginning with eight different initial values. In Figure 3(A), starting from different initial values, the threshold size x_{T} converged to the same value, although the time required for the convergence might differ according to the initial conditions. In contrast, Figure 3(B) presents the case in which the trajectories converged into two final values. This is the case in which the evolutionary endpoint depends on the initial value.

Figure 4(A) illustrates the threshold size x_{T} at the end of the evolutionary changes for different values of the strength of feedback *k*, which is indicated on the

horizontal axis. It represents the last 100 out of 100,000 time steps of eco-evolutionary dynamics. The small black points indicate the values when the initial value of x_{T} is 100, and the large gray points indicate those when the initial value of x_{T} is 50.

For $k < 0.26$ and $k > 0.74$, the threshold size evolved into a single value regardless of the initial condition, just as in Figure 3(A). Figure 4(B) illustrates the location of the final values of the evolutionary dynamics of x_{T} and the population dynamics of the density of the residents *D*. Both values converged into a single value. We designate this as "Type I" (see below).

Figure 4(A) reveals that, for $0.26 \leq k \leq 0.74$, there are two different values of x_{T} in the evolution. These appear as two curves in Figure 4(A), both of which are stable. This represents the evolutionary bistability, in which the threshold size evolved into one of the two values, depending on the initial value. The dynamics are similar to that illustrated in Figure 3(B). Figure 4(C) illustrates the evolutionary dynamics of x_{T} and the population dynamics of the density of the residents *D*. Herein, there are two evolutionarily stable values of x_{T}, which are the same as those illustrated in Figure 4(A). In the case illustrated in Figure 4(C), one of the two evolutionarily stable threshold sizes $(x_{\mathrm{T}} = 35.48)$ corresponds to the stable equilibrium of D $(D = 4.64)$, and the other stable threshold size $(x_{\mathrm{T}} = 73.70)$ corresponds to a fluctuating D within a period of 2 years ($D = 0.43$ and $D = 4.90$), which are indicated by two solid circles connected by arrows. We designate this as "Type III" (see below).

Between these two types, there is one value, $x_{\mathrm{T}} = 63.50$, that represents another evolutionarily unstable equilibrium. Even if we started from an initial value

relatively close to it, $x_{\mathrm{T}} = 63.50$ evolved and deviated from it; hence, it is difficult to determine it using direct simulation of the evolutionary process. The value for unstable evolutionary equilibrium can be obtained using the selection gradient method, as explained in Appendix C. If we fix x_{T}, the dynamics of the density of the resident populations fluctuate within a period of 2 years, which are indicated by two crosses in Figure 4(C).

4.1 Three types of outcome of eco-evolutionary dynamics

We can classify the outcome of eco-evolutionary dynamics into the following three types:

1. Type I: Evolution of x_{T} converged into a single value. The ecological dynamics converged into a stable fixed point. In this case, x_{T} evolved into a value that satisfied the following evolutionarily stable strategy (ESS) derived by Tachiki and Koizumi (2016):

$$S_{\mathrm{M}} = \sum_{\tau=0}^{\infty} S_{\mathrm{R}}{}^{\tau} C(x'_{\mathrm{T}} + \Delta l\tau | x'_{\mathrm{T}}). \qquad (10)$$

Type I represents the large *k* and small *k* in Figure 4(A).

2. Type II: Evolutionary dynamics converge into a single equilibrium, which corresponds to the ecological dynamics that continue to fluctuate perpetually within period of two. In this case, the evolutionary outcome of the threshold trait does not satisfy Equation (10). In the case illustrated in Figure 4, there is no parameter corresponding to Type II; however, this will be explained in Figure 5.

3. Type III: The evolutionary dynamics have multiple equilibria that are

simultaneously stable (or, more precise, continuously stable). Type III represents intermediate values of k in Figure 4(A).

As far as we examined over biologically plausible range of parameters, we observed only those types.

4.2. Selection gradient

We can evaluate the selection gradient numerically using the method developed by Tachiki and Iwasa (2012), as explained in Appendix C. Figure 5 illustrates the selection gradient calculated using this method. Horizontal and vertical axes represent the strength of feedback k and the threshold size, respectively. Figure 5(A) supports the results of Figure 4. In Figure 5, the arrows in each panel indicate the direction of the evolution predicted by the selection gradient. The curves for the boundary between different regions are the evolutionary singular points. Solid curves where the negative selection gradient lies above them and the positive selection gradient below them correspond to the set of convergence stable points or attractors. In contrast, dashed curves correspond to the set of repeller, which are unstable.

For $k = 0.2$ (Fig. 4[B]), there is only one evolutionary singularity, which is an attractor. This results in the Type I classification by examining the dynamics of D_t.

In contrast, for $k = 0.4$ (Fig. 4[C]), we have stable equilibrium of $x_{\mathrm{T}} = 35.48$, unstable equilibrium of $x_{\mathrm{T}} = 63.50$, and a second stable equilibrium of $x_{\mathrm{T}} = 73.70$, which correspond to the three values illustrated in Figure 4(C). This corresponds to Type III.

As parameters gradually change, the system reveals a discontinuous change. For example, in Figure 4(A), starting from $k = 0.4$, k increases gradually. An attractor (the stable evolutionary equilibrium) and a repeller (unstable evolutionary equilibrium) fuse when $k = 0.74$ and then disappear when $k > 0.74$ (Fig. 4[A]). This behavior is called "saddle-node bifurcation." Similarly, the saddle-node bifurcation occurred when we tested other parameters, such as survivorship of residents and migrants (Fig. 5B, C).

5. Discussion

In stream ecosystems, as an outcome of competition for food resources, dominance hierarchy (Nakano, 1995) and habitat segregation (Nakano, 1999) have been demonstrated among salmonids. In addition, the resource competition causes a density-dependent suppression of growth (Post et. al., 1999; Jenkins et al., 1999). In this paper, we proposed a new model for the eco-evolutionary dynamics of alternative life-history tactics when juvenile growth is suppressed in a density-dependent manner.

If the growth of juveniles is suppressed by the resident population of adult males, fewer individuals grow larger than the threshold value, which results in reduced abundance of resident adults in the following year. In contrast, a low resident density in a year should allow more juvenile growth, which will tend to stay in the stream and result in an increased abundance of residents in the next year. This causes a large fluctuation in the population size between years, either in a periodic or chaotic manner (Fig. 2).

We then studied the evolution of the threshold size in a system combining the

interference competition with the threshold evolution. For certain parameters, the threshold size evolved into a single value and the population dynamics converged into a stable equilibrium, as in Figure 4(B); for other parameters, however, the threshold body size evolved into one of the two values, both of which were convergence stable. If the threshold converged into one value, the population dynamics also converged into a stable equilibrium; however, if it converged into a second value, the population dynamics fluctuated with large amplitude, as presented in Figure 4(C). This is the case of evolutionary bistability.

We can derive several useful implications from the results of this model. First, the abundance of the resident males who remain in the stream all the year round might fluctuate between years due to the negative feedback caused by the density-dependent juvenile growth coupled with the threshold reaction of the life-history tactics. In a population of masu salmon, all the individuals who stay in the stream are males who exhibit the resident tactic, because all females migrate to the ocean. The population size of the resident males remaining in the stream is easier to trace than that of the females and the migrant males in the ocean. We presume that the model can be tested by a long-term observation of a stream population of masu salmon.

Second, we might be able to trace the number of individuals who return to their natal stream from the ocean (salmon-run). The model indicates that the number of juveniles who remain in the river might fluctuate among years due to ecological feedback (Fig. 2a), even if that the total number of juveniles is constant. This suggests that the number of males who return to their natal stream may fluctuate, but the number

of returning females is constant over the years because all females choose migratory tactic without any life-history decisions. If so, the model proposes an interpretation to the field observation that the number of males who return to their natal stream for breeding fluctuates with a greater magnitude than the number of returning females. However, we admit that it might be difficult to confirm this prediction due to the several processes that modify the abundance of both males and females in the ocean. In addition, the number of individuals who return to their natal stream for breeding is unlikely to reflect the number of juveniles who migrated to the ocean in the previous years; however, it might be worthwhile to test this prediction.

Third, the eco-evolutionary dynamics suggest that there are distinct dynamic behaviors, both of which are stable. Different local populations of masu salmon might exhibit distinct dynamic behavior. For example, consider that populations in different local streams cannot mix with each other, even if they mix during the growing period in the ocean. Then, the number of resident males in one stream might be stable between years, whereas that in the nearby stream might fluctuate wildly between years. The model predicts that the two populations might differ in the threshold size at which the juveniles exhibit either the migratory or resident tactic.

Fourth, any natural populations suffer stochasticity from either environmental fluctuations or a small population size. The results of selection gradient revealed that a saddle-node bifurcation of the evolutionary equilibria occurred when we gradually changed demographic parameters (Fig. 5). This implies that the slight change in the demographic parameter due to environmental stochasticity might result in large change

in the evolutionary consequence of trait value (x_{T}), and hence the resulting ecological dynamics might be changed from stable to oscillating state.

Finally, as the environment gradually changes, for example, global warming, our model predicts that evolutionary bistability will suddenly disappear and then transit into a single globally stable evolutionary equilibrium. This is suggested by the saddle-node bifurcations exhibited in Figures 4(A) and 5(A, B).

In this paper, we assumed that the juveniles become migrants or residents based on whether their body size at a critical age exceeds a threshold value. This is the rule of the "absolute assessment model" by Tachiki and Koizumi (2016). Tachiki and Koizumi also studied a case in which the juveniles become migrants or residents based on their relative size among all juveniles born in that year. This "relative assessment model" produces a distinct behavior—the fractions of residents and migrants are always stable (Tachiki and Koizumi, 2016). To study the effect of the density-dependent growth on the relative assessment rule will be an important future theoretical work as a continuation of the present paper.

Experienced density might affect the alternative life-history tactics, causing an extensive feedback to the population dynamics, which might not be observed only in salmonid fishes but also other organisms such as insect polymorphism (Gross, 1996). For example, in aphids, the density that is experienced by the mother is known to affect whether her offspring are with or without wings (Sutherland, O. R. W.,1969), and in plant hoppers, the density experienced by the juveniles is known to affect whether they develop into adults with long wings or short wings (Kishimoto, 1956). These life-

history decisions should modify the dispersal tactic for individuals and control the local population density, and also influence the population dynamics as a result of the complex interaction with plant (Denno and Peterson, 1995). The experimental studies revealed the existence of tactile stimuli that affect the life-history characteristics, even under conditions in which food abundance is controlled. In this paper, we assumed that juvenile males become migrants or residents based on their size at a critical life stage, which can be affected by a food shortage. Traditionally, the population dynamics and the evolutionary change related to life history have been studied separately. However, in some cases they are very tightly linked and the study of their close interaction need more attention in theoretical and empirical study.

Acknowledgments

This study was conducted in support of JSPS Overseas Research Fellowship, a Grant-in-Aid for Young Scientists No. 17K1597, a Grant-in-Aid for Scientific Research (B) No. 16H04845 to Y.T., and a Grant-in-Aid for Scientific Research (B) No. 15H04423 to Y.I. We would like to thank the following people for their helpful comments: H. Araki, H. Haeno, S. Iwami, Y. Kakizoe, M. Seki, T. Sato, and S. Satoi.

References

Brown, J. S., & Vincent, T. L. (1987). Predator-prey coevolution as an evolutionary game. In *Applications of Control Theory in Ecology* (pp. 83-101). Springer Berlin Heidelberg.

Denno, R. F., Olmstead, K. L., & McCLOUD, E. R. I. C. (1989). Reproductive cost of flight capability: a comparison of life history traits in wing dimorphic planthoppers. *Ecological Entomology*, *14*(1), 31-44.

Denno, R. F., & Peterson, M. A. (1995). Density-dependent dispersal and its consequences for population dynamics. Population dynamics: new approaches and synthesis, 113-130.

Dieckmann, U., & Law, R. (1996). The dynamical theory of coevolution: a derivation from stochastic ecological processes. *Journal of mathematical biology*, *34*(5-6), 579-612.

Dodson, J. J., Aubin-Horth, N., Thériault, V., & Páez, D. J. (2013). The evolutionary ecology of alternative migratory tactics in salmonid fishes. *Biological Reviews*, *88*(3), 602-625.

Fricke, H., & Fricke, S. (1977). Monogamy and se*x* change by aggressive dominance in coral reef fish. *Nature*, *266*(5605), 830-832.

Gross, M. R. (1996). Alternative reproductive strategies and tactics: diversity within sexes. *Trends in Ecology & Evolution*, *11*(2), 92-98.

Iwasa, Y., Pomiankowski, A., & Nee, S. (1991). The evolution of costly mate preferences II. The “handicap” principle. *Evolution*, *45*(6), 1431-1442.

Jenkins, T. M., Diehl, S., Kratz, K. W., & Cooper, S. D. (1999). Effects of population density on individual growth of brown trout in streams. *Ecology*, *80*(3), 941-956.

Kuwamura, T., & Nakashima, Y. (1998). New aspects of sex change among reef fishes: recent studies in Japan. In *Fish biology in Japan: an anthology in honour of Hiroya Kawanabe* (pp. 125-135). Springer Netherlands.

Kishimoto, R. 1956. Effect of crowding during the larval period on the determination of the wing-form of an adult plant-hopper. *Nature*, **176**: 641–642.

Koseki, Y., & Maekawa, K. (2000). Sexual selection on mature male parr of masu salmon (Oncorhynchus masou): does sneaking behavior favor small body size and less-developed sexual characters?. *Behavioral Ecology and Sociobiology*, *48*(3), 211-217.

Miyakoshi, Y., & Saitoh, S. I. (2011). Effects of smolt size and timing of migration on recovery rate of wild masu salmon Oncorhynchus masou. *Fisheries Science*, *77*(6), 939-944.

Morita, K., & Nagasawa, T. (2010). Latitudinal variation in the growth and maturation of masu salmon (Oncorhynchus masou) parr. *Canadian Journal of Fisheries and Aquatic Sciences*, 67(6), 955-965.

Morita, K., Tamate, T., Kuroki, M., & Nagasawa, T. (2014). Temperature-dependent variation in alternative migratory tactics and its implications for fitness and population dynamics in a salmonid fish. *Journal of Animal Ecology*, *83*(6), 1268-1278.

Munday, P. L., Buston, P. M., & Warner, R. R. (2006). Diversity and flexibility of sex-

change strategies in animals. *Trends in Ecology & Evolution*, *21*(2), 89-95.

Piché, J., Hutchings, J. A., & Blanchard, W. (2008). Genetic variation in threshold reaction norms for alternative reproductive tactics in male Atlantic salmon, Salmo salar. *Proceedings of the Royal Society of London B: Biological Sciences*, *275*(1642), 1571-1575.

Post, J. R., Parkinson, E. A., & Johnston, N. T. (1999). Density-dependent processes in structured fish populations: interaction strengths in whole-lake experiments. *Ecological Monographs*, *69*(2), 155-175.

Roff, D. A. (1986). The evolution of wing dimorphism in insects. *Evolution*, *40*(5), 1009-1020.

Roff, D. A. (1996). The evolution of threshold traits in animals. *The Quarterly Review of Biology*, *71*(1), 3-35.

Rosenzweig, M. L. (1987). Habitat selection as a source of biological diversity. *Evolutionary Ecology*, *1*(4), 315-330.

Sutherland, O. R. W. (1969). The role of crowding in the production of winged forms by two strains of the pea aphid, Acyrthosiphon pisum. *Journal of Insect Physiology*, *15*(8), 1385-1410.

Tachiki, Y., & Iwasa, Y. (2012). Evolutionary jumping and breakthrough in tree masting evolution. *Theoretical population biology*, *81*(1), 20-31.

Tachiki, Y., & Koizumi, I. (2016). Absolute versus Relative Assessments of Individual Status in Status-Dependent Strategies in Stochastic Environments. The American Naturalist, 188(1), 113-123.

Warner, R. R., & Robertson, D. R. (1978). Sexual Patterns in the Labroicl Fishes of the Western Caribbean, I: The Wrasses (Labridae). *Smithsonian Contributions to Zoology*, *254*, 1-27.

Watanabe, M., Takamura, S., & Maekawa, K. (2008). Effects of timing of nest entry and body size on the fertilization success of alternative male reproductive phenotypes of masu salmon (Oncorhynchus masou). *Canadian Journal of Zoology*, *86*(10), 1121-1130.

Zera, A. J., & Denno, R. F. (1997). Physiology and ecology of dispersal polymorphism in insects. *Annual review of entomology*, *42*(1), 207-230.

Appendix A

Stability of the population dynamics of residents

We consider a small deviation of D_t from D^* in Equation (5). We replace $D_t = D^* + \Delta D_t$, in Equation (5), then

$$D^* + \Delta D_{t+1} = S_{\mathrm{R}} N \int_{x_{\mathrm{T}}}^{\infty} p_t(x, D^* + \Delta D_t)\, dx + S_{\mathrm{R}}(D^* + \Delta D_t). \tag{A.1}$$

We calculate the Taylor expansion of the first term on the right-hand side of Equation (A.1)

$$D^* + \Delta D_{t+1} = S_{\mathrm{R}} N \left\{ \int_{x_{\mathrm{T}}}^{\infty} p_t(x, D^*)\, dx + \Delta D_t \frac{d\left(\int_{x_{\mathrm{T}}}^{\infty} p_t(x, D_t) dx\right)}{dD} + \frac{\Delta D_t{}^2}{2} \frac{d^2\left(\int_{x_{\mathrm{T}}}^{\infty} p_t(x, D_t) dx\right)}{dD^2} + \cdots \right\} + S_{\mathrm{R}}(D^* + \Delta D_t) \tag{A.2}$$

If ΔD_t is significantly smaller, we can neglect the higher order terms, then

$$D^* + \Delta D_{t+1} = S_{\mathrm{R}} N \left\{ \int_{x_{\mathrm{T}}}^{\infty} p_t(x, D^*)\, dx + \Delta D_t \frac{d\left(\int_{x_{\mathrm{T}}}^{\infty} p_t(x, D_t) dx\right)}{dD} \right\} + S_{\mathrm{R}}(D^* + \Delta D_t) \ . \tag{A.3}$$

From Equation (5) in the text,

$$\Delta D_{t+1} = S_{\mathrm{R}} \left\{ 1 + N \frac{d\left(\int_{x_{\mathrm{T}}}^{\infty} p_t(x, D_t) dx\right)}{dD} \right\} \Delta D_t \ . \tag{A.4}$$

From Equation (A.4), we obtain the condition for the density of resident males to be stable as follows:

$$\left| S_{\mathrm{R}} \left\{ 1 + N \frac{d\left(\int_{x_{\mathrm{T}}}^{\infty} p_t(x, D_t) dx\right)}{dD} \right\} \right| < 1. \tag{A.5}$$

Here, we note

$$\frac{d\left(\int_{x_{\mathrm{T}}}^{\infty} p_t(x, D_t) dx\right)}{dD} = \frac{d\left(\int_{x_{\mathrm{T}}}^{\infty} p_t(x, D_t) dx\right)}{d\mu} \frac{d\mu}{dD} \ . \tag{A.6a}$$

$$\int_{x_{\mathrm{T}}}^{\infty} p_t(x, D_t)\, dx = \int_{x_{\mathrm{T}}}^{\infty} \frac{1}{\sqrt{2\pi}\sigma} \exp\left[-\frac{\left(x - \mu(D_t)\right)^2}{2\sigma^2} \right] dx$$

$$= 1 - \frac{1}{2}\left(1 + \mathrm{erf}\left[\frac{x-\mu(D_t)}{2\sigma}\right]\right) \quad . \tag{A.6b}$$

$$\frac{d\left(\int_{x_T}^{\infty} p_t(x,D_t)dx\right)}{d\mu} = -\frac{1}{2}\frac{d}{d\mu}\int_0^{\frac{x-\mu(D_t)}{2\sigma}} e^{-x^2}\, dx \frac{d}{d\mu}\left(\frac{x-\mu(D_t)}{2\sigma}\right)$$

$$= \frac{1}{\sqrt{2\pi}\sigma}\exp\left[-\frac{\left(x-\mu(D_t)\right)^2}{2\sigma^2}\right] \quad . \tag{A.6c}$$

$$\frac{d\mu}{dD} = \frac{d}{dD}\left(\mu_0 + \mu_1 erf[k(\theta - D)]\right)$$

$$= \mu_1 \frac{d}{dD}\int_0^{k(\theta-D)} e^{-x^2}\, dx \frac{d}{dD}\ (k(\theta - D))$$

$$= \frac{-2k\mu_1}{\sqrt{\pi}}\exp[-k^2(\theta - D)^2] \quad . \tag{A.6d}$$

From Equations (A.6a, b, c, and d),

$$\frac{d\left(\int_{x_T}^{\infty} p_t(x,D_t)dx\right)}{dD} = \frac{-2k\mu_1}{\pi\sigma}\exp\left[-\frac{\left(x-\mu(D_t)\right)^2}{2\sigma^2} - k^2(\theta - D)^2\right] \ . \tag{A.7}$$

therefore, the condition for the stability of resident male density Equation (A.5)

becomes

$$\left|S_{\mathrm{R}}\left\{1 + \frac{-\sqrt{2}Nk\mu_1}{\pi\sigma}\exp\left[-\frac{\left(x-\mu(D_t)\right)^2}{2\sigma^2} - k^2(\theta - D)^2\right]\right\}\right| < 1 \quad . \tag{A.8}$$

Appendix B

Derivation of size distribution of the residents

The fraction of juveniles who stay in the stream is a step function of the body size *x*:

$$X(x|x_{\mathrm{T}}) = \begin{cases} 1 & x \geq x_{\mathrm{T}} \\ 0 & x < x_{\mathrm{T}} \end{cases} \quad . \tag{B.1}$$

Using Equations (1) and (2), the size distribution of residents in year *t* can be described as follows:

$$n_{\mathrm{R},t}(x) = \sum_{\tau=1}^{\infty} {S_R}^{\tau} X(x - \tau\Delta l|x_{\mathrm{T}}) N_{t-\tau} \hat{p}_{t-\tau}(x - \tau\Delta l, \mu_{t-\tau}) \quad . \tag{B.2}$$

The annual increment in the body size, measured in terms of the fork length, is assumed to be constant Δl, as is often assumed in fishery sciences (e.g., Morita et al., 2014). S_R is the annual survivorship and τ is the cohort age.

Appendix C

Selection gradient and evolutionary bifurcation

To understand the bifurcation structure of eco-evolutionary dynamics, we examine the selection gradient. When the mean body size fluctuates, fitness changes with time. To evaluate the invisibility of mutants, we calculate the long-term geometric mean fitness of the mutant (Hasting and Caswell, 1979; Hamilton, 1980; Venable, 1989; Tachiki and Iwasa, 2012) as

$$W(x'_{\mathrm{T}}) = \sqrt[t]{W(x'_{\mathrm{T}}, \mu_1) W(x'_{\mathrm{T}}, \mu_2) \ldots W(x'_{\mathrm{T}}, \mu_t)}. \quad \text{(C.1)}$$

Since it is difficult to differentiate function $W(x'_{\mathrm{T}})$ with respect to x'_{T}, we numerically evaluated the selection gradient $\delta W(x'_{\mathrm{T}})$ using the finite-difference method as follows:

$$\delta W(x'_{\mathrm{T}}) = \frac{W(x_{\mathrm{T}}+h) - W(x_{\mathrm{T}}-h)}{2h}, \quad \text{(C.2)}$$

where δ is the central difference operator $(h = 0.001)$ and $W(x_{\mathrm{T}})$ is the geometric mean fitness. We compared the prediction by selection gradient with the numerical simulation of eco-evolutionary dynamics.

Figures

Figure 1. Masu salmon adopt remarkable alternative life-history tactics

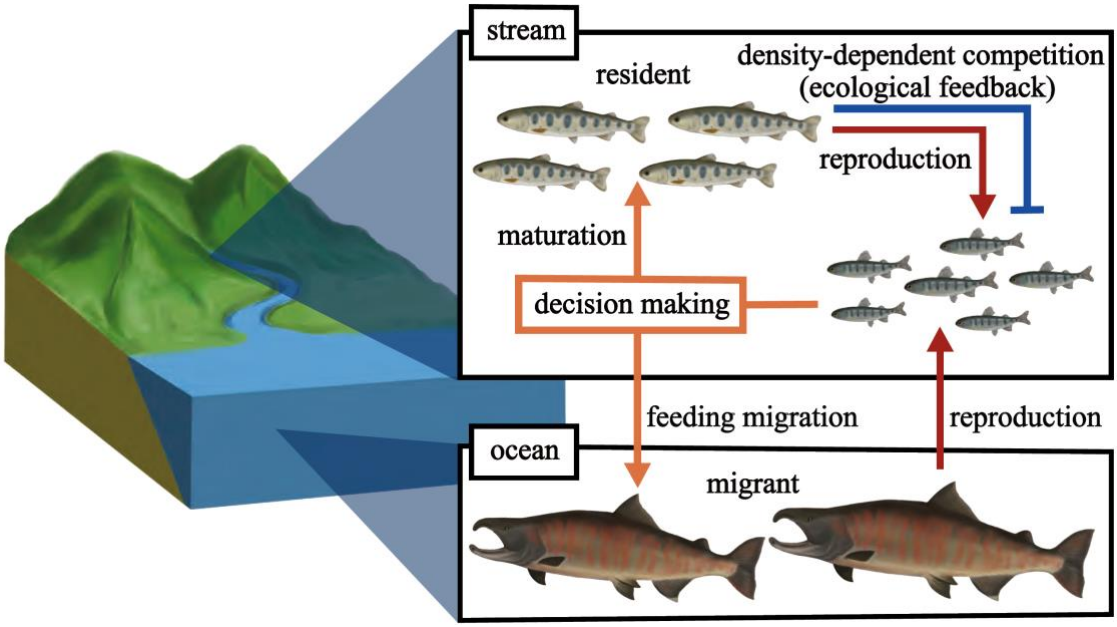

Certain individuals complete their entire life cycle in freshwater streams (residents), whereas others migrate to the ocean (migrants) to feed and mature. Residents reproduce in the year they hatched and survive for multiple years (iteroparity). Migrants mature in the ocean and reproduce in the river at 2+ years and then die (semelparity).

Figure 2. Population dynamics of the density of resident males

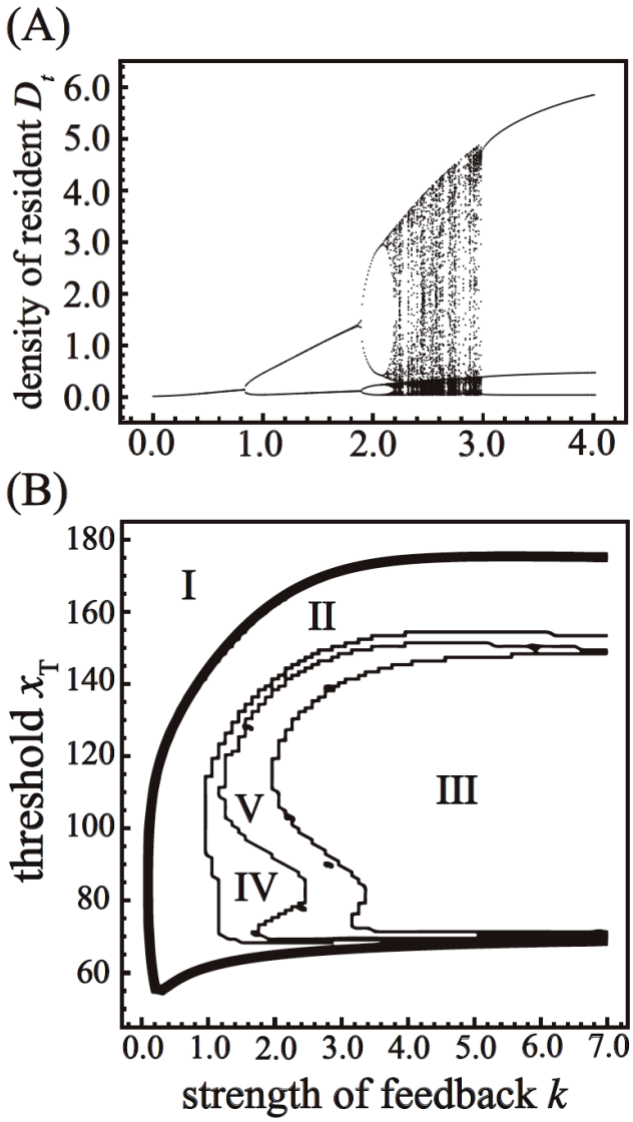

(A) Bifurcation diagram of the system. Horizontal and vertical axes represent the strength of feedback k and the fraction of residents among juveniles, respectively. When $k < 0.82$, the fraction of residents reaches a stable equilibrium. If $k \geq 0.82$, the fraction of the residents continues to fluctuate. For the intermediate values of k, the system reveals chaotic fluctuation. (B) Phase diagram. Horizontal and vertical axes are

the strength of the feedback k and threshold x_{T}, respectively. AreaIrepresents the dynamics converged into the equilibrium. Areas II, III, and IV indicate the parts in which the system converged into the oscillation within 2, 3, and 4 years, respectively. AreaV indicates the part that is a cycle of ≥5.0 years, or chaotic fluctuation. The boundary between areasIand II was calculated analytically using Equation (6). Boundaries between areas II and V were calculated numerically.

Figure 3. The evolutionary trajectories of the threshold juvenile size x_{T} that separate migrants from residents

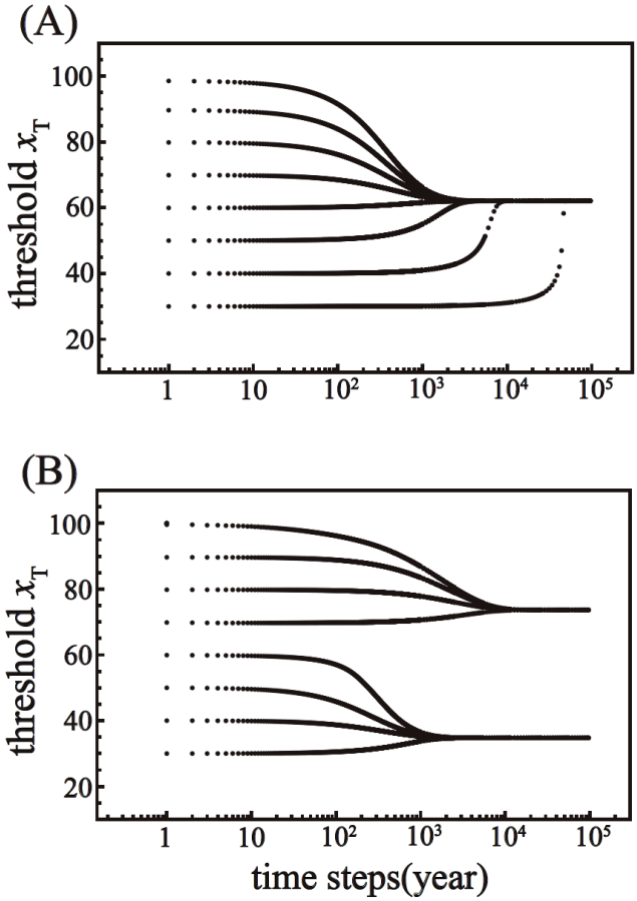

Trajectories starting from eight different initial values are presented. The horizontal axis represents time and is expressed by the number of generations on a logarithmic scale. (A) Trajectories from different initial values converge into a single value. There was no initial value dependence in the evolution. Feedback strength was $k = 0.1$. (B) Trajectories from different initial states converged into one of the two values. Dependence on the initial conditions exists. Feedback strength was $k = 0.5$. Other parameters were $\mu_0 = 100.0, \mu_1 = 50.0, \theta = 0.4, \Lambda = 500.0, \sigma = 13.0,\ S_{\mathrm{R}} = 0.05, S_{\mathrm{M}} = 0.5 \times 10^{-4}, \Delta l\ = 40.0, N = 100.0, \mathrm{c0} = 0.1,$ and $\mathrm{c1} = 5.0$.

Figure 4. Eco-evolutionary dynamics of the system for different feedback strengths *k*

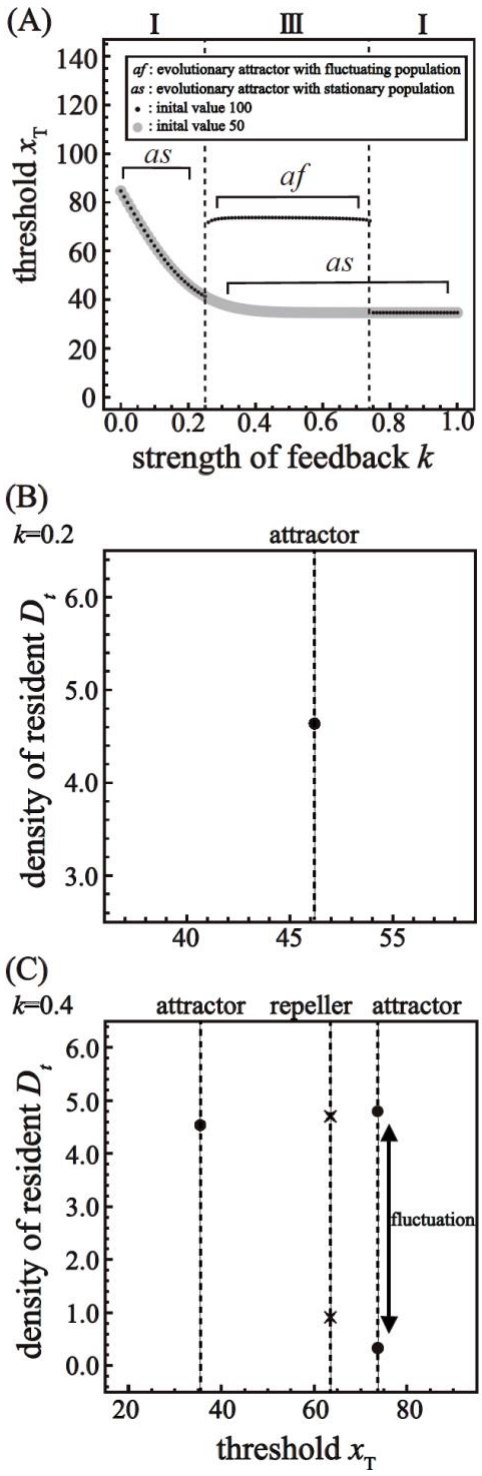

(A) The evolutionary endpoint of the threshold x_{T}. The horizontal axis represents the feedback strength k. For $k < 0.26$ and for $k > 0.74$, there is a single evolutionary endpoint; for $0.26 \leq k \leq 0.74$, there were two evolutionary endpoints, both of which were stable. The system was bistable. The evolutionary endpoint is illustrated by points (i.e., attractor). The small black points are the result of an initial value of $x_{\mathrm{T}} = 100$. The larger grey points are the result of an initial value of $x_{\mathrm{T}} = 50$. Curves labeled "*as*" indicate the evolutionary attractor with that the density of residents becomes stable; Curves labeled "*af*" indicate the evolutionary attractor with that the density of residents fluctuates within a period of 2 years Parameters were $\mu_0 = 100.0, \mu_1 = 50.0, \theta = 0.4, \sigma = 13.0,\ S_{\mathrm{R}} = 0.05, S_{\mathrm{M}} = 0.5 \times 10^{-4}, \Delta l\ = 40.0, N = 100.0, c_0 = 0.1,$ and $c_1 = 5.0$.

(B) The location of the final values of the evolutionary dynamics of x_{T} and population dynamics of resident male density *D*. Both of these values converged into a single value. This is Type I. Feedback strength was$k = 0.2$.

(C) The location of the final values of the evolutionary dynamics of x_{T} and population dynamics of the resident male density *D*. There are two evolutionarily stable values of x_{T}, which are the same two values illustrated in Figure 4(A). One of the two evolutionarily stable threshold sizes $(x_{\mathrm{T}} = 35.48)$ corresponds to the stable equilibrium of $D = 4.64$. The other stable threshold size $(x_{\mathrm{T}} = 73.70)$ corresponds to a fluctuating *D* within a period of 2 years $(D = 0.43$ and $D = 4.90)$, which are indicated by two solid circles connected by arrows. This is Type III. Between these two values, is $x_{\mathrm{T}} = 63.50$, which is another equilibrium that is evolutionarily unstable. Even

if the initial value is close to it, the value evolved to deviate from it. Feedback strength was $k = 0.4$.

Figure 5. Sign of the selection gradient δW with respect to x_T

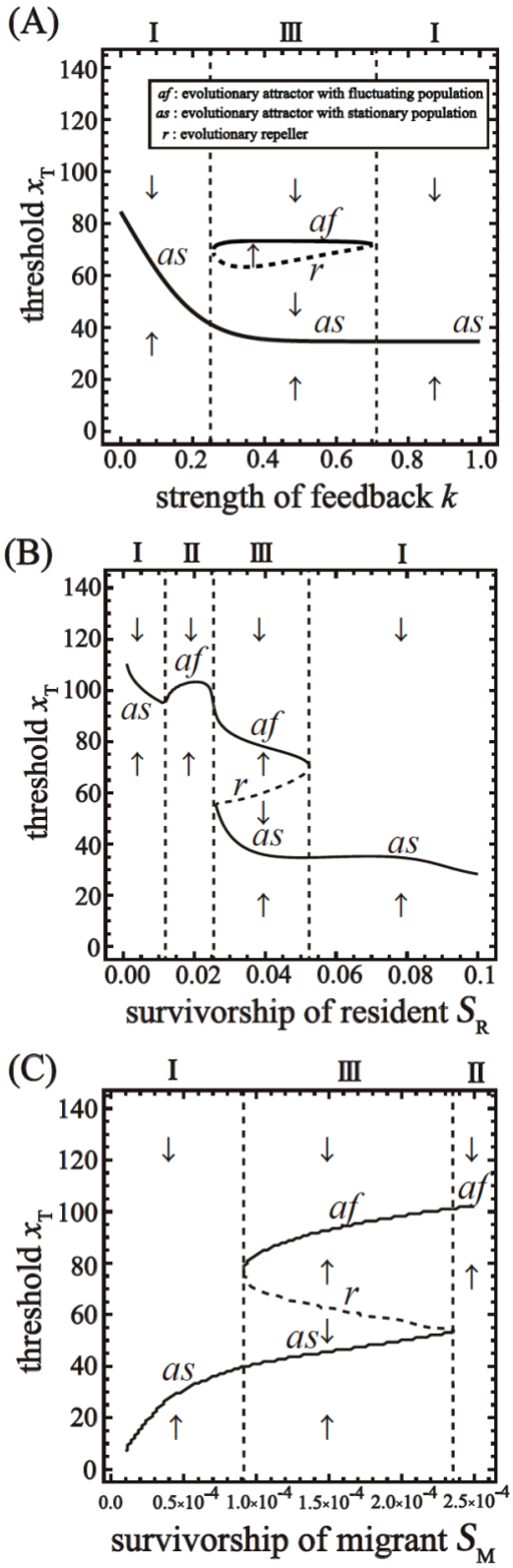

The vertical axis is x_{T}. The horizontal axis is a parameter. Upper arrows indicate that the trait value x_{T} increases evolutionarily in the corresponding regions (i.e., $\delta W > 0$). In the region designated by lower arrows, $\delta W < 0$ holds. Solid curves are the set of convergence stable points (i.e., attractor). The dashed curves are the set of evolutionarily unstable points (i.e., repeller). Curves labeled "*as*" indicate the evolutionary attractor with that the density of residents becomes stable; Curves labeled "*af*" indicate the evolutionary attractor with that the density of residents fluctuates within a period of 2 years; a line labeled "*r*" indicates the evolutionary repeller.

(A) The horizontal axis is the feedback strength *k*. For $k < 0.26$ or $k > 0.71$, the evolutionary dynamics of x_{T} converged into a single globally stable point. The ecological dynamics of the resident density converged into a stable fixed point (results not shown). This is Type I. For $0.26 \leq k \leq 0.71$, the evolutionary dynamics of x_{T} converged into one of the two stable values, depending on the initial condition. The system was evolutionarily bistable. The ecological dynamics of the resident density for one evolutionary stable equilibrium converged into a stable fixed point; however, that for the other evolutionary stable equilibrium continued to fluctuate within a period of 2 years (result not shown). This is Type III. There was an intermediate x_{T} that is an unstable evolutionarily equilibrium. Other parameters were $\mu_0 = 100.0, \mu_1 = 50.0, \theta = 0.4, \sigma = 13.0, S_{\mathrm{R}} = 0.05, S_{\mathrm{M}} = 0.5 \times 10^{-4}, \Delta l = 40.0, N = 100.0, c0 = 0.1,$ and $c1 = 5.0$.

(B) The horizontal axis represents the annual survivorship of resident males S_{R}. For $0.011 < S_{\mathrm{R}} \leq 0.026$, the evolution of x_{T} converged to a single globally stable value;

however, the population dynamics of resident males continued to fluctuate within a period of 2 years. This is Type II. For $0.026 < S_R \leq 0.052$, we observed the behavior of Type III (evolutionary bistability). For the remaining values of S_{R}, we observed the behavior of Type I (convergence to a single globally stable equilibrium at which the population dynamics are stable). The feedback strength was $k = 0.5$. Other parameters were the same as those in Figure 4(A) except for$S_{\mathrm{R}} = 0.05$.

(C) The horizontal axis represents the annual survivorship of migrant males S_{M}. The model reveals Type III behavior for $0.93 \times 10^{-4} \leq S_{\mathrm{M}} < 2.38 \times 10^{-4}$; the model reveals Type II behavior for $2.38 \times 10^{-5} \leq S_{\mathrm{M}}$; all other values represent Type I behavior. The feedback strength was $k = 0.5$. Other parameters were the same as those in Figure 4(A), except for$S_{\mathrm{M}} = 0.5 \times 10^{-4}$.

Chapter 3 Eco-evolutionary dynamics may show an irreversible regime shift, illustrated by salmonids facing climate change

The study in this chapter, done in collaboration with Dr. Yuuya Tachiki and Dr. Yoh Iwasa, was published in Theoretical Ecology 14: 345–357 in 2021.

Abstract

The enhanced or reduced growth of juvenile masu salmon (*Oncorhynchus masou masou*), may result from climate changes to their environment and thus impact on the eco-evolutionary dynamics of their life-history choices. Male juveniles with status, i.e., if their body size is larger than a threshold, stay in the stream and become resident males reproducing for multiple years, while those with smaller status, i.e., their body size is below the threshold, migrate to the ocean and return to the stream one year later to reproduce only once. Since juvenile growth is suppressed by the density of resident males, the fraction of resident males may stay in equilibrium or fluctuate wildly over a 2-year period. When the threshold value evolves, the convergence stable strategy may generate either an equilibrium or large fluctuations of male residents. If environmental changes occur faster than the rate of evolutionary adaptation, the eco-evolutionary dynamics exhibit a qualitative shift in the population dynamics. We also investigated the relative assessment models, in which individual life-history choices are made based on the individual's relative status within the juvenile population. The eco-evolutionary dynamics are very different from the absolute assessment model, demonstrating the importance of understanding the mechanisms of life history choices when predicting the impacts of climate change.

keywords: climate change, alternative life-history tactics, anadromous fish, status-dependent strategy, interference competition.

1. Introduction

Alternative tactics, utilized by many species at some point in their lives, describe discontinuous patterns of phenotypic variation, expressed by the same genotype, that result in divergent developmental programs (Roff 1996). For example, among adult dung beetles, individuals that have large horns behave as fighters, while those that do not become sneakers (Emlen 1997). In earwigs, small individuals have short forceps and large ones have long forceps; differences that originate due to the amount of proteins they acquired during development (Tomkins 1999). Salmonid fishes exhibit remarkable alternative life-history tactics. While some individuals migrate to the ocean to feed, grow to very large sizes, and then return to the natal stream to reproduce (migratory tactic), others complete their entire life cycle in freshwater streams (resident tactic) (Morita and Nagasawa 2010; Morita et al. 2014).

The coexistence of alternative tactics within a population is often explained as a status-dependent strategy (SDS; Gross 1996). If several tactics are available, and if the fitness of each tactic depends on the status (e.g., body size), the individual chooses the tactic with the highest expected fitness gain, given their status. Here, the phenotype of an individual switches based on whether the status is above or below a threshold. The value of the threshold should evolve to an evolutionarily stable strategy (Gross 1996).

A general trend observed throughout anadromous salmonids is that larger juveniles tend to remain in their natal streams (residents) (Piché et al. 2008). In a status-dependent strategy model for life-history tactics in salmonids (Morita et al. 2014), body size measurements, such as fork length and body mass, are considered to be the

determinants for whether the fish stays in or leaves its natal stream (Dodson et al. 2013). Body size may depend on several factors, such as interactions among individuals, environmental stochasticity, and climate changes, and subsequently these factors can influence the fraction of juveniles that employ each of the two tactics. For example, the growth of a juvenile can be suppressed by competition with other juveniles and adults in the stream, resulting in a decrease in the overall size and number of juveniles (Brown trout: Jenkins et al. 1999; Rainbow trout: Post et al. 1999). It can be predicted then, that the number of juveniles developing to residents, should decrease as the density increases.

Climate changes also affect migratory tactics in several different ways. Recently, global warming is considered to have affected environmental habitats, resulting in a shift of fish body sizes (Perry et al., 2005; Crozier et al. 2008; Daufresne et al. 2009; Satterthwaite et al. 2010). Naturally, we may imagine that a higher temperature might enhance the growth rate of juveniles due to the enhanced productivity of their environments (Crozier et al. 2008). However, Daufresne et al. (2009) demonstrated that an increase in the water temperature resulted in a decrease in the body size of aquatic species, due to their increased metabolic activity. The change in the growth rate, caused the body sizes of the juveniles to change, which affected the life-history choices of the masu salmon, and subsequently, a change in the fraction of migrant fishes (versus resident fishes). Further, Finstad and Hein (2012) predicted that the fraction of migrants Arctic char that are important for the fishing industry, will be reduced by increasing terrestrial productivity, under climate change scenarios.

In many models of life history choices, individuals are assumed to choose tactics based on their absolute status (such as body size), with a threshold value (Gross 1996). Tachiki and Koizumi (2016) proposed an alternative mechanism of life-history choices, called a relative assessment model, in which each juvenile makes a life-history choice based on their relative status within the juvenile population, estimated by the interactions among individuals. Tachiki and Koizumi (2016) showed that relative assessment stabilizes the fractions of the two tactics, and that it is evolutionarily favored under a stochastic environment, in comparison with the absolute assessment model (Gross 1996).

In this paper, we consider the size of individuals affected by climate change, represented as a monotonic change of temperature, that might either increase or decrease their growth rate. We focus on salmonids, a taxon that exhibits alternative life-history tactics. We examine how their eco-evolutionary dynamics as well as the fraction of migrant tactics and the evolution of the threshold status, responds to climate change. We first consider the case in which life-history choices are made based on absolute assessments, but we later examine the case with a relative assessment model. These two cases are very different, and indicate the importance of understanding the underlying mechanisms of how individuals make life-history decisions in predicting the impact of climate change on wild life resources.

2. Life history choices affected by density-dependent growth

We begin with a mathematical model for the life-history choice of masu salmon

(*Oncorhynchus masou masou*). Some males complete their entire life cycle in freshwater streams (residents), whereas others migrate to the ocean (migrants). In contrast, all females become migrants, as in several other salmonids (Dodson et al. 2013). Resident males can start reproduction in the year they hatch and continue to reproduce for multiple years (iteroparity). In contrast, migrant males mature in the ocean and return to their natal stream at the age of 2+ years, to reproduce once and then die (semelparity). Large juveniles tend to be residents (Piché et al. 2008), which has been regarded as the optimal tactic in the status-dependent strategy (SDS) model (Morita et al. 2014). The life-history choice of juveniles depends on whether their body size exceeds a threshold value, and the growth of juveniles is suppressed when there are many older resident males. An abundant number of residents in a year, should reduce the growth of juveniles and result in fewer juveniles staying in the stream, leading to fewer resident males in the subsequent years. This causes a delayed feedback of fish density in the stream and may result in fluctuations of the juvenile body size and of the fractions of migrants and residents (Horita et al. 2018). In this section, we explain the population dynamic model for males, and summarize the results that will be the basis of the analysis of the evolutionary outcomes.

2.1. The choice of life history by juveniles in absolute assessment model

Let x be the body size of a juvenile when the life-history choice is made. We assume that x has a normal distribution with mean μ_t and standard deviation σ:

$$\hat{p}_t(x, \mu_t) = \frac{1}{\sqrt{2\pi}\sigma} \exp\left(-\frac{(x-\mu_t)^2}{2\sigma^2}\right). \quad (1)$$

The mean body size μ_t, may vary between years, being affected by competition for food and space with other river residents, and by environmental conditions.

We assume that a juvenile becomes a resident if its body size *x* is larger than a threshold x_{T}; it becomes a migrant if *x* is smaller than x_{T} (absolute assessment model). The probability to be a resident is:

$$X(x|x_{\mathrm{T}}) = \begin{cases} 1 & x \geq x_{\mathrm{T}} \\ 0 & x < x_{\mathrm{T}} \end{cases}. \quad (2)$$

Let D_t be the density of stream residents in year *t*. It is obtained by integrating the size distribution of individuals employing the resident tactic, multiplied by N_t, the number of juveniles in year *t*. We have:

$$D_t = \sum_{\tau=1}^{\infty} {S_{\mathrm{R}}}^{\tau} N_{t-\tau} \int_{-\infty}^{\infty} X(x|x_{\mathrm{T}}) \hat{p}_t(x, \mu_{t-\tau})\, dx. \quad (3a)$$

The size distribution of residents in year *t* is given as follows:

$$n_{R,t}(x|x_{\mathrm{T}}) = \sum_{\tau=1}^{\infty} {S_{\mathrm{R}}}^{\tau} X(x - \tau\Delta l|x_{\mathrm{T}}) N_{t-\tau} \hat{p}_{t-\tau}(x - \tau\Delta l, \mu_{t-\tau}). \quad (3b)$$

where S_{R} and Δl are annual survivorship and size increments of the residents, respectively.

2.2. Density-dependent growth and ecological dynamics

In the stream, when the density of residents is higher, the growth of juveniles becomes slower, due to competition for resources. Hence, the mean body size of juveniles is a decreasing function of the density of the residents (e.g., Brown trout: Jenkins et al.

1999; Rainbow trout: Post et al. 1999). Horita et al. (2018) considered the case when the mean body size of juveniles μ_t decreases with D_t, that the density of the resident males is as follows:

$$\mu_t = \mu_0 + \mu_1 \operatorname{erf}[k(\theta - D_t)], \tag{4}$$

where parameter μ_0 determines the intermediate value of the body size μ_t. Hereafter, we call it the intermediate size. We may regard μ_0 as an index of juvenile growth rate. In all of the analyses in this paper, we assume that μ_0 is larger (or smaller) if the juvenile growth rate is faster (or slower), due to climate changes. μ_1 determines a range of the function μ_t. θ is the population density when the mean body size μ_t is equal to μ_0. μ_t converges to $\mu_0 + \mu_1$ when the density is very low, and to $\mu_0 - \mu_1$ when it is very high. k determines the slope of the function, and we call *k,* the "strength of ecological feedback." The strength of ecological feedback (k) affects the stability of the fraction of juveniles who become migrants. When k is small, the fraction of migrant males is stable. As k increases, the fraction of migrants becomes unstable, and fluctuates over a period of two years. Further increases in k make the amplitude of the fluctuation larger (Horita et al. 2018).

Since μ_t in Eq. (4) is a function of the density of male residents, the size distribution of juveniles in year t is a function of D_t, expressed as $p_t(x, D_t) = p_t(x, \mu_t(D_t))$. The residents in subsequent years, comprise the resident juveniles of the current year who remain in the stream, plus the surviving residents in the current year. We define the population dynamics of D_t as:

$$D_{t+1} = S_{\mathrm{R}} N \int_{-\infty}^{\infty} X(x|x_{\mathrm{T}}) p_t(x, D_t)\, dx + S_{\mathrm{R}} D_t, \tag{5}$$

where the first term on the right-hand side indicates the contribution of juveniles from the current year who remain in the stream, and $S_{\mathrm{R}} D_t$ represents that by the residents in the current year. Eq. (5) indicates that the density of residents in year t+1 can be calculated from the density in year t.

The population dynamics Eq. (5) may converge either to a stable equilibrium or to a 2-year cycle with a large amplitude (Horita et al. 2018). This can be explained in an intuitive manner as follows: when the threshold value x_{T} is clearly higher than the mean size of the juveniles, most juveniles migrate to the ocean and will be back to the stream later for reproduction. Then, only a small fraction of juveniles will remain in the stream and become residents in the following years, causing reduced growth suppression on juveniles. This creates a delayed negative feedback in the density of residents, and may produce two-year fluctuations of the mean body size of juveniles, the fraction of migrants, and the density of residents. In contrast, if the threshold body size x_{T} is rather small, compared with the mean body size of juveniles, a large fraction of juveniles remain in the stream and become residents in the following year.

2.3. Monotonic changes of the environment

We have considered the effect of the slow and steady change of the environment, which causes monotonic increases or decreases in the intermediate size, μ_0. In the numerical analyses, we start with stable environmental conditions, in which the intermediate size

μ_0 is fixed for a very long time. Then, climate changes start to modify the intermediate size μ_0, as follows:

$$\mu_{0,t+1} = \mu_{0,t} + mt. \tag{6}$$

The mean body size was stopped when it reached a particular value. We assume that the mean size is a linear function of time for simplicity (Prentice et al. 1993). The parameter m, indicates the rate of change in μ_0. m is positive if the environmental change enhances the juvenile growth, but negative if it reduces it. Gregory et al. (2017) showed that the body size of Atlantic salmon increased more than 10 (mm) in 20 years (0.5 [mm/year]). According to these literatures, we adopted the plausible value as the parameter of body size change ($0.01 \leq m \leq 0.6$ [mm/year]). We investigated climate change for 100 years as in many other studies (e.g. Finstad & Hein 2012; Lehodey et al. 2013; Lehodey et al. 2015). We classified the dynamical behavior of the system in terms of ecology and evolution. In experimental studies, when the water temperature increases, the growth rate first increases and then starts to decrease due to metabolic disorder (Satterthwaite et al. 2010). In our simulation, we consider a monotonical change to simplify the model.

The fraction of migrants decreased with an increase in the intermediate body size μ_0 (Fig. 1a). The change of stability in the ecological dynamics may occur both from equilibrium to fluctuation and from fluctuation to equilibrium. Hereafter, we call it "regime shift". In figure 1b, the fraction of migrants was stable initially, but it became destabilized as μ_0 changed. In figure 1c, the fraction of migrants fluctuated initially within the 2-year period, but it stabilized as μ_0 changed. When the intermediate size

decreased (Fig. 1d, 1e, & 1f), the fraction of migrants increased (Fig. 1d), and the ecological dynamics may change from an equilibrium to a 2-year cycle (Figs. 1e & 1f).

3 Evolutionary dynamics

To explore the evolution of the threshold trait, x_{T}, which is expressed only in males, we consider the competition among males for mating opportunities. We adopted the fitness function formalized by Tachiki and Koizumi (2016), in which the fitness of a male is defined as a lifetime siring success for each tactic. Notably, population growth is independent of the threshold trait and population size does not change, because all females are migrants. We hence assumed that *N*, the number of new born individuals, is a constant. The evolutionary change in the threshold trait might affect the fraction of males who exhibit alternative life-history tactics.

3.1 Evolutionary change of the threshold trait

The spawning group of masu salmon, consists of a female and several males including both migrants and residents (Watanabe et al. 2008; Esteve et al. 2011). Migrant males attack other males, whereas resident males adopt a sneaking tactic (Koseki and Maekawa 2000; Watanabe et al. 2008). Further, sneaker males attack each other, resulting in a dominance hierarchy among sneaker males (Koseki and Maekawa 2000; Esteve et al. 2011). Due to this interference competition, the competitive ability of resident males with body size *x* becomes a decreasing function of the density of resident males larger than *x*. We here assume that the competitive ability of a resident male with

size x is given as follows:

$$C_t(x|x_{\mathrm{T}}) = c_0 exp\left[-c_1 \int_x^{\infty} n_{\mathrm{R},t}(y|x_{\mathrm{T}})\, dy\right], \tag{7}$$

where c_0 is the relative competitive ability of the strongest resident relative to a migrant, and c_1 is a constant that mediates the strength of the interference of the competition among the residents. $n_{\mathrm{R},t}(y)$ is the size distribution of the residents (Eq. 3b). Eq. (7) could be interpreted as the product of c_0 and the probability that an individual with size x does not encounter larger individuals in the same spawning group. The number of spawning females and eggs produced does not change between years, because all females are migrants and the sex ratio and survivorship are constant. The migrants return to their natal stream to reproduce once after several years in the ocean for growth. Miyakoshi and Saitoh (2011) reported that the adult size and ocean survival of masu salmon are independent of their size at smoltification.

We assume here that the competitive ability of a migrant can be expressed as the product of constant survivorship, S_{M}, and the size-independent competitive ability of the migrant, which is normalized to 1. We also consider that the situation is one where there are a few rare mutants in a population dominated by the wild type. Let the trait value of mutant x'_{T} be slightly different from that of wild type x_{T}. The fitness of a mutant (i.e., invasion fitness) is given as follows (Tachiki and Koizumi 2016):

$$W_t(x'_{\mathrm{T}}|x_{\mathrm{T}}) = f_t(x'_{\mathrm{T}})/f_t\,(x_{\mathrm{T}}), \tag{8a}$$

where

$$f_t(x'_{\mathrm{T}}) = S_{\mathrm{M}} \int_{-\infty}^{\infty} \left(1 - X(x|x'_{\mathrm{T}})\right) p(x, D_{t-2}) dx$$

$$+\int_{-\infty}^{\infty} X(x|x_{\mathrm{T}}') \sum_{\tau=0}^{\infty} {S_R}^{\tau} C(x+\tau\Delta l|x_{\mathrm{T}})\, p(x, D_{t-\tau}) dx\,. \tag{8b}$$

The first term on the right-hand side of Eq. (8b) is the reproductive success of migrants. The survivorship, S_{M}, is multiplied by the probability that a juvenile migrates to the ocean. Notably, the mating success of migrants when they successfully return to their natal stream is normalized as unity. The second term of the right-hand side of Eq. (8b) is the contribution of residents. It is the product of survivorship during τ years and the competitive ability summed over the years and averaged with the probability distribution.

Here, we adopt the evolutionary dynamics as follows:

$$x_{\mathrm{T}_{t+1}} = x_{\mathrm{T}_t} + \Lambda \frac{\partial}{\partial x_{\mathrm{T}}'} \ln W(x_{\mathrm{T}}'|x_{\mathrm{T}})\Big|_{x_{\mathrm{T}}'=x_{\mathrm{T}}}\,. \tag{9}$$

where, Λ is equal to the additive genetic variance (Iwasa et al., 1991) and mediates the rate of the evolution. Concerning the threshold size of maturation in salmonid fishes, there is no appropriate dataset estimating the additive genetic variance. However, there is a literature that estimates the genetic variance of threshold for smoltification in rainbow trout (Phillis et al. 2016). While there is substantial difference between threshold of smoltification and that of early maturation, we tested Λ for a wide range including the value estimated by Phillis et al. (2016) and examined how Λ modified the eco-evolutionary consequence.

3.2. Evolution of threshold size in a constant environment

Figure 2 indicates the selection gradient of the threshold trait x_{T}, i.e., the direction of

evolutionary change. Here, all of the parameters are constant (no climate change). The horizontal axis is survivorship, S_{R} in figure 2. The evolutionary attractors may be single values, or two different values, depending on S_{R} (Fig. 2a). The system exhibits saddle-node bifurcation in which bistability of evolutionary outcomes occurs for a particular range of the parameter S_{R} (see Horita et al. 2018). These two evolutionary attractors differ in the stability of ecological dynamics (i.e., time series of the fraction of migrants). When the threshold trait is at the evolutionary attractor of a larger x_{T}, the ecological dynamics exhibit a fluctuation with 2-year period. The evolutionary attractor of a smaller x_{T} corresponds to the ecological dynamics of a stable equilibrium (Horita et al. 2018).

The threshold size evolves to the evolutionarily stable value. When the survivorship of resident males in the stream, S_{R} is high, the threshold x_{T} evolves to be small and the fraction of resident males evolves to be large, resulting in stable population dynamics (denoted as "E" in Fig. 2a). In contrast when the survivorship of resident males, S_{R} is small, x_{T} evolves to be large, and the fraction of migrant males fluctuates wildly between high and low values over a 2-year period (denoted as "C" in Fig. 2a). Interestingly, when the survivorship of residents is an intermediate value, the system is evolutionarily bistable. Depending on the initial value, either a large threshold size, x_{T} with a fluctuating fraction of migrants/residents evolves, or a low threshold size x_{T} with a stable and large fraction of migrants (i.e. a small fraction of residents) evolves.

Figure 3 also indicates the evolutionary outcomes, x_{T} in a constant

environment in which the horizontal axis is the intermediate size of juveniles μ_0. As μ_0 increases, the threshold value x_{T} that is convergence stable increased accordingly (Fig. 3a & 3b).

4. Eco-evolutionary dynamics in changing environments

In this section, we investigate the impact of slow and steady environmental changes over a period of years on the eco-evolutionary dynamics of the life-history choices of masu salmon. We ran numerical analyses of the eco-evolutionary dynamics under the conditions in which the intermediate size μ_0 was changed according to Eq. (6).

4.1. Evolutionary trajectories of threshold x_{T} with climate change

Figure 4 illustrates the evolutionary trajectories of the system, in which μ_0 changes due to environmental changes and these drive the evolutionary changes in x_{T}. Here, the horizontal axis is for μ_0, and the vertical axis is for x_{T}. The parameters were selected as those that correspond to figure 3b. For each value of μ_0 (horizontal axis), there are two evolutionary stable values of x_{T} (evolutionary attractors); and one evolutionary unstable value (evolutionary repeller) located between them (Fig. 3b). Only the difference between figure 4a and 4b is the rate of change in μ_0 (designated by m).

If the environment does not change, μ_0 remains at a particular value, and the evolution of the system should converge to either one of the two attractors, as shown in figure 3b. However, climate change causes an increase in μ_0, making the system deviate from the attractor. As a result, the trajectory of the threshold trait (x_{T}),

illustrated by the black arrows, always stayed a little below the attractors (gray lines), instead of exactly on them (Fig. 4). When climate change ends and μ_0 becomes fixed to its final value, the evolution can make straight forward movements to the attractor, which is indicated as a vertical trajectory in figure 4a and 4b.

If the rate of change in μ_0 is sufficiently small in comparison with the rate of evolution (Fig. 4a), the evolutionary trajectory during environmental change has a slope similar to the three lines indicating two attractors and a repeller. This implies that if the system starts from near the attractor, corresponding to stable equilibrium population dynamics, then the evolutionary trajectory kept close to the attractor. In contrast if the system started near the attractor corresponding to a 2-year cycle, then the system keeps close to the attractor with the 2-year cycle. Hence, we can conclude that the population dynamics remain unchanged during and after climate change, if the rate of the evolution is sufficiently fast compared with climate changes.

Figure 4b shows the case where the rate of the evolution is slower than that of climate change. Here, climate changes make the system move from the attractor corresponding to the fluctuating population dynamics to the attractor corresponding to the stable equilibrium dynamics. Hence the population dynamics exhibit a transition of their dynamical behavior.

4.2. Regime shift in the eco-evolutionary dynamics caused by climate change

Figure 5 shows the eco-evolutionary dynamics under the same parameter set as that of figure 3a, in which there was only one evolutionary equilibrium which was convergence

stable. When the rate of the evolution Λ was too small to follow the change in the intermediate size μ_0 (i.e. the rate of climate change was too fast to keep up with), the evolution of the threshold trait could not follow climate change. Hence, the difference between the trait value adopted in the population and the evolutionary convergence stable strategy, under given μ_0, increased while climate change occurred ($T_1 < t < T_2$; in Fig. 5a). This results in a large fluctuation of the fraction of migrants among males (Fig. 5b). Even after climate change stopped ($t > T_2$), the evolution of the threshold still continued, and gradually converged to an equilibrium. Taking 4 or 5 times longer transient time than that of climate change, the threshold trait x_{T} finally reached the convergence stable strategy. During this long transient (Hasting et al. 2018), the stability of the ecological dynamics changed once the frequency of migrants converged to a particular value, and then fluctuated again and finally returned to stable two-year cycle with the same amplitude with that before climate change (Fig. 5b). Such a complex pattern of dynamical behavior was realized because the combination of trait value x_{T} and the intermediate size μ_0 was in the parameter region for a 2-year cycle most of the time, but in the one for stable equilibrium for some period of time (Fig. S1 in online resource 1). The fraction of migrants recovered to the same level as before the environmental change (Fig. 5a). Depending on the parameter set, there were various patterns of ecological dynamics generated with a change in intermediate size μ_0. See Appendix A and figure S2 (online resource 1) for a detailed explanation.

Figure 6 shows the eco-evolutionary dynamics in the case of figure 3b, in which there are three evolutionary equilibria, one is the repeller (dotted line in Fig. 3b)

and others are convergence stable (solid lines in Fig. 3b). Before climate change started ($t < T_1$), the threshold trait x_{T} was equal to an evolutionary attractor (Fig. 6a, which corresponds to the upper attractor in Fig. 4b,). In this state, the fraction of migrants oscillates over a 2-year period (Fig. 6b). When intermediate size μ_0 increased with time ($T_1 < t < T_2$), the threshold trait, once increased slightly but then suddenly decreased (Fig. 6a). This occurred when the threshold trait crossed the repeller (tipping point [Hastings et al. 2018]), and it attracted another evolutionary equilibrium (Fig. 4b). At the same time, the fraction of migrants was stabilized (Fig. 6b). Even after the environmental changes ceased ($t > T_2$), the evolution of the threshold trait x_{T} continued and finally stopped at the evolutionary equilibrium after long transient. In this case, the ecological dynamics were qualitatively different before and after the environmental changes, caused by the transition of the evolutionary attractor, from the upper one to the bottom one in figure 4a. Hereafter, we call it "evolutionary regime shift". For a more detailed explanation see Appendix A and figure S3 (online resource 1).

This evolutionary regime shift was caused by the balance between the rate of change in the intermediate size m, and that of evolution Λ. We examined whether the evolutionary regime shift occurred or not, by running the eco-evolutionary dynamics. When the rate of the evolution was large enough, the evolutionary regime shift did not occur (Fig. 7). If the evolution was too slow to follow climate change, the trait value deviated from the attractor converged formerly and then reached the repeller. When the trait value crossed the repeller, it was attracted by another evolutionary attractor.

5. Relative assessment of the rules

Animals learn their relative status or social rank in a population from experiences by interacting with other individuals and adjust their behavior accordingly (Fricke and Fricke 1977; Warner and Robertson 1978; Kuwamura and Nakashima, 1998; Munday et al., 2006). In the relative assessment models (Tachiki and Koizumi 2016), each individual is assumed to estimate its relative status in the population *z* by Bayesian inference. Let *z* be the difference of an individual's own status to the population median status ($z = 0$ if its status is equal to the median of the population). We assume that individuals have a prior distribution for *z* that follows a normal distribution, with mean 0 and standard deviation σ. It obtains a difference of its own status (i.e., body size) and that for a randomly chosen opponent, and then calculates posterior distribution. Each individual updates posterior distribution *n* times (Bayesian update). Each juvenile chooses the resident tactic if the estimated status is higher than a threshold value z_{T}.

Let $\Phi(x|z_{\mathrm{T}})$ be the probability that an individual with true absolute status *x*, estimates its own relative status *z*, to be larger than the threshold z_{T}. According to the derivation in Appendix B (online resource 1), Φ becomes,

$$\Phi(x|z_{\mathrm{T}}) = \frac{1}{2}\left(1 + \mathrm{erf}\left[\frac{n(x-\mu) - (n+2)z_{\mathrm{T}}}{2\sigma\sqrt{n+2}}\right]\right). \tag{10}$$

In the case of the relative assessment, we obtain the same statistics from Eqs. (3a & 3b) by replacing x_{T} and $X(x|x_{\mathrm{T}})$ with z_{T} and $\Phi(x|z_{\mathrm{T}})$, respectively.

Eq. (10) is a sigmoidal function of true size *x*, and the number of Bayesian update *n*, mediates the slope of the function. In the limit of very large *n*, Φ becomes a

step function in which Φ is 1 if $x > z_{\mathrm{T}} + \mu$, and otherwise Φ equals 0.

We have examined the relative assessment models by applying all the analyses adopted to absolute assessment models in previous sections. First, in relative assessment models, the change in the status of all the juveniles in the population simultaneously, does not impact on the fraction of migrants, as illustrated in figure 8a. In addition, the ecological dynamics are always stable. Second, we can compute the evolution of threshold traits in the relative assessment models, with the same scheme as for the case of absolute assessment in the previous sections, but the variable to evolve is z_{T}, instead of x_{T}, the results were:

[1] There was only one stable attractor (Fig. 2b). There was no parameter set that showed bistability of evolutionary attractors. The evolutionary consequence of the threshold trait z_{T}, that was convergence stable, decreased with an increase in survivorship of resident S_{R}. Ecological dynamics were always stable in this case.

[2] The threshold value z_{T} at the stable attractor was independent of the intermediate size μ_0 (Fig. 3c).

[3] In eco-evolutionary dynamics, the threshold value z_{T} hardly changed with an increase in intermediate size μ_0 (Fig. 8b). Slight changes in trait values were observed during the environmental changes ($T_1 < t < T_2$), and they were caused by the changes in the population structure of the residents. The changes in the intermediate size did not influence the ecological dynamics (Fig 8c). These outcomes of the responses of eco-evolutionary dynamics to climate change (formalized as Eq. (10)) are greatly different from those of the absolute assessment models. This suggests that the responses to

climate changes critically depend on the manner in which life-history choice is performed by the organism.

6. Discussion

Population respond to climate changes both ecologically and/or evolutionarily (Bradshaw et al. 2006; Charmantier et al. 2008; Chevin et al. 2010). Traits change as evolution operates on fitness differences in the environment and also by phenotypic plasticity depending on the conditions of the environment. These responses may enable the population to survive under environmental changes (Ashander et al. 2019). While some recent studies in chaos and dynamics in eco-evolutionary models under changing environment have focused on the phase transition (Gilpin and Feldman 2017) and predictability (Rego-Costa et al. 2018), the relationship between the rate of climate change and that of evolution was underexplored. We here explored the possibility that the irreversible regime shift was caused depending on the balance of these two.

6.1 Eco-evolutionary responses to change may result in long transient, or even irreversible changes to population dynamics

In this study, we have investigated the effects of climate change on population dynamics. In cases where individuals made decisions based on their own status, such as body size (absolute assessment), the fraction of migrants was changed because of climate change (Fig. 1). As the intermediate size μ_0 increased, the number of juveniles

becoming larger surpassed the threshold, resulting in a greater fraction of juveniles employing resident tactics. Climate change may also affect the qualitative behavior of the population dynamics (Figs. 1b, and 1c).

These changes in the ecological dynamics could be reverted to those before climate change occurred, when we consider the evolution of threshold traits (Fig. 5), given that the rate of the evolution is fast enough when compared with the environmental change, and the threshold trait that was convergence stable, linearly increased with increasing intermediate size, μ_0 (Fig. 3a). During climate changes, the threshold did not evolve linearly, and hence the difference between the evolutionary attractor and the threshold traits adopted in the population increased (Fig. 5a). This caused considerable change in the ecological dynamics, in terms of both the fraction of migrants and the stability of the system (Fig. 5b). However, if there was only one evolutionary equilibrium, the evolutionary dynamics finally converged to the equilibrium (Fig. 5a), and this resulted in the recovery of the ecological dynamics, to the same qualitative behavior as that prior to climate changes (Fig. 5b).

On the other hand, when there were multiple equilibria in the threshold trait (Fig. 3b), increasing the intermediate size μ_0 might cause the transition of trait values from one evolutionary equilibrium to another (Fig. 6a). This resulted in irreversible changes in the dynamic behavior of the system (Fig. 6b). This evolutionary regime shift occurred when the rate of climate change was sufficiently large in comparison with the rate of the evolution (Fig. 4a, and 7). In order to demonstrate potential behavior of the model, in this paper we adopted arbitrary values as the rate of the evolution and climate

change in our simulation, and based on the analyses we concluded that the balance between these parameter is important in a factor realizing the evolutionary regime shift (Fig. 7). Phillis et al. (2016) evaluated the rate of the evolution of threshold trait of smoltification in the system of rainbow trout. Quantitative study of measuring the rate of evolution is important because it will allow us to know whether or not the evolutionary regime shift likely to occur under natural situations. These results highlight the importance of reducing the rate of climate change. Bradshaw et al. (2006) claimed that organisms respond evolutionarily to climate changes and they are able to adapt to the environment however, the survival of organisms will be in danger if we do not reduce the rate of climate change. Thomas et al. (2004), also called attention to the importance of reducing the rate of climate change, to avoid a crisis of extinction for organisms. In this study, we showed that the mismatch of a threshold trait in a given environment, caused by climate change, might consequently cause a regime shift of the ecological dynamics (Fig. 1). This would result in phenotypically different population dynamics. Since we cannot modify the rate of the evolution for natural populations without significant interventions, reducing the rate of climate change may be one potential policy to prevent irreversible changes to the natural populations.

We examined the distance between the upper attractor and repeller when evolutionary bistability occurred (Fig. S4 in online resource 1), and found that it increased with a decrease in survivorship of residents S_{R}, and increased with an increase in the survivorship of migrants S_{M}. In other words, when the survivorship of residents was small and that of the migrants was large, the evolutionary regime shift

would be unlikely.

6.2 Relative versus absolute assessment rules

In the cases where individuals make the decision based on the estimated social ranks in the population (relative assessment), climate change had no effect on the evolutionary dynamics (Fig. 8a). The threshold trait hardly changed when we considered the evolution of the threshold with the occurrence of climate change (Fig. 8b), and there were no situations in which evolutionary bistability occurred. The ecological dynamics of the relative assessment model were less severely affected by climate change than those of the absolute assessment model. Relative assessment can be regarded as a form of phenotypic plasticity. In general, phenotypic plasticity is known to help the maintenance of a population in the face of climate change (Chevin et al., 2010). Charmantier et al. (2008) showed that the phenotypic plasticity might allow the population to cope with rapid climate change. Hence, it is important to know whether the salmonids make the decision by relative assessment or absolute assessment. In natural situations, organisms may adopt a mixture of absolute and relative assessments. To predict the outcomes of climate change in relation to eco-evolutionary dynamics, it is important to know how relative elements influence life-history decision making, and this should be the focus of more research in the future.

In this study, we assumed that climate change affects the body size only, because the size directly affects life-history choices. There are, however, documentations that climate changes affect organisms from multiple aspects

simultaneously (Walther et al., 2002), such as body size (Crozier et al. 2008; Daufresne et al. 2009), habitat (Perry et al. 2005, Warren et al. 2001), phenology (Przybylo et al. 2000), survivorship (Ozgul et al. 2010, Satterthwaite et al. 2010), and species interactions (Tylianakis et al. 2008). These will change the eco-evolutionary dynamics, and it is necessary to consider which changes are significant when we study the effects of climate change on particular organisms. Furthermore, we here focused only on the life-history of males, because most female exhibits migrant tactic in masu salmon. There are however some species in which females also show alternative life-history tactics (e.g. brown trout: Jonsson et al. 2001; masu salmon: Morita & Nagasawa 2010). Since female directly affect the population dynamics, considering the decision making in both sexes enables us to explore the dynamical change and population persistence of whole population as consequences of environmental change.

7. Conclusion

The present study demonstrated the importance of understanding the mechanisms of life history choices in predicting the impacts of climate change. The way in which life history choice mechanisms respond to change also is important. Bradshaw and Holzapfel (2008) conjectured that both phenotypic plasticity and genetic evolution mitigate the harmful effects of climate change on organisms. However, the present study showed that, when the rate of climate change is too fast, traits may shift to different evolutionary attractors, and these shifts may be irreversible. As a result, the ecological dynamics can become qualitatively different from the initial ones.

Acknowledgements

This study was conducted in support of JSPS Overseas Research Fellowship for Young Scientists (DC1) from the Japan Society for the Promotion of Science (JSPS) to J.H., by a Grant-in-Aid for JSPS Fellows award (19J21686) to J.H., and by a Grant-in-Aid for Young Scientists award (17K1597), and a Grant-in-Aid for Scientific Research (B) award (16H04845) to Y.T. We would like to thank the following people for their helpful comments: A. Hara, S. Iwami, Y. Kakizoe, I. Koizumi, K. Morita, K. Nagata, G. Sahashi, A. Satake, T. Sato, S. Satoi, and M. Seki.

References

Ashander, J., Thompson, L. C., Sanchirico, J. N., & Baskett, M. L. (2019). Optimal investment to enable evolutionary rescue. *Theoretical Ecology*, 12(2), 165-177.

Bradshaw, W. E., & Holzapfel, C. M. (2006). Evolutionary response to rapid climate change. *Science*, 312(5779), 1477-1478.

Bradshaw, W. E., & Holzapfel, C. M. (2008). Genetic response to rapid climate change: it's seasonal timing that matters. *Molecular Ecology*, 17(1), 157-166.

Charmantier, A., McCleery, R. H., Cole, L. R., Perrins, C., Kruuk, L. E., & Sheldon, B. C. (2008). Adaptive phenotypic plasticity in response to climate change in a wild bird population. *Science*, 320(5877), 800-803.

Chevin, L. M., Lande, R., & Mace, G. M. (2010). Adaptation, plasticity, and extinction in a changing environment: towards a predictive theory. *PLoS biology*, 8(4), e1000357.

Crozier, L. G., Hendry, A. P., Lawson, P. W., Quinn, T. P., Mantua, N. J., Battin, J., ... & Huey, R. B. (2008). Potential responses to climate change in organisms with complex life histories: evolution and plasticity in Pacific salmon. *Evolutionary Applications*, 1(2), 252-270.

Daufresne, M., Lengfellner, K., & Sommer, U. (2009). Global warming benefits the small in aquatic ecosystems. *Proceedings of the National Academy of Sciences*, 106(31), 12788-12793.

Dodson, J. J., Aubin-Horth, N., Thériault, V., & Páez, D. J. (2013). The evolutionary ecology of alternative migratory tactics in salmonid fishes. *Biological*

Reviews, 88(3), 602-625.

Emlen, D. J. (1997). Alternative reproductive tactics and male-dimorphism in the horned beetle Onthophagus acuminatus (Coleoptera: Scarabaeidae). *Behavioral Ecology and Sociobiology*, 41(5), 335-341.

Esteve, M., McLennan, D. A., & Kawahara, M. (2011). Sexual behaviour of a masu salmon parr, with implications for the evolution of parr sexual behaviour in the salmonines. *Ecology of Freshwater Fish*, 20(3), 492-494.

Finstad, A. G., & Hein, C. L. (2012). Migrate or stay: terrestrial primary productivity and climate drive anadromy in Arctic char. *Global Change Biology*, 18(8), 2487-2497.

Fricke, H., & Fricke, S. (1977). Monogamy and sex change by aggressive dominance in coral reef fish. *Nature*, 266(5605), 830.

Gilpin, W., & Feldman, M. W. (2017). A phase transition induces chaos in a predator-prey ecosystem with a dynamic fitness landscape. *PLoS computational biology*, 13(7), e1005644.

Gregory, S. D., Nevoux, M., Riley, W. D., Beaumont, W. R., Jeannot, N., Lauridsen, R. B., ... & Roussel, J. M. (2017). Patterns on a parr: Drivers of long-term salmon parr length in UK and French rivers depend on geographical scale. *Freshwater Biology*, 62(7), 1117-1129.

Gross, M. R. (1996). Alternative reproductive strategies and tactics: diversity within sexes. *Trends in Ecology and Evolution*, 11(2), 92-98.

Hastings, A., Abbott, K. C., Cuddington, K., Francis, T., Gellner, G., Lai, Y. C., ... &

Zeeman, M. L. (2018). Transient phenomena in ecology. *Science*, 361(6406).

Horita, J., Iwasa, Y., & Tachiki, Y. (2018). Evolutionary bistability of life history decision in male masu salmon. *Journal of theoretical biology*, 448, 104-111.

Iwasa, Y., Pomiankowski, A., & Nee, S. (1991). The evolution of costly mate preferences II. The "handicap" principle. *Evolution*, 45(6), 1431-1442.

Jenkins, T. M., Diehl, S., Kratz, K. W., & Cooper, S. D. (1999). Effects of population density on individual growth of brown trout in streams. *Ecology*, 80(3), 941-956.

Kuwamura, T., & Nakashima, Y. (1998). New aspects of sex change among reef fishes: recent studies in Japan. *Environmental Biology of Fishes*, 52(1-3), 125-135.

Koseki, Y., & Maekawa, K. (2000). Sexual selection on mature male parr of masu salmon (Oncorhynchus masou): does sneaking behavior favor small body size and less-developed sexual characters?. *Behavioral Ecology and Sociobiology*, 48(3), 211-217.

Lehodey, P., Senina, I., Calmettes, B., Hampton, J., & Nicol, S. (2013). Modelling the impact of climate change on Pacific skipjack tuna population and fisheries. *Climatic change*, 119(1), 95-109.

Lehodey, P., Senina, I., Nicol, S., & Hampton, J. (2015). Modelling the impact of climate change on South Pacific albacore tuna. *Deep Sea Research Part II: Topical Studies in Oceanography*, 113, 246-259.

Morita, K., & Nagasawa, T. (2010). Latitudinal variation in the growth and maturation of masu salmon (Oncorhynchus masou) parr. *Canadian Journal of Fisheries and Aquatic Sciences*, 67(6), 955-965.

Morita, K., Tamate, T., Kuroki, M., & Nagasawa, T. (2014). Temperature-dependent variation in alternative migratory tactics and its implications for fitness and population dynamics in a salmonid fish. *Journal of Animal Ecology*, 83(6), 1268-1278.

Munday, P. L., Buston, P. M., & Warner, R. R. (2006). Diversity and flexibility of sex-change strategies in animals. *Trends in Ecology and Evolution*, 21(2), 89-95.

Ozgul, A., Childs, D. Z., Oli, M. K., Armitage, K. B., Blumstein, D. T., Olson, L. E., Tuljapurkar, S. & Coulson, T. (2010). Coupled dynamics of body mass and population growth in response to environmental change. *Nature*, 466(7305), 482.

Perry, A. L., Low, P. J., Ellis, J. R., & Reynolds, J. D. (2005). Climate change and distribution shifts in marine fishes. *science*, 308(5730), 1912-1915.

Phillis, C. C., Moore, J. W., Buoro, M., Hayes, S. A., Garza, J. C., & Pearse, D. E. (2016). Shifting thresholds: rapid evolution of migratory life histories in steelhead/rainbow trout, Oncorhynchus mykiss. *Journal of Heredity*, 107(1), 51-60.

Piché, J., Hutchings, J. A., & Blanchard, W. (2008). Genetic variation in threshold reaction norms for alternative reproductive tactics in male Atlantic salmon, Salmo salar. *Proceedings of the Royal Society of London B: Biological Sciences*, 275(1642), 1571-1575.

Post, J. R., Parkinson, E. A., & Johnston, N. T. (1999). Density-dependent processes in structured fish populations: interaction strengths in whole-lake experiments. *Ecological Monographs*, 69(2), 155-175.

Prentice, I. C., Sykes, M. T., & Cramer, W. (1993). A simulation model for the transient effects of climate change on forest landscapes. *Ecological modelling*, 65(1-2), 51-70.

Przybylo, R., Sheldon, B. C., & Merilä, J. (2000). Climatic effects on breeding and morphology: evidence for phenotypic plasticity. *Journal of Animal Ecology*, 69(3), 395-403.

Rego-Costa, A., Debarre, F., & Chevin, L. M. (2018). Chaos and the (un) predictability of evolution in a changing environment. *Evolution*, 72(2), 375-385.

Roff, D. A. (1996). The evolution of threshold traits in animals. *The Quarterly Review of Biology*, 71(1), 3-35.

Satterthwaite, W. H., Beakes, M. P., Collins, E. M., Swank, D. R., Merz, J. E., Titus, R. G., ... & Mangel, M. (2010). State-dependent life history models in a changing (and regulated) environment: steelhead in the California Central Valley. *Evolutionary Applications*, 3(3), 221-243.

Tachiki, Y., & Koizumi, I. (2016). Absolute versus relative assessments of individual status in status-dependent strategies in stochastic environments. *The American Naturalist*, 188(1), 113-123.

Thomas, C. D. et al. (2004). Extinction risk from climate change. *Nature*, 427(6970), 145.

Tomkins, J. L. (1999). Environmental and genetic determinants of the male forceps length dimorphism in the European earwig Forficula auricularia L. *Behavioral Ecology and Sociobiology*, 47(1-2), 1-8.

Tylianakis, J. M., Didham, R. K., Bascompte, J., & Wardle, D. A. (2008). Global change and species interactions in terrestrial ecosystems. *Ecology letters*, 11(12), 1351-1363.

Walther, G. R., Post, E., Convey, P., Menzel, A., Parmesan, C., Beebee, T. J., Fromentin, J. M., Hoegh-Guldberg, O. & Bairlein, F. (2002). Ecological responses to recent climate change. *Nature*, 416(6879), 389.

Warner, R. R., & Robertson, D. R. (1978). Sexual Patterns in the Labroid Fishes of the Western Caribbean, I the Wrasses (Labridae).

Warren, M. S., Hill, J. K., Thomas, J. A., Asher, J., Fox, R., Huntley, B., Roy, D. B., Telfer, M. G., Jeffcoate, S., Harding, P., Jeffcoate, G., Willis, S. G., Greatorex-Davies, J. N., Moss, D. & Thomas, C. D. (2001). Rapid responses of British butterflies to opposing forces of climate and habitat change. *Nature*, 414(6859), 65.

Watanabe, M., Takamura, S., & Maekawa, K. (2008). Effects of timing of nest entry and body size on the fertilization success of alternative male reproductive phenotypes of masu salmon (Oncorhynchus masou). *Canadian Journal of Zoology*, 86(10), 1121-1130.

Appendix A

Complex dynamical behavior caused by environmental changes.

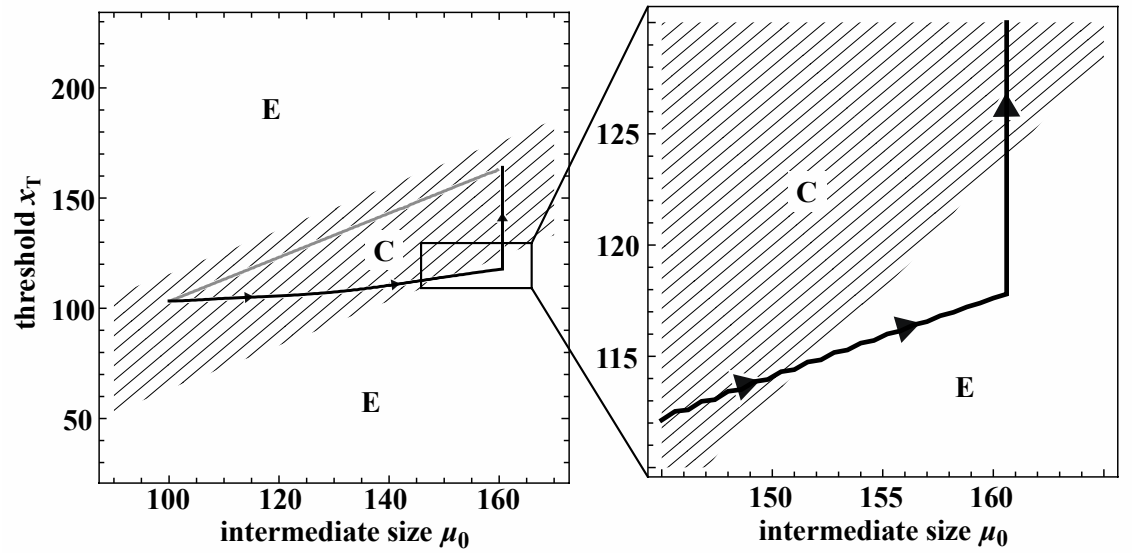

Figure S1: Evolutionary trajectory. See explanation in the text.

Figure S1 illustrates an evolutionary trajectory. Vertical axis and horizontal axis indicate intermediate size μ_0 and threshold trait x_T, respectively. The gray solid line is the convergence stable threshold when x_T evolves with μ_0 fixed. Solid curve with arrows is an evolutionary trajectory. Shaded region with label C and white regions with label E are given in the caption of Fig. 4. Parameters were the same as those for Fig. 5.

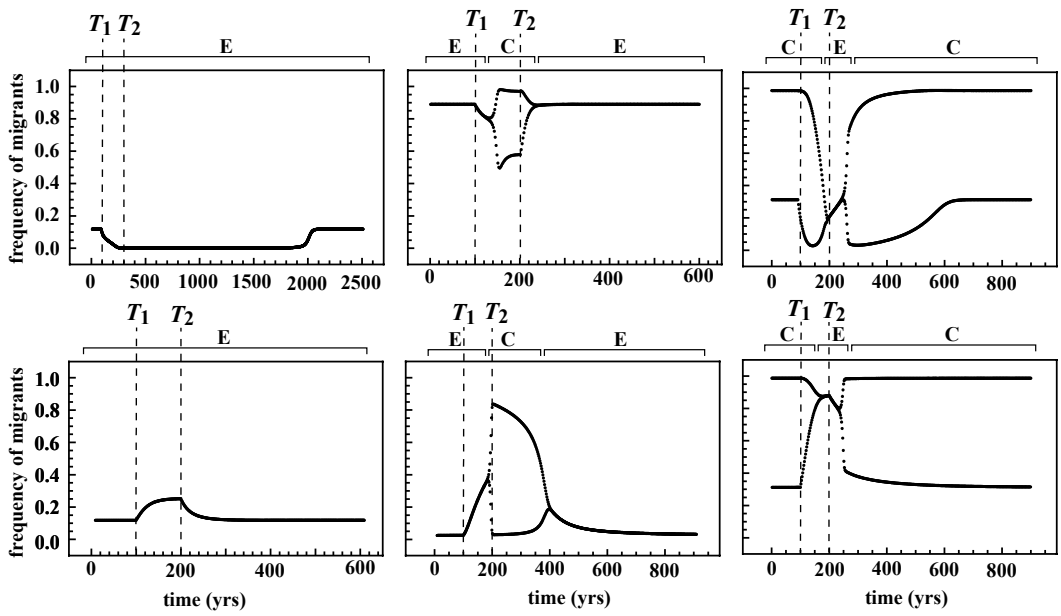

Figure S2: Fraction of migrants among male juveniles when the threshold evolves. Symbols "T_1", "T_2", "E" and "C" are the same as those in Fig. 1. In S2a, S2b & S2c, intermediate size μ_0 increased with time. In the other cases, intermediate size μ_0 decreased (d, e, & f) . Even after the environmental change stopped (T_2<t), the evolution of threshold still continued and then it stopped when the fraction of migrants returned to the initial level. (a) Parameters were: feedback strength $k = 0.1$, rate of body size change $m = 0.3$, rate of threshold evolution $\Lambda = 100.0$, survivorship of residents $S_{\mathrm{R}} = 0.05$, and that of migrants $S_{\mathrm{M}} = 0.5 \times 10^{-4}$. (b) Parameters were: $k = 0.5$, $m = 0.6$, $\Lambda = 50.0$, $S_{\mathrm{R}} = 0.02$, and $S_{\mathrm{M}} = 7.0 \times 10^{-4}$. (c)Parameters were: $k = 0.5$, $m = 0.6$, $\Lambda = 10.0$, $S_{\mathrm{R}} = 0.02$, and $S_{\mathrm{M}} = 0.5 \times 10^{-4}$. (d) Parameters were: $k = 0.1$, $m = -0.6$, $\Lambda = 100.0$, $S_{\mathrm{R}} = 0.05$, and $S_{\mathrm{M}} = 0.5 \times 10^{-4}$. (e) Parameters were: $k = 0.5$, $m = -0.6$, $\Lambda = 20.0$, $S_{\mathrm{R}} = 0.05$, and $S_{\mathrm{M}} = 0.5 \times 10^{-4}$. (f) Parameters were: $k = 0.5$, $m = -0.6$, $\Lambda = 10.0$, $S_{\mathrm{R}} = 0.02$, and $S_{\mathrm{M}} = 0.5 \times 10^{-4}$. Other parameters were $\mu_0 = 100.0, \mu_1 = 50.0, \theta = 0.4, \sigma = 13.0, \Delta l = 40.0, N = 100.0, c_0 = 0.1$ and $c_1 = 5.0$.

Fig. S2 shows the eco-evolutionary dynamics when there is only one equilibrium. The fraction of migrants decreased with an increase in the intermediate body size μ_0 ($T_1 < t < T_2$), and after the climate change ceased ($t > T_2$), population dynamics returned to the initial level (Fig. S2a). Qualitative transition of population dynamics may occur both from equilibrium to cycle and from cycle to equilibrium. In Fig. S2b, the fraction of migrants was stable initially, but it became destabilized as μ_0 changed ($T_1 < t < T_2$). In Fig. S2c, the fraction of migrant fluctuated initially, but it became stabilized as μ_0 changed ($T_1 < t < T_2$). When the intermediate size decreased (Figs. S2d, S2e & S2f; $T_1 < t < T_2$), the fraction of migrant increased (Fig. S2d; $T_1 < t < T_2$), and the ecological dynamics may change from equilibrium to two-year cycle (Figs. S2e & S2f; $T_1 < t < T_2$). These regime shifts returned to the initial level after the climate change stopped ($t > T_2$).

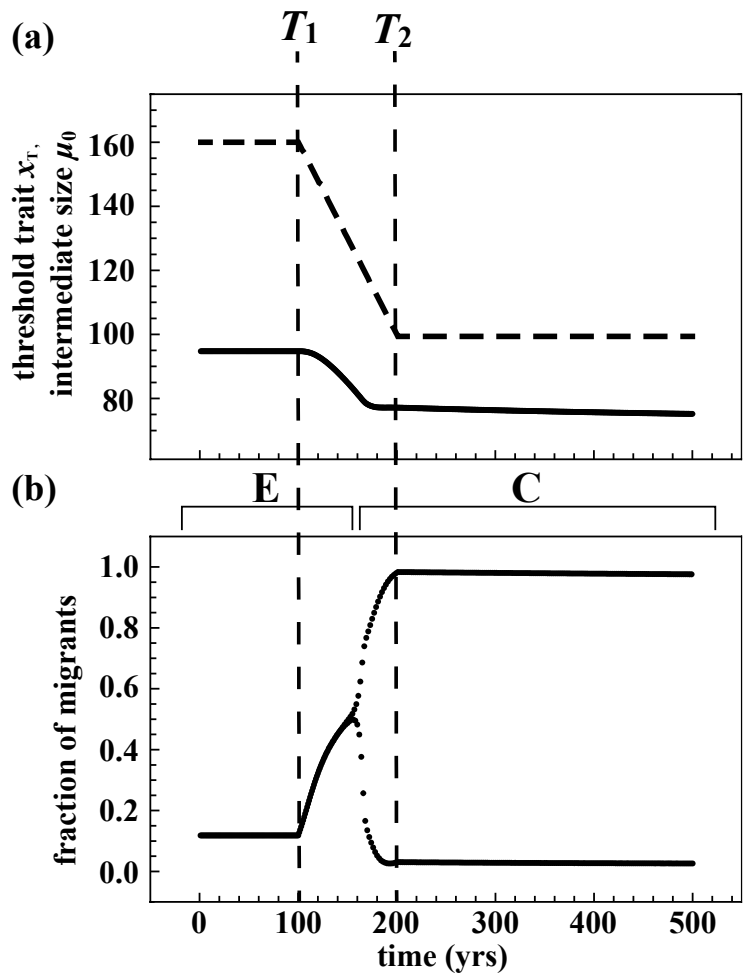

Figure S3: Eco-evolutionary dynamics under the climate change for the case of evolutionary bistability. Symbols "T_1", "T_2", "E" and "C" indicate the same as those in Fig. 1. (a) Solid line and dotted line indicate the same as those in Fig.5a. As the intermediate size decreased, an evolutionary regime shift occurred. The difference between intermediate size and threshold changed after the climate change. (b)The fraction of migrants exhibited different dynamics: it converged the equilibrium to cycle with period of 2 year. The rate of climate change was $m = -0.6$ and the rate of evolution was $\Lambda = 50.0$. Other parameters were the same as for Fig. 3b.

Fig. S3 shows the eco-evolutionary dynamics in which the intermediate size μ_0 decreased with time. Before the environmental change started ($t < T_1$), the threshold trait x_{T} was located on an evolutionary attractor (Fig.S3a, which corresponds to the lower attractor in Fig. 4.), and the fraction of migrants was stabilized (Fig. S3b). As intermediate size μ_0 decreased with time ($T_1 < t < T_2$), the threshold trait decreased (Fig. S3a). The fraction of migrants started fluctuating with 2-year cycle (Fig. S3b). After the environmental change was stopped ($t > T_2$), the threshold trait evolved to a value, and the population dynamics became qualitatively different from before the climate change (evolutionary regime shift).

Appendix B

Probabilistic Reaction Norm of Relative Assessment based on Bayesian Decision Making

Let x and z be the true and estimated relative status, respectively. Here, estimated relative body size is defined as the deviation from the population-mean value. Note that no individual knows the population-mean status initially. Let the distribution of the status follows a normal distribution, with mean μ and standard deviation σ:

$$p(x) = \frac{1}{\sqrt{2\pi}\sigma} \exp\left(-\frac{(x-\mu)^2}{2\sigma^2}\right) dx. \tag{B.1}$$

The prior distribution of the estimated status z is assumed to be a normal distribution, with mean equal to 0 and standard deviation σ:

$$p_x^{\text{prior}}(z) = \frac{1}{\sqrt{2\pi}\sigma} \exp\left(-\frac{z^2}{2\sigma^2}\right). \tag{B.2}$$

This implies that each individual has no idea about their relative body size but speculates that their status is equivalent to other individuals they encounter in the population. Each individual is assumed to obtain the data through contact (or fight) with a randomly selected opponent. The probability that an individual with status x deviates from the status value (Δx) of an opponent is as follows:

$$p_x(\Delta x) = \frac{1}{\sqrt{2\pi}\sigma} \exp\left(-\frac{\left(\Delta x-(x-\mu)\right)^2}{2\sigma^2}\right). \tag{B.3}$$

The probability that an individual with relative body size z obtains data for Δx (i.e., likelihood) is

$$L(\Delta x|z) = \frac{1}{\sqrt{2\pi}\sigma} \exp\left(-\frac{(\Delta x-z)^2}{2\sigma^2}\right). \tag{B.4}$$

The expected likelihood function of an individual with true body size x after one

contact is

$$E_x[L(\Delta x|z)] = \int_{-\infty}^{\infty} p_x(\Delta x) L(\Delta x|z) d\Delta x. \tag{B.5}$$

When each individual makes contact with others *n* times, based on the Bayesian updating, the expected likelihood is

$$E_x[L(\Delta \boldsymbol{x}|z)] = \int_{\mathbb{R}^n} p_x^n(\Delta \boldsymbol{x}) \prod_{i=1}^{n} L(\Delta x_i|z)\, d\Delta \boldsymbol{x}, \tag{B.6}$$

where Δx is an *n*-dimensional vector of the data experienced by the focal individual. The posterior distribution of the estimated relative body size distribution is

$$p_x^{\text{posterior}}(z|\Delta x) = \frac{E_x[L(\Delta \boldsymbol{x}|z)] p_x^{\text{prior}}(z)}{\int_{-\infty}^{\infty} E_x[L(\Delta \boldsymbol{x}|z)] p_x^{\text{prior}}(z) dz}. \tag{B.7}$$

Let z_{T} be the threshold trait. Suppose that an individual chooses tactic α if its estimated relative status is larger than z_{T}; otherwise, it chooses the alternative tactic β. The probability that an individual with true status x chooses tactic α is

$$\Phi(x) = \int_{z_{\mathrm{T}}}^{\infty} p_x^{\text{posterior}}(z|\Delta x)\mathrm{d}z = \frac{1}{2}\left(1 + \mathrm{erf}\left[\frac{n(x-\mu) - (n+2)z_{\mathrm{T}}}{2\sigma\sqrt{n+2}}\right]\right) \tag{B.8}$$

If n is very large, each individual can accurately assess its relative status; and the reaction norm Φ approximates a step function:

$$\Phi(x|z_{\mathrm{T}}) \xrightarrow[n\to\infty]{} \begin{cases} 1 \text{ if } x > z_{\mathrm{T}} + \mu \\ 0 \quad \text{otherwise.} \end{cases}$$

Hence, the individual's decision making becomes similar to the absolute assessment model when *n* is very large, but the condition term contains the population mean status μ. This indicates that the phenotypic threshold value in the relative assessment model changes if the population-mean status changes, whereas the threshold does not change

in the absolute assessment model (Eq. 2 in the main text).

Appendix Figure S4

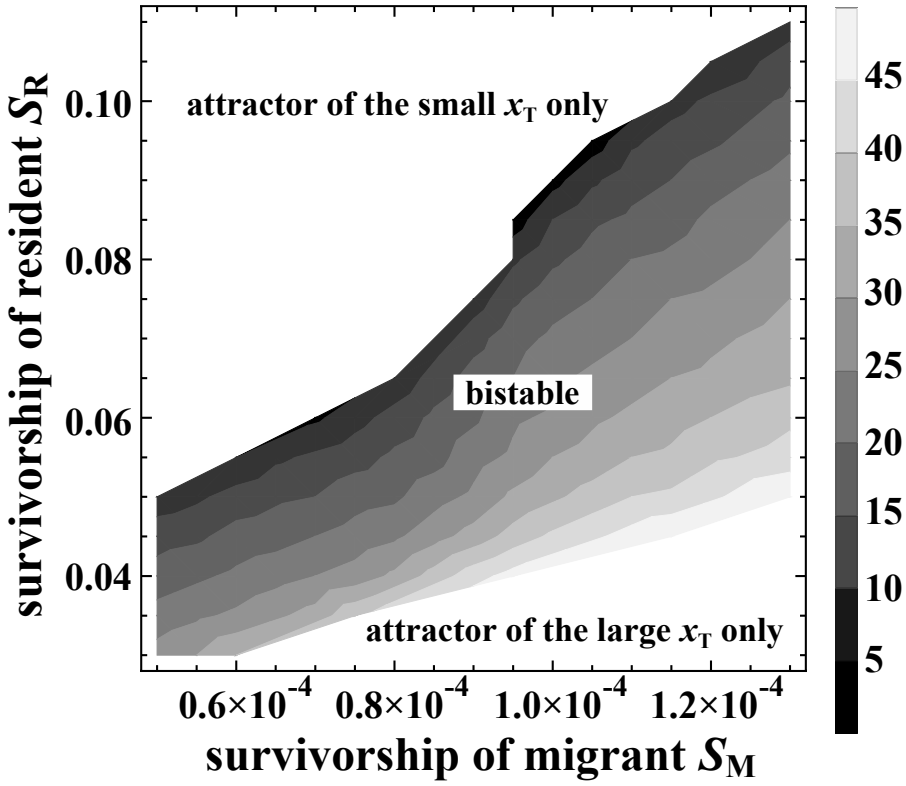

Figure S4: The distance between the attractor of the larger x_T and the repeller, in the evolution of x_T. Horizontal axis and vertical axis indicate the survivorship of migrant S_M and that of resident S_R, respectively. In shaded area, evolutionary bistability was observed. In the white area, there is only one equilibrium. The magnitude of the distance is indicated by the darkness of shading: the darker area indicates the condition for a shorter distance between upper attractor and repeller (i.e., the attractor is less robust). The distance decreased with a larger survivorship of migrant S_M, and a smaller survivorship of resident S_R. Parameters were: $\mu_0 = 160.0, \mu_1 = 50.0, m = 0.01, \theta = 0.4, \sigma = 13.0, \Delta l = 40.0, N = 100.0, c_0 = 0.1$and $c_1 = 5.0$.

Figures

Figure 1 Fraction of male juveniles to be migrants when the threshold is fixed

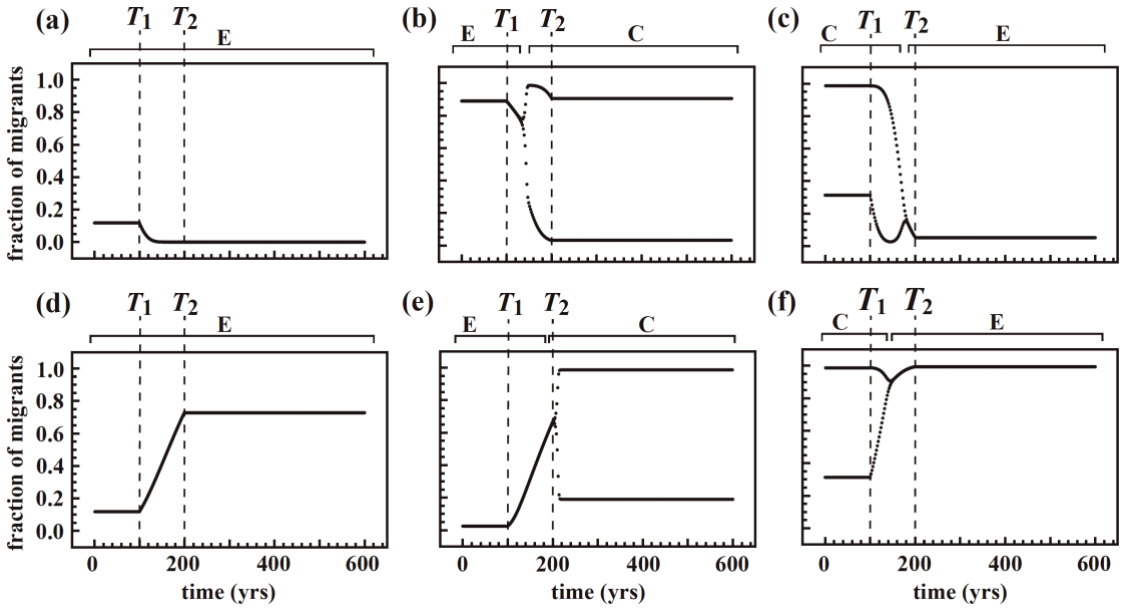

Climate changes occurred between T_1 and T_2. The signs "E" and "C" indicate that the ecological dynamics are equilibrium and cycle over a 2-year period, respectively. In 1a, 1b, and 1c, intermediate size μ_0 increased. In the other cases, intermediate size decreased. (a) The fraction of migrants decreased with an increase in μ_0. Parameters: feedback strength $k = 0.1$; the rate of climate change $m = 0.6$; survivorship of residents $S_{\mathrm{R}} = 0.05$; and that of migrants $S_{\mathrm{M}} = 0.5 \times 10^{-4}$. (b) The stability of the fraction of migrants that changed from equilibrium to cycle. Parameters: $k = 0.5$; $m = 0.6$; $S_{\mathrm{R}} = 0.02$; and $S_{\mathrm{M}} = 7.0 \times 10^{-4}$. (c) The stability of the fraction of migrants that changed from cycle to equilibrium. Parameters: $k = 0.5$; $m = 0.6$; $S_{\mathrm{R}} = 0.02$; and $S_{\mathrm{M}} = 0.5 \times 10^{-4}$. (d) The fraction of migrants that increased with a decrease in μ_0. Parameters: $k = 0.1$; $m = -0.4$; $S_{\mathrm{R}} = 0.05$; and $S_{\mathrm{M}} = 0.5 \times 10^{-4}$. (e) The stability of the fraction of migrants that changed from equilibrium to cycle. Parameters: $\mu_{0,0} =$

160.0; $k = 0.5$; $m = -0.6$; $S_{\mathrm{R}} = 0.05$; and $S_{\mathrm{M}} = 0.5 \times 10^{-4}$. (f) The stability of the fraction of migrants that changed from cycle to equilibrium. Parameters: $k = 0.5$; $m = -0.4$; $S_{\mathrm{R}} = 0.02$; and $S_{\mathrm{M}} = 0.5 \times 10^{-4}$. Other parameters were: $\mu_{0,0} = 100.0$; $\mu_1 = 50.0$; $m = 0.01$; $\theta = 0.4$; $\sigma = 13.0$; $\Delta l = 40.0$; $N = 100.0,$; $= 0.1$; and $c_1 = 5.0$.

Figure 2 Evolutionary consequences of threshold trait

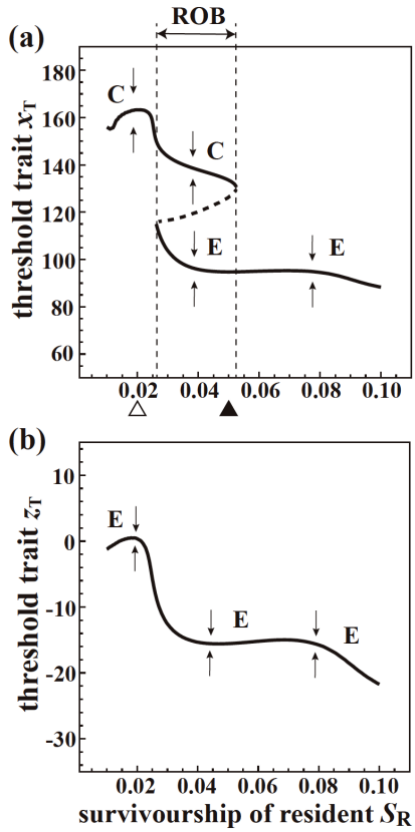

The horizontal axis is the survivorship of resident S_R. The vertical axis is the threshold trait. The signs "E" and "C" indicate the same as those in Fig. 1. Upper (lower) arrows indicate that the trait values increase (decrease) in evolution. Solid curves are the set of convergence stable points (attractor). The dotted curves are the set of evolutionarily unstable points (repeller). The ROB (range of bistability) indicates the range for which the evolutionary bistability occurs. (a) In the case of absolute assessment, for $S_R < 0.026$ or $0.052 < S_R$, the evolutionary dynamics of x_T converged into a single stable point. For $0.026 \leq S_R \leq 0.052$, the evolutionary dynamics of x_T converged into one of the two stable values, depending on the initial values. Open and solid triangles correspond to the parameter sets of Fig 3a and 3b, respectively. Other parameters were:

$k = 0.5$; $\mu_0 = 100.0$; $\mu_1 = 50.0$; $\theta = 0.4$; $\sigma = 13.0$; $S_{\mathrm{M}} = 2.5 \times 10^{-4}$; $\Delta l = 40.0$; $N = 100.0$; $c_0 = 0.1$; and $c_1 = 5.0$. (b) In the case of the relative assessment, the evolutionary dynamics of z_{T} always converged to a stable equilibrium. The number of Bayesian update was $n = 100.0$. Other parameters were the same as those in Fig. 2a.

Figure 3 Evolutionary consequences of threshold trait

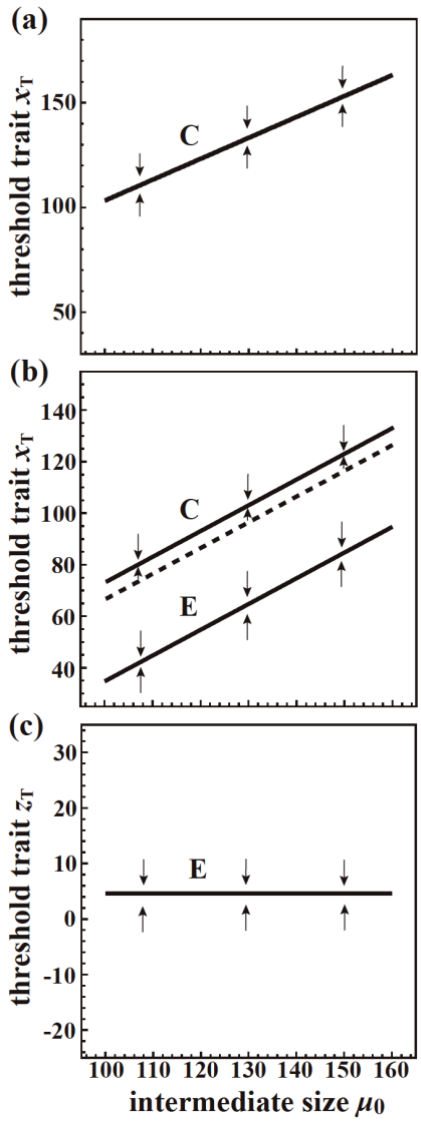

The horizontal axis is the intermediate size μ_0. The signs "E" and "C" indicate the same as those in Fig. 1. Arrows indicate the same as those in Fig. 2. (a) In the case of absolute assessment with only one evolutionary equilibrium (in Fig. 2a, it is donated by the open triangle), the convergence stable point increased with an increase in μ_0. Survivorship of resident was $S_R = 0.02$. Survivorship of migrant was $S_M = 0.5 \times 10^{-4}$. (b) In the case of the absolute assessment with three evolutionary equilibria (in Fig. 2a, it is donated by the solid triangle). Two attractors and one repeller increased

with an increase in μ_0. Parameters were: $S_{\mathrm{R}} = 0.05$ and $S_{\mathrm{M}} = 0.5 \times 10^{-4}$. (c) In the case of relative assessment, the convergence stable threshold value did not correlate with μ_0. Parameters were: $S_{\mathrm{R}} = 0.08$ and $S_{\mathrm{M}} = 2.5 \times 10^{-4}$. The number of Bayesian update was $n = 100.0$. Other parameters were: $k = 0.5$; $\mu_1 = 50.0$; $\theta = 0.4$; $\sigma = 13.0$; $\Delta l = 40.0$; $N = 100.0$; $c_0 = 0.1$; and $c_1 = 5.0$.

Figure 4 Evolutionary trajectories

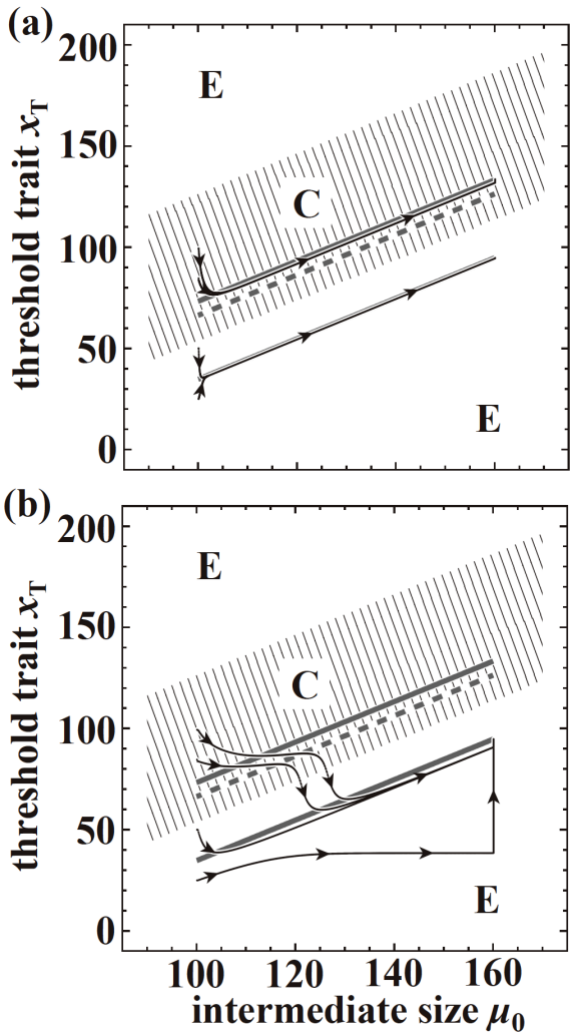

The horizontal and vertical axis represent the intermediate size μ_0 and threshold trait x_T, respectively. Black arrows indicate the evolutionary trajectories of the system. The solid gray line indicates the convergence stable threshold, and the dotted gray line is the repeller. In the dashed shading region, where is donated by sign "C", ecological dynamics fluctuated over a 2-year cycle, and in the white region, denoted by the sign "E", ecological dynamics were at an equilibrium. (a) When the rate of the evolution was faster than the rate of climate change, the evolution could keep up with climate change. The rate of climate change was m = 0.01 (b) When the rate of the evolution was slower

than the rate of climate change, the threshold trait converged to the lower attractor by crossing the repeller. The rate of climate change was $m = 0.1$. Other parameters were: $\Lambda = 100.0$; $k = 0.5$; $\mu_{0,0} = 100.0$; $\mu_1 = 50.0$; $\theta = 0.4$; $\sigma = 13.0$; $S_{\mathrm{R}} = 0.05$; $S_{\mathrm{M}} = 0.5 \times 10^{-4}$; $\Delta l = 40.0$; $N = 100.0$; $c_0 = 0.1$; and $c_1 = 5.0$.

Figure 5 Eco-evolutionary dynamics with climate change in the case of single equilibrium

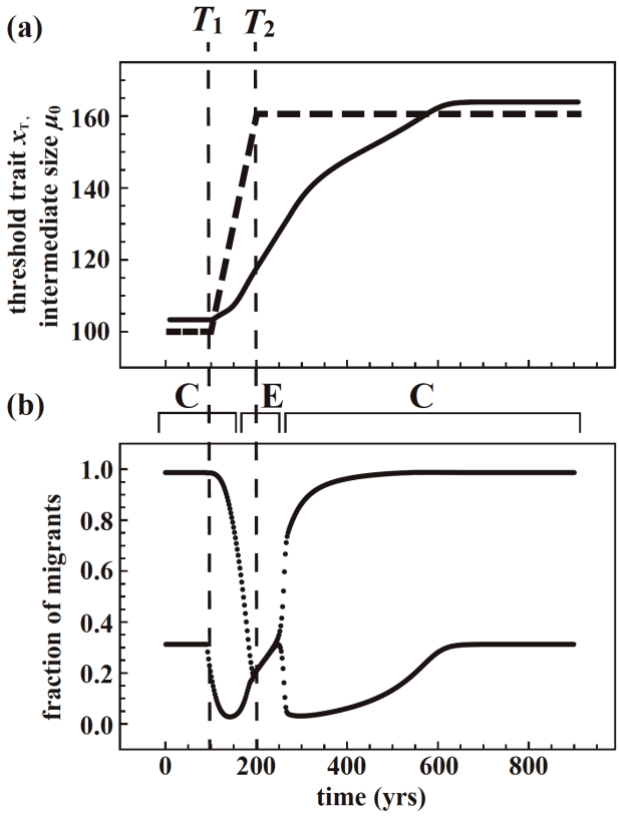

The signs "T_1", "T_2", "E" and "C" indicate the same as those in Fig. 1. (a) The solid line is the trajectory of threshold trait x_{T}, and the dotted line is the intermediate size μ_0. The threshold value increased with evolution with an increase in intermediate size. The interval of values of intermediate size and thresholds had been changed before and after climate changes. (b)The stability of the time series of the fraction of migrants was temporarily changed, such as fluctuated to equilibrium with the effects of climate change, and then the stability returned to the initial level by threshold evolution. Parameters were: $k = 0.5$; $m = 0.6$; $\mu_{0,0} = 100.0$; $\mu_1 = 50.0$; $\theta = 0.4$; σ 13.0; $\Lambda = 10.0$; $S_{\mathrm{R}} = 0.02$; $S_{\mathrm{M}} = 0.5 \times 10^{-4}$; $\Delta l = 40.0$; $N = 100.0$; $c_0 = 0.1$; and $c_1 = 5.0$.

Figure 6 Eco-evolutionary dynamics with climate change and the case of bistability

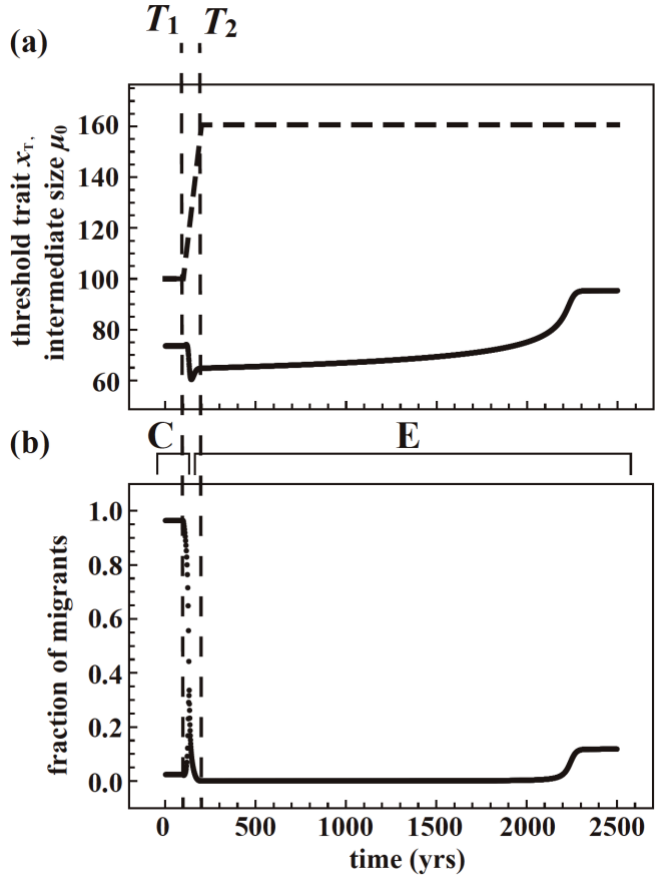

The signs "T_1", "T_2", "E" and "C" indicate the same as those in Fig. 1. (a) The solid line and dotted line indicate the same as those in Fig.5a. By increasing the value of the intermediate size, the regime shift of the threshold occurred and it converged to the other attractor. The interval of values of intermediate size and threshold had been changed before and after climate changes. (b) The stability of the timeseries of the fraction of migrants changed from unstable to stable. The fraction of migrants are finally fixed at a specific value, which is different from the initial situation. Parameters were: $k = 0.5$; $m = 0.6$; $\mu_{0,0} = 100.0$; $\mu_1 = 50.0$; $\theta = 0.4$; $\sigma = 13.0$; $\Lambda = 50.0$; $S_{\mathrm{R}} = 0.05$; $S_{\mathrm{M}} = 0.5 \times 10^{-4}$; $\Delta l = 40.0$; $N = 100.0$; $c_0 = 0.1$; and $c_1 = 5.0$.

Figure 7 The conditions under which the evolutionary regime shift occurs

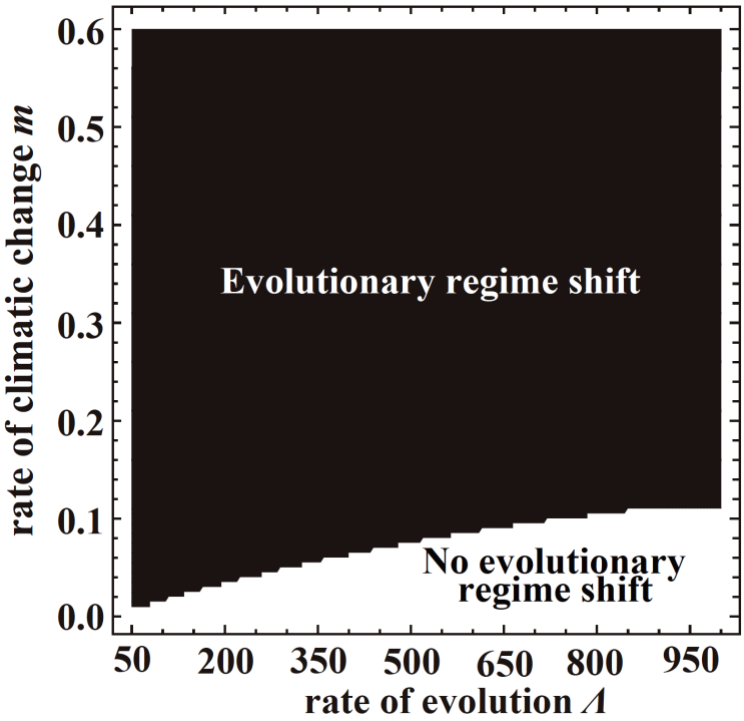

The horizontal axis and vertical axis indicate the rate of threshold evolution Λ, and rate of climate change m, respectively. The black area indicates where evolutionary regime shifts (threshold converges to the other attractor) have occurred. The white area indicate where evolutionary regime shifts have not occurred. When the rate of the evolution was large, the evolutionary regime shift of the threshold by climate change hardly occurs. Parameters were: $k = 0.5$; $\mu_{0,0} = 100.0,$; $\mu_1 = 50.0$; $\theta = 0.4$; $\sigma = 13.0$; $S_{\mathrm{R}} = 0.05$; $S_{\mathrm{M}} = 0.5 \times 10^{-4}$; $\Delta l = 40.0$; $N = 100.0$; $c_0 = 0.1$; and $c_1 = 5.0$.

Figure 8 Ecologically and eco-evolutionary dynamics with climate change in the case of the relative assessment

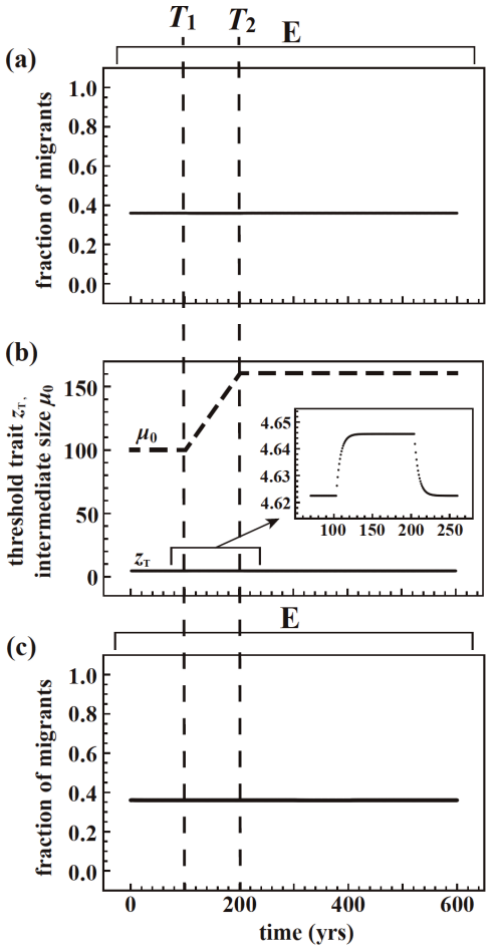

The signs "T_1", "T_2" and "E" indicate the same as those in Fig. 1. (a) When the threshold trait is fixed. The frequency of migration was not changed by climate change. (b) The dotted line is the intermediate value μ_0, and the solid line is the threshold trait, z_{T}. When the threshold trait evolves, the value of z_{T} hardly changed with an increase in intermediate size. (c) The fraction of migrants did not change with an increase in intermediate size in the case of (b). Parameters were: $k = 0.5$; $\mu_{0,0} = 100.0$; $\mu_1 = 50.0$; $m = 0.6$; $\theta = 0.4$; $\sigma = 13.0$; $\Lambda = 50.0$; $S_{\mathrm{R}} = 0.08$; $S_{\mathrm{M}} = 2.5 \times 10^{-4}$; $\Delta l = 40.0$; $N = 100.0$; $n = 100.0,$; $c_0 = 0.1$; and $c_1 = 5.0$.